

UC Irvine

UC Irvine Previously Published Works

Title

Simulation of fusion plasmas: Current status and future direction

Permalink

<https://escholarship.org/uc/item/2h6476c8>

Journal

Plasma Science and Technology, 9(3)

ISSN

1009-0630

Authors

Batchelor, DA

Beck, M

Becoulet, A

et al.

Publication Date

2007-06-01

DOI

10.1088/1009-0630/9/3/13

Peer reviewed

Simulation of Fusion Plasmas: Current Status and Future Direction

D.A. Batchelor¹, M. Beck², A. Becoulet³, R.V. Budny⁴, C.S. Chang⁵,
P.H. Diamond⁶, J.Q. Dong⁷, G.Y. Fu^{*4}, A. Fukuyama⁸, T.S. Hahn⁴,
D.E. Keyes⁹, Y. Kishimoto¹⁰, S. Klasky¹, L.L. Lao¹¹, K. Li¹², Z. Lin^{*13},
B. Ludaescher¹⁴, J. Manickam⁴, N. Nakajima¹⁵, T. Ozeki¹⁶, N. Podhorszki¹⁴,
W.M. Tang⁴, M.A. Vouk¹⁷, R.E. Waltz¹¹, S.J. Wang¹⁸, H.R. Wilson¹⁹, X.Q. Xu²⁰,
M. Yagi²¹, F. Zonca²²

¹ Oak Ridge National Laboratory, Oak Ridge, TN 37831, USA

² 1122 Volunteer Blvd, Suite 203, Knoxville, TN 37996-3450, USA

³ Association EURATOM-CEA sur la Fusion Contrôlée, CEA Cadarache, 13108 Saint Paul
lez Durance Cedex, France

⁴ Princeton Plasma Physics Laboratory, Princeton University, Princeton, NJ 08543, USA

⁵ Courant Institute of Mathematical Sciences, New York University, 251 Mercer Street,
New York, NY 10012, USA

⁶ University of California at San Diego, Dept. of Physics and Center for Astrophysics and
Space Sciences, La Jolla, CA 92093, USA

⁷ Southwestern Institute of Physics, Chengdu 610041, China

⁸ Department of Nuclear Engineering, Kyoto University, Kyoto 606-8501, Japan

⁹ Columbia University, Department of Applied Physics and Applied Mathematics, MC 4701,
New York, NY 10027, USA

¹⁰ Department of Fundamental Energy Science, Graduate School of Energy Science,
Kyoto University, Gokasho, Uji, Kyoto 611-0011, Japan

¹¹ General Atomics, P.O. Box 85608, San Diego, CA 92186, USA

¹² Department of Computer Science, Princeton University Princeton, NJ 08544, USA

¹³ Department of Physics and Astronomy, University of California, Irvine, CA 92697, USA

¹⁴ Department of Computer Science University of California, Davis, CA, 95616, USA

¹⁵ National Institute for Fusion Science, Toki, Gifu 509-5292, Japan

¹⁶ Japan Atomic Energy Research Institute, Naka Fusion Research Establishment,
Naka-machi, Ibaraki-ken, Japan

¹⁷ Department of Computer Science, North Carolina State University, Raleigh, NC 27695,
USA

¹⁸ Department of Physics, Fudan University, 200433 Shanghai, China

¹⁹ EURATOM/UKAEA Culham Science Centre, Abingdon, Oxon OX1 3DB, United
Kingdom

²⁰ Lawrence Livermore National Laboratory, Livermore, CA 94550, USA

²¹ Research Institute for Applied Mechanics, Kyushu University, Kasuga 816-8580, Japan

²² Associazione Euratom-ENEA sulla fusione, CR Frascati, Casella Postale 65-00044,
Frascati, Italy

- I. Introduction (Z. Lin, G. Y. Fu, J. Q. Dong)
- II. Role of theory and simulation in fusion sciences
 - 1. The Impacts of theory and simulation on tokamak experiments (H. R. Wilson, T.S. Hahm and F. Zonca)
 - 2. Tokamak Transport Physics for the Era of TIER: Issues for Simulations (P.H. Diamond and T.S. Hahm)
- III. Status of fusion simulation and modeling
 - 1. Nonlinear Governing Equations for Plasma Simulations (T. S. Hahm)
 - 2. Equilibrium and stability (L.L. Lao, J. Manickam)
 - 3. Transport modeling (R.E. Waltz)
 - 4. Nonlinear MHD (G.Y. Fu)
 - 5. Turbulence (Z. Lin and R.E. Waltz)
 - 6. FRO heating and current drive (D.A. Batchelor)
 - 7. Edge physics Simulations (X.Q. Xu and C.S. Chang)
 - 8. Energetic particle physics (F. Zonca, G.Y. Fu and S.J. Wang)
 - 9. Time-dependent Integrated Modeling (R.V. Budny)
 - 10. Validation and verification (J. Manickam)
- IV. Major initiatives on fusion simulation
 - 1. US Scientific Discory through Advanced Computing (SciDAC) Program & Fusion Energy Science (W. Tang)
 - 2. EU Integrated Tokamak Modelling (ITM) Task Force (A. Becoulet)
 - 3. Fusion Simulations Activities in Japan (A. Fukuyama, N. Nakajima, Y. Kishimoto, T. Ozeki, and M. Yagi)
- V. Cross-disciplinary research in fusion simulation
 - 1. Applied mathematics: Models, Discretizations, and Solvers (D.E. Keyes)
 - 2. Computational Science (K. Li)
 - 3. Scientific Data and Workflow Management (S. Klasky, M. Beck, B. Ludaescher, N. Podhorszki, M.A. Vouk)
 - 4. Collaborative tools (J. Manickam)

I Introduction

(Z. Lin, G. Y. Fu, J. Q. Dong)

After half a century of intense pursuit, magnetic fusion has made tremendous progress toward the goal as an attractive energy solution for the world's increasingly critical energy problem. The key obstacle for reaching the ignition has been the lack of fundamental understanding, and thus the limited ability to control the complex, nonlinear, and dynamical system characteristic of high temperature plasma in fusion tokamak experiments. Renewed optimism in magnetic confinement has come from recent progress marked by the strong coupling between experiment, theory, and simulation. In particular, large-scale simulations enabled by the ever increasing power of modern computers are rapidly advancing fusion energy science. Numerical simulations, in tandem with analytic theories and experimental measurements, have helped to discover fundamental physics in fusion plasmas, to understand tokamak experimental results, to guide the design and installation of advanced tokamak diagnostics, to control plasma behavior, and to optimize tokamak operation regimes.

The International Thermonuclear Experimental Reactor (ITER) experiment is the crucial next step in the quest for fusion energy. Theory and simulation will play an even bigger role in the ITER project as we explore the new regime of burning plasma physics. First-principles simulations could directly address the parameter regimes inaccessible by conventional experimental and analytic techniques. Predictive simulation tools could enhance the efficiency of the utilization and optimize operation configurations for ITER, and could aid the physics design of DEMO, the successor to ITER for the engineering demonstration of a fusion power plant.

Fusion simulations fall broadly into two categories. The first type, referred to as "modeling" in this paper, is a reduced model incorporating all known physics and empirical scaling for unknown physics. Examples include the re-construction of magnetohydrodynamic equilibrium and transport modeling. Modeling is the essential tool for assisting experimental operations and data interpretation, and for projecting the performance of future burning plasma experiments. These areas are relatively mature thanks to research efforts over the past three decades. The second type, referred to as "physics simulation", is a direct numerical simulation using first-principles equations. The goal is to identify and discover the fundamental physics in fusion plasmas, and to provide a physics basis for innovative confinement approaches and advanced operation regimes. Such physics simulations provide the building blocks for modeling and are the current focus in the world fusion community. Examples include nonlinear magnetohydrodynamics (MHD), turbulence, heating and current drive, boundary physics, and energetic particle physics. Theory plays a critical role in the physics simulations by deducing basic equations, interpreting simulation re-

sults, and constructing physics models.

ITER simulations focus on the extension of current simulation capabilities into the burning plasma regime and on integrated simulations addressing simultaneously multiple scales and multiple processes in fusion plasmas. A central theme is the predictive simulation integrating both modeling and physics simulation codes for the purpose of benchmarking on existing tokamak experiments, with the ultimate goal of providing a comprehensive simulation package for ITER plasmas. Major initiatives toward integrated simulation with predictive capability have been launched by several ITER partners. In US, large scale fusion simulation projects including nonlinear MHD, turbulent transport, RF-heating, and other areas are currently supported as part of the Scientific Discovery through Advanced Computing (SciDAC) initiative funded by the Department of Energy (DOE). Each project typically involves 15-30 researchers in 5-10 institutions. In addition to addressing key science area, fusion SciDAC supports three prototype centers for a fusion simulation project (FSP) targeting integrative simulation of burning plasmas. The burning Plasma Simulation Initiative (BPSI) organized as joint university group, the Numerical Experiment of Tokamak (NEXT) organized by JAEA, and the multi-scale fusion plasma simulation organized by the NIFS group, have been proposed in Japan, which may play a central role for the ITER simulation center for fusion science. The European Union (EU) has launched an Integrated Tokamak Modeling (ITM) initiative in Europe for ITER.

Addressing the dynamical processes in fusion plasmas characterized by a large number of degree of freedom and disparate spatial-temporal scales, fusion simulation is a grand challenge from both the physics and computing points of view. Consequently, cross-disciplinary collaboration has become a clearly visible trend in fusion simulations, which often involve computational and analytical plasma physicists, applied mathematicians, computational and computer scientists. Therefore, it is crucial to carefully plan the coordination and collaboration across the boundaries of disciplines and institutions. Another important observation is that fusion simulation is one of the key applications driving the hardware and software developments for high performance computers. Large-scale physics simulations can effectively utilize the computing power of thousands of processors using the most powerful massively parallel computers.

Recognizing the importance of theory and simulation in fusion research and the collaborative nature of ITER simulation, a Workshop on ITER Simulation sponsored by the ITER-China participation team (ITER-CN-PT) was held in Beijing, May 15-19, 2006. The meeting drew about one hundred fusion researchers, students, and managers from US, Japan, Europe, and China to discuss the present status and future collaborations on fusion simulations in support of the ITER project. This article is a direct product of the carefully planned pro-

gram of comprehensive review presentations by many active researchers at the forefront of fusion simulations. The topics covered include the role of theory and simulation in fusion science, the status of fusion simulation and modeling, the major initiatives of fusion simulation among ITER partners, and the cross-disciplinary research in fusion simulation. In addition to presenting the state-of-the-art in fusion theory and simulations, many of the Workshop participants express a sense of urgency to establish plasma programs at top universities in China for training the next generation of fusion researchers and a desire to initiate international collaborations on fusion theory and simulations under the ITER framework.

The paper is organized as follows. Chapter II discusses the role of theory and simulation in fusion sciences including important issues for simulations in the area of tokamak transport physics. Chapter III reviews the status of fusion simulation and modeling covering 10 areas: III.1 Nonlinear governing equations for plasmas simulations, III.2 equilibrium and stability, III.3 transport modeling, III.4 nonlinear MHD, III.5 turbulence simulations, III.6 RF heating and current drive, III.7 edge physics simulations, III.8 energetic particle physics, III.9 time-dependent integrated modeling, and III.10 code validation and verification. Chapter IV gives an overview of major fusion simulation initiatives in US, Europe, and Japan. Finally, Chapter V review cross-disciplinary research in fusion simulation including applied mathematics, computational science, data structure, and collaborative tool.

II Role of theory and simulation in fusion sciences

II.1 The impact of theory and simulation on tokamak experiments (H. R. Wilson, T.S. Hahm, and F. Zonca)

In this section, we consider how theory and simulation have influenced tokamak experiments. Over the years, there have been numerous examples, and it is not possible to review all of them in this section. Instead, we have identified a number of areas that raise key research issues for ITER: either for its performance, or for its structural integrity. Although the review is not exhaustive, it does provide an illustration of how the theoretical physics community helps to shape and guide the experimental programmes on the world's tokamaks. We have listed a number of important references. Again, it is not possible to include all references, but we have aimed to construct a representative list which will provide access to the wider literature in these areas.

Edge localised modes

Edge-Localised Modes, or ELMs, are instabilities associated with a transport barrier at the tokamak plasma edge [Zohm96, Connor98a, Suttrop00, Be-

coulet03, Huysmans05]. Each ELM results in an eruption of particles and energy from the plasma, which then flow along the scrape-off layer to the divertor target. Extrapolations using data from existing tokamaks give concern that the resulting heat loads on ITER could be intolerable, but the uncertainties are large. In an effort to reduce the uncertainty, significant theoretical effort has been devoted to improve our understanding of the processes which govern the ELM, and a lot of progress has been made over the past decade [Huysmans05, Wilson06].

It is now widely accepted that a particular type of plasma instability, the “peeling-ballooning” mode, is responsible for triggering the ELM [Connor98b, Snyder02]. This model predicts that as the edge current density and pressure gradient rise beyond critical values, the plasma becomes unstable, triggering an ELM event. The model has been tested on a large number of tokamaks around the world, comparing the predicted critical values with the experimental pressure gradient and current density at the edge just prior to an ELM [Snyder02, Saarelma05]. In general, the current density cannot yet be measured, but is instead calculated (for example using the theoretical prediction for the bootstrap current [Bickerton71]). An example of the good agreement is shown in Fig. II.1.1 for JET. Just before the ELM, the plasma is approaching the predicted stability boundary.

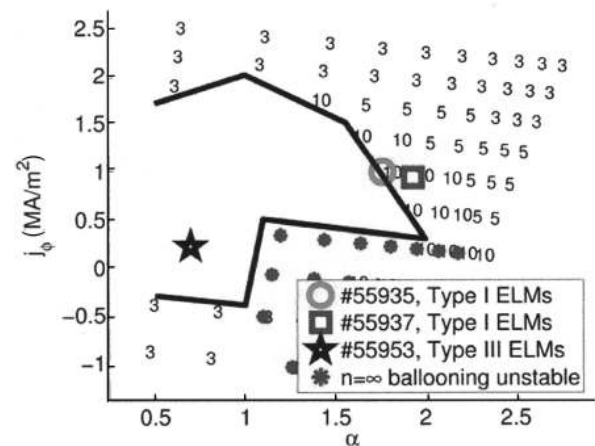


Fig. II.1.1 Edge stability diagram for a typical JET discharge. The figure shows that the two large Type I ELM discharges are close to the stability boundary, while the smaller type III ELM discharge is away from the stability boundary. The numbers correspond to the most unstable toroidal mode number; the full curve is the stability boundary. The axes are toroidal current density, j_ϕ , and normalised pressure gradient, α . [Saarelma05]

Motivated by the theory, the role of the edge current in triggering the ELM has been explored on both COMPASS-D [Fielding96] and TCV [Degeling03]. They confirmed that transiently suppressing (or enhancing) the edge current suppressed (or triggered) ELMs. Most recently, as a consequence of the growing realisation that the current density is an impor-

tant parameter, there has been much effort to design a diagnostic to actually measure this quantity in the plasma edge region. The team on DIII-D have led the way [Thomas04], successfully installing a diagnostic that exploits the Zeeman effect in lithium, and are beginning to make the first measurements. Initial results indicate that the theoretical predictions based on the bootstrap current are generally reasonably accurate (see Fig. II.1.2).

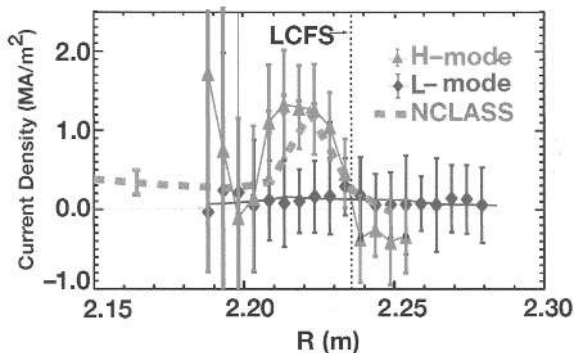


Fig.II.1.2 Measurements of edge current density using the LIBEAM diagnostic on DIII-D for H-mode (triangles) and L-mode (diamonds) discharges. The theoretical prediction for the bootstrap current is shown as the dashed curve (Figure from [Thomas04])

To begin to understand the range of energy loss from ELMs observed in experiments, theory and simulation have extended the studies to address non-linear effects. Analytic theory predicts the existence of filamentary structures that can be ejected into the scrape-off layer [Wilson04]. This result has been confirmed in large scale numerical calculations which employ more realistic plasma physics models and are not constrained by the orderings necessary to make analytic progress (eg, see [Snyder05]). This new picture of the ELM motivated experiments on MAST to search, and find, these filamentary structures [Kirk04], and also provided an interpretation of results from ASDEX-Upgrade [Eich03]. Evidence for filamentary structures has now been found on many tokamaks, world-wide. Although their precise role still remains to be clarified, the filaments appear to be ejected into the scrape-off layer on the outboard side, but remain attached to the core plasma on the high field side. This suggests that they could either act as a conduit allowing hot core plasma to escape along them into the scrape-off layer, or they could act to suppress the flow shear, causing a collapse of the transport barrier.

The existence of filaments has raised a new concern for ITER: if the filaments should strike the vessel wall, where there is limited protection, they could do serious damage. Experiments have confirmed that a significant fraction of the ELM energy can be deposited in localised regions on the vessel wall [Herrmann04], but the implications for ITER remain uncertain.

Filamentary structures are also predicted to arise from so-called “blob” theories [Yu06], which may be

of relevance in the later stages of the ELM.

Based to some extent on our theoretical knowledge of the ELM process, there have been a number of encouraging experiments recently that offer the prospect of ELM control on ITER. These include using coils to modify the magnetic field topology near the plasma edge [Evans04] and injection of pellets into the pedestal region [Lang04].

Neoclassical tearing modes

Neoclassical tearing modes (NTMs) are instabilities of the core plasma that modify the magnetic topology and thereby dramatically degrade the confinement [Hegna98, Sauter97, Wilson96a]. Indeed, they can lead to a loss of plasma control, and a subsequent disruption. The instabilities were first predicted by theory two decades ago [Qu85, Carrera86], but it was not until the mid 1990’s that they were finally observed on TFTR [Chang95], and they became a major concern for ITER. These and subsequent experiments on other tokamaks demonstrated the existence of a threshold: NTMs require a “seed” magnetic perturbation that exceeds a critical amplitude. The sawtooth instability associated with the plasma centre can provide a sufficiently large seed and trigger the NTM, provided the plasma collisionality is sufficiently low. Two theoretical models were proposed for the observed threshold: one based on the finite ratio of the cross-field to parallel transport processes [Fitzpatrick95], and one based on the polarization current [Wilson96b]. Neither of these processes are fully understood, but models based on them have been tested extensively in experiments. These experiments have not been able to differentiate between the models, and it is possible that both are playing a role. The polarization current model provides a firm prediction that the threshold will scale with the Larmor radius, normalized to the plasma radius, ρ^* . Careful experiments on ASDEX-Upgrade supported such a scaling [Gunter99], and when this was confirmed using a multi-machine data-base involving JET, ASDEX-Upgrade and DIII-D [laHaye00] (see Fig. II.1.3), concern grew that the threshold would be very low on

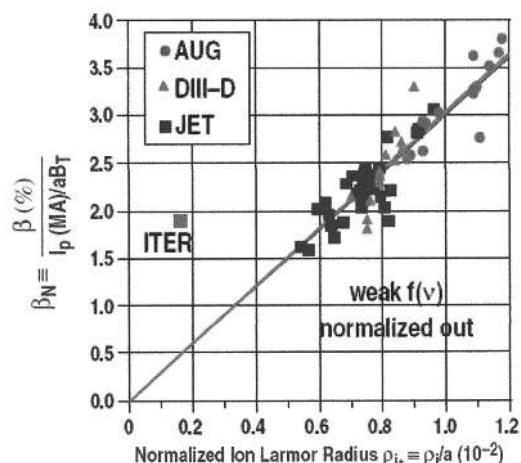


Fig.II.1.3 Threshold β for the onset of NTMs as a function of ρ^* (from Ref [laHaye00])

ITER (which has a low value of ρ_*). However, data from JET suggests that the scaling of threshold β with ρ_* may be a consequence of a co-linearity in the data set between these two parameters [Buttery04]. Here, β is the ratio of the thermal plasma energy, to the energy stored in the magnetic fields. Despite the success of the polarization current model, in particular the predicted scaling of the threshold with ρ_* , it is not universally accepted. Indeed, results of numerical modelling have provided an alternative explanation of the ρ_* scaling of the threshold [Poli02, Poli05]. This is an area that would benefit from an increased effort in large-scale numerical calculations to improve our understanding of the dominant threshold mechanisms.

Theory predicts that NTMs grow as a consequence of a “hole” in the bootstrap current. If this current is replaced using current drive techniques, then it is possible to reduce the size of the NTM below the threshold so that it is again stabilised [Hegna97, Zohm97]. Subsequent experiments on ASDEX-Upgrade [Gantenbein00], DIII-D [laHaye02] and JT-60U [Isayama03] confirmed the success of this technique, which will be employed on ITER. While there is a small residual concern that multiple NTMs could appear in principle on ITER, in which case it would be difficult to control all of them, it is widely believed that NTMs are no longer the major concern for ITER they once were. Nevertheless, they rightly remain an important area of tokamak research.

Resistive wall modes

One goal of tokamak research is to maximize β . Recall that β is the ratio of the thermal plasma energy to the energy stored in the magnetic fields. The former is a measure of the fusion performance, while the latter is a measure of the cost; β is therefore an indicator of the efficiency of a fusion power plant. In addition, the bootstrap current, essential if we wish to operate the tokamak in steady state (rather than as a pulsed device), increases with β . Theory predicts that the maximum value of β is typically limited by a violent type of plasma instability known as the kink mode. By placing an infinitely conducting wall sufficiently close to the plasma surface this β -limit can be significantly increased. Of course, real materials are not infinitely conducting. The consequence is that the plasma is not completely stabilized, and a new type of instability called the resistive wall mode RWM grows at a rate that depends on the wall resistivity. Although the RWM grows more slowly than the kink mode that the wall suppresses, it still eventually leads to a disruption, and discharge termination.

Codes based on the ideal magneto-hydrodynamics model of the plasma have predicted the no-wall and infinitely conducting wall β -limits for many years with some accuracy, confirmed by numerous experiments on tokamaks. However, it is only relatively recently that we are starting to understand the full physics of the resistive wall mode. For example, theory predicts that sufficient plasma rotation can stabilize the RWM, al-

lowing higher values of β to be achieved [Bondesson94, Fitzpatrick96, Betti95, Finn95, Chu04]. Experiments, notably on DIII-D confirm that provided rotation can be maintained, the RWM is indeed stabilized and values of β well above the no-wall limit can be reached [Strait03]. However, these experiments show that it is difficult to maintain the rotation: the mode itself tries to slow the plasma down and, once the plasma has slowed sufficiently, the RWM grows, eventually leading to a disruption. There is recent evidence to suggest that, in fact, relatively little rotation is required to stabilize the RWM [Garofalo06, Takechi06]. Nevertheless, on ITER, where there is little momentum injection, it is prudent to develop alternative ways to control the instability.

Theory provides another idea for RWM stabilization that can be used together with plasma rotation: to use a system of current-carrying coils [Bishop89, Jensen97]. Codes have been developed to calculate the optimum coil designs for existing tokamaks, as well as ITER [Liu00, Bialek01, Chu04]. A set of such coils (so-called I-coils) have recently been installed inside the vacuum vessel of DIII-D, designed on the basis of our theoretical understanding of the properties of the RWM. Initial experiments with these coils have demonstrated that β can be increased to a value significantly above the no-wall limit, even with very little flow in the plasma [Okabayashi05]. This is well into the regime where RWMs would be expected to terminate the discharge (without the coils). Although we still do not have a complete understanding of the RWM, this combination of theory and experiment provides confidence that similar high β discharges can be achieved on ITER.

Mean $\mathbf{E} \times \mathbf{B}$ shear flow and turbulence-driven zonal flows:

Although a complete theoretical picture remains elusive, flows are thought to play a key role in the generation of improved confinement regimes, such as the H-mode. Extensive experimental investigation in the 90's of the physics of transport barrier formation produced significant insight into turbulence suppression by the mean sheared $\mathbf{E} \times \mathbf{B}$ flow, as reviewed almost a decade ago [Burrell97, Synakowski97]. The theory of how the $\mathbf{E} \times \mathbf{B}$ flow leads to nonlinear decorrelation was first developed in a simple geometry [Biglari90], and then extended to general toroidal geometry [Hahm95]. These theories, combined with nonlinear gyrofluid simulations [Waltz94], have led to an approximate criterion for ion thermal transport barrier formation: namely that the ratio of the $\mathbf{E} \times \mathbf{B}$ shearing rate [Hahm95] to the maximum linear growth rate of micro-instabilities should exceed a critical value. While this is an over-simplified “rule of thumb”, rather than a final statement of the $\mathbf{E} \times \mathbf{B}$ shear suppression, it has proved useful for the experimental community as an approximate measure to assess the role of $\mathbf{E} \times \mathbf{B}$ shear in transport barrier formation. Now there is a significant effort toward self-consistent, nonlinear dynamic simulations of transport barrier formation.

While the physics of the mean $E \times B$ flow is relatively well-established [Terry00], the study of turbulence driven zonal flows is an active area of current research in both the theory and experimental communities. Zonal flows are $E \times B$ flows associated with azimuthally ($n = 0$) and poloidally ($m = 0$) symmetric, but radially varying electric potential fluctuations. Therefore, zonal flows are not directly responsible for radial transport and, unlike various instabilities in confined plasmas, cannot grow at the expense of the expansion free energy associated with the radial gradient of either temperature or density. Thus, zonal flows are linearly stable, and can only grow at the expense of fluctuation energy through a nonlinear interaction. Zonal flows coexist with, and are excited by, ambient turbulence developed from a variety of collective instabilities; they regulate transport by shearing the ambient turbulence. Unlike the mean $E \times B$ flow which can be driven externally (for instance, by neutral beam injection) and can exist in the absence of turbulence, zonal flows are spontaneously generated by turbulence [Diamond05].

Zonal flows are of practical importance since they reduce transport, and shift the effective threshold condition for the onset of significant transport. In the magnetic fusion community, the possible importance of self-generated zonal flows in regulating turbulence and transport was first recognized in fluid simulations of drift wave turbulence [Hasegawa87]. In recent years, with emerging nonlinear gyrokinetic simulations [Lin98] with more realistic kinetic dynamics and a proper treatment of the undamped zonal flow component in collisionless toroidal geometry [Rosenbluth98], it is now widely recognized that understanding zonal flow dynamics is essential for predicting confinement in future devices [Dimits00].

Advances in theory and simulation of zonal flows have influenced the experimental community as described in a recent review [Diamond05]. In particular, characterization of the experimentally measurable features of zonal flow properties from nonlinear gyrokinetic simulations [Hahm00] has motivated experimental measurements. In toroidal plasmas, GAMs (geodesic acoustic modes) consisting of the ($n = 0, m = 1$) up-down asymmetric side band pressure perturbation linearly coupled to the ($n = 0, m = 0$) electric field potential perturbation via geodesic curvature [Winsor68], can also be nonlinearly excited, in addition to the low frequency (near zero) zonal flow [See Fig. II.1.4]. The low frequency component of zonal flows is believed to be more important in regulating core turbulence [Hahm99]. In various tokamak experiments around the world, fluctuations which look like GAMs (Geodesic Acoustic Modes) have been detected using BES [McKee03], reflectometry [Conway05], Langmuir probes [Xu04], and HIBP [Ido06, Melnikov05, Schoch03] at the edge, partly due to their well defined non-zero frequency. More recent measurements further into the tokamak core, with an enhanced signal-to-noise ratio, have begun to identify a low frequency feature as well,

which looks like the zonal flow [Gupta06]. Stronger evidence of the existence of low frequency zonal flows has come from HIBP measurements on stellarators [see Fig. II.1.4]. There are many such on-going projects in the world that are aiming to provide a more definite experimental verification of zonal flows and their importance for confinement [Itoh05].

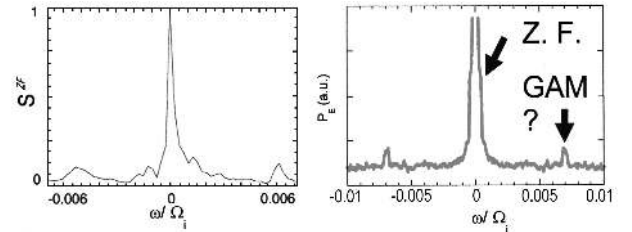


Fig.II.1.4 On the left, frequency spectrum of zonal flow intensity from the GTC gyrokinetic simulation of tokamak core (ITG) turbulence exhibits two distinct features, one at near zero frequency, and another at GAM frequency [Hahm 2000]. On the right, from Heavy Ion Beam Probe (HIBP) measurements of CHS stellarator plasmas, power spectrum of electrostatic potential difference at two toroidal locations separated by 90 degrees is plotted.

There remain a number of outstanding issues in zonal flow physics which need to be addressed in the near future [Itoh06]. For example, a more direct link between the zonal flow amplitude and enhancement of confinement needs to be demonstrated. There have been some systematic, but limited, scans on the collisional damping of zonal flows [Lin99], and the q -dependence of zonal flow properties [Miyato04, Angelino05] and their effect on confinement. However, in most cases the effects of zonal flows have been exhibited in case by case simulations [Beer96, Dimits00, Lin98, Waltz94] or in the context of simple nonlinear models [Diamond98, Chen00]. Another issue that limits our predictive capability is the need to improve our understanding of key elements of the theory, such as how zonal flows saturate in collisionless plasmas. By addressing these outstanding issues, we may be able to identify practical ways to generate zonal flows, and so influence the confinement in reactor relevant future devices such as ITER.

Fast particle instabilities

Fusion-relevant tokamak plasmas have an energetic particle population, either as a consequence of the plasma heating schemes or, as with ITER, the products of the fusion reactions. In both cases, it is essential that the energetic particles are retained in the plasma until they give up their energy to heat the fuel. A concern is that there is a class of plasma instabilities that arises as a consequence of these energetic particles, and these instabilities could lead to their premature ejection [Pinches04]. There are numerous examples (covered in detail in Section III.8), but the best-known is probably the Toroidal Alfvén Eigenmode (TAE mode). First predicted theoretically [Cheng 85], the existence of the TAE mode was confirmed later on several tokamaks

around the world. However, there remains an element of uncertainty in the predictions for whether or not this mode will be unstable in ITER. Linear theory predicts that the mode will be unstable when the drive due to the fast particle population exceeds the damping arising from the thermal plasma. Calculations of the damping are extremely difficult, involving complicated plasma physics processes, and so there is considerable variation in the predictions for ITER, with a corresponding uncertainty. In an attempt to eliminate damping models, and so improve the predictions for ITER, measurements of the damping rate have been made by externally driving an Alfvén wave in a plasma that is stable to the TAE mode, and then measuring how rapidly its amplitude decays (see, for example, [Fasoli 95]).

To understand how this class of instabilities influences the fast particle confinement, it is necessary to address, and test, the non-linear theory. There are numerous aspects of this (e.g. see [Fasoli 95]), but we shall focus on just one example here. Theory predicts that close to the threshold for instability, the non-linear evolution depends on the competition between the drive (a measure of the wave-particle interaction) and the collisions (a measure of the restoring effect on the particle distribution function). For sufficiently low drive, a saturated solution is predicted, but this becomes unstable for larger drives, and limit cycles are predicted [Berk97]. This leads to a splitting of the spectral lines for TAE modes, which were subsequently observed on JET [Fasoli98]. This provides important experimental support for the theory, which is now being taken forward through numerical simulations to improve the understanding in the strongly non-linear regime [Vann05].

Summary

Theory and simulation have provided additional guidance and focus to tokamak experiments in many areas of crucial importance for ITER. We have only been able to give a few examples in this section, which provides a flavor of the important role that theory and simulation play in the international fusion energy research community.

References

[Angelino05] P. Angelino, et al. 2006, Plasma Phys. Control. Fusion, 48: 557
 [Becoulet03] M. Becoulet, et al. 2003, Plasma Phys. Contr. Fusion, 45: A93
 [Beer96] M. A. Beer, G. W. Hammett. 1996, Phys. Plasmas, 3: 4046
 [Berk97] H. L. Berk, B. N. Breizman, M. S. Pekker. 1997, Plasma Phys. Rep., 23: 778
 [Betti95] R. Betti, J. P. Freidberg, 1995, Phys. Rev. Lett., 74: 2949
 [Bialek01] J. Bialek, et al. 2001, Phys Plasmas, 8: 2170
 [Bickerton71] R. J. Bickerton, J. W. Connor, J. B. Taylor. 1971, Nature, 229: 110

[Biglari90] H. Biglari, P. H. Diamond, P. W. Terry. 1990, Phys. Fluids B, 2: 1
 [Bishop89] C. M. Bishop. 1989, Plasma Phys Contr Fusion, 31: 1179
 [Bondeson94] A. Bondeson, D. J. Ward. 1994, Phys. Rev. Lett., 72: 2709
 [Burrell97] K. H. Burrell. 1997, Phys. Plasmas, 4: 1499
 [Buttery04] R. J. Buttery, et al. 2004, Nucl. Fusion, 44: 678
 [Carrera86] R. Carrera, R. D. Hazeltine, M. Kotschenreuther. 1986, Phys Fluids, 29: 899
 [Chang95] Z. Chang, et al. 1995, Phys Rev Lett. 74: 4663
 [Chen00] L. Chen, Z. Lin, R. B. White. 2000, Phys. Plasmas, 7: 3129
 [Cheng85] C. Z. Cheng, L. Chen, M. S. Chance. 1985, Ann Phys (N.Y.), 21: 161
 [Chu04] M. S. Chu, et al. 2004, Phys Plasmas, 11: 2497
 [Connor98a] J. W. Connor. 1998, Plasma Phys Contr Fusion, 40: 531
 [Connor98b] J. W. Connor, et al. 1998, Phys Plasmas, 5: 2687
 [Conway05] G. D. Conway, et al. 2005, Plasma Phys. Control. Fusion, 47: 1165
 [Degeling03] A. W. Degeling, et al. 2003, Plasma Phys Contr Fusion, 45: 1637
 [Diamond98] P. H. Diamond, et al. 1998, Dynamics of zonal flows and self-regulating drift wave turbulence, in Plasma Phys. and Controlled Nuclear Fusion Research (IAEA, Vienna, 1998) IAEA-CN-69/TH3/1.
 [Diamond05] P. H. Diamond, et al. 2005, Phys. Plasmas. Control. Fusion, 47: R35
 [Dimits00] A. Dimits, et al. 2000, Phys. Plasmas, 7: 969
 [Eich03] T. Eich, et al. 2003, Phys. Rev. Lett., 91: 195003
 [Evans04] T. E. Evans, R. A. Moyer, et al. 2004 Phys. Rev. Lett., 92: 235003
 [Fasoli95] A. Fasoli, et al. 1995, Phys. Rev. Letts., 75: 645
 [Fasoli98] A. Fasoli, et al. 1998, Phys. Rev. Letts., 81: 5564
 [Fielding96] S. J. Fielding, et al. 1996, Plasma Phys. Contr. Fusion, 38: 1091
 [Finn95] John M. Finn. 1995, Phys. Plasmas, 2: 198
 [Fitzpatrick95] R. Fitzpatrick. 1995, Phys. Plasmas, 2: 825
 [Fitzpatrick96] R. Fitzpatrick, A. Y. Aydemir. 1996, Nucl Fusion, 36: 11
 [Gantenbein00] G. Gantenbein, et al. 2000, Phys. Rev. Lett., 85: 1242
 [Garafalo06] A. M. Garafalo, et al. Active Control of Resistive Wall Modes in High Beta, Low Rotation DIII-D Plasmas, 21st IAEA Fusion Energy Conf. (Chengdu, China, 2004) Ex/7-1Ra (Vienna, IAEA)
 [Gunter99] S. Günter, et al. Plasma Phys Contr Fusion, 41: B231
 [Gupta06] D. K. Gupta, et al. 2006, Detection of Rosenbluth-Hinton Flows in the core of a High-Temperature Tokamak Plasma. Phys. Rev. Lett., Submitted
 [Hahm95] T. S. Hahm, K. H. Burrell. 1995, Phys. Plasmas, 2: 1648
 [Hahm99] T. S. Hahm, et al. 1999, Phys. Plasmas, 6: 922
 [Hahm00] T. S. Hahm, et al. 2000, Plasma Phys. Contr.

- Fusion, 42: A205
 [Hegna97] C. C. Hegna, J.D. Callen. 1997, Phys. Plasmas, 4: 2940
 [Hegna98] C. C. Hegna. 1998, Phys. Plasmas, 5: 1767
 [Herrmann04] A. Herrmann, et al. 2004, Plasma Phys. Contr. Fusion, 46: 971
 [Hasegawa87] A. Hasegawa, M. Wakatani. 1987, Phys. Rev. Lett., 59: 1581
 [Huymans05] G. T. A. Huymans, et al. 2005, Plasma Phys Contr Fusion, 47: B165
 [Ido06] T. Ido, et al. 2006, Plasma Phys. Contr Fusion, 48: S41
 [Isayama03] A. Isayama, et al. 2003, Nucl. Fusion, 43: 1272
 [Itoh05] S.-I. Itoh. 2005, Plasma Phys. Contr. Fusion, 48: S, Editorial
 [Itoh06] K. Itoh. et al. 2006, Phys. Plasmas 13: 055502
 [Jensen97] T. H. Jensen, R. Fitzpatrick. 1997, Phys. Plasmas 4: 2997
 [Kirk04] A. Kirk, et al. 2004, Phys. Rev. Lett., 92: 245002
 [laHaye00] R. J. la Haye, et al. 2000, Phys. Plasmas, 7: 3349
 [laHaye02] R. J. la Haye, et al. 2002, Phys. Plasmas, 9: 2051
 [Lang04] P.T. Lang, et al. 2004 Nucl. Fusion, 44: 665
 [Lin98] Z. Lin, et al. 1998, Science, 281: 1835
 [Lin99] Z. Lin, et al. 1999, Phys. Rev. Lett., 83: 3645
 [Liu00] Y. Q. Liu, et al. 2000, Phys. Plasmas, 7: 3681
 [Melnikov05] A. V. Melnikov, et al. 2005, Czech. J. Phys., 55: 349
 [McKee03] G. R. McKee, et al. 2003, Phys. Plasmas, 10: 1712
 [Miyato04] N. Miyato, Y. Kishimoto. 2004, Phys. Plasmas, 11: 5557
 [Okabayashi05] M. Okabayashi, et al. 2005, Nucl. Fusion, 45: 1715
 [Pinches04] S. D. Pinches, et al. 2004, Plasma Phys. Contr. Fusion, 46: B187
 [Poli02] E. Poli, et al. 2002, Phys. Rev. Lett., 88: 075001
 [Poli05] E. Poli, A. Bergmann, A. G. Peeters. 2005, Phys. Rev. Lett., 95: 205001
 [Qu85] W. X. Qu, J. D. Callen 1985, University of Wisconsin Report, number UWPR 85-5. Copies may be ordered from the National Technical Information Service, Springfield, VA 22161
 [Rosenbluth98] M. N. Rosenbluth, F. L. Hinton. 1998, Phys. Rev. Lett., 80: 724
 [Saarelma05] S. Saarelma, et al. 2005, Plasma Phys Contr Fusion, 47: 713
 [Sauter97] S. Sauter, et al. 1997, Phys. Plasmas, 4: 1654
 [Schoch03] P. M. Schoch et al. 2003, Rev. Sci. Instrum., 74: 1846
 [Snyder02] P. B. Snyder, et al. 2002, Phys. Plasmas, 9: 2037
 [Snyder05] P. B. Snyder, H. R. Wilson, X. Q. Xu. 2005, Phys Plasmas, 12: 056115
 [Strait03] E. J. Strait, et al. 2003, Nucl Fusion, 43: 430
 [Suttrop00] W. Suttrop, et al. 2000, Plasma Phys. Contr. Fusion, 42: A1
 [Synakowski97] E. J. Synakowski, et al. 1997, Phys. Plasmas, 4: 1736
 [Tekechi06] M. Tekechi, et al. Plasma Rotation and Wall effects on Resistive Wall Mode in JT-60U, 21st IAEA Fusion Energy Conf. (Chengdu, China, 2004) Ex/7-1Rb (Vienna, IAEA)
 [Terry00] P. W. Terry. 2000, Rev. Mod. Phys., 72: 109
 [Thomas04] D. Thomas, et al. 2004, Phys. Rev. Lett., 93: 065003
 [Vann05] R. G. L. Vann, R. O. Dendy, M. P. Gryaznevich. 2005, Phys Plasmas, 12: 032501
 [Waltz94] R. Waltz, G. Kerbel, J. Milovich. 1994, Phys. Plasmas, 1: 2229
 [Wilson96a] H. R. Wilson, et al. 1996, Plasma Phys. Contr. Fusion, 38: A149
 [Wilson96b] H. R. Wilson, et al. 1996, Phys Plasmas, 3: 248
 [Wilson04] H. R. Wilson, S. C. Cowley. 2004, Phys. Rev. Lett., 92: 175006-1
 [Wilson06] H. R. Wilson, et al. 2006, Plasma Phys Contr Fusion, 48: A71
 [Winsor68] N. Windsor, J. L. Johnson, J. M. Dawson. 1968, Phys. Fluids, 11: 2448
 [Xu04] G. S. Xu, et al. 2004, 20th IAEA Fusion Energy Conf. (Vilamoura, Portugal, 2004) Ex/8-4Rb, IAEA -CSP-5/CD (Vienna, IAEA)
 [Yu06] G. Q. Yu, S. I. Krasheninnikov, P. N. Guzdar. 2006, Phys Plasmas, 13: 042508 (and references therein)
 [Zohm96] H. Zohm, et al. 1996, Plasma Phys Contr Fusion, 38: 105
 [Zohm97] H. Zohm. 1997, Phys Plasmas, 4: 3433

II.2 Tokamak transport physics for ITER: issues for simulation (P.H. Diamond and T.S. Hahm)

In this section we discuss scientific issues in tokamak transport physics which are important to ITER and which are amenable to study using numerical simulation. We emphasize important questions which are open or otherwise unsolved, and do not dwell on the past glory of solved problems. This note is necessarily brief, and thus should not in any sense, be regarded as a ‘review’. Rather, it should be thought of as an essay, and one which certainly reflects the opinions and biases of its authors.

The topics in the theory of transport of greatest relevance to ITER include:

- i.) breakdown of gyroBohm scaling: underlying physical processes
- ii.) electron thermal transport - a persistent dilemma...
- iii.) L-H transition and hysteresis - how big is the margin?
- iv.) ‘spontaneous’ toroidal rotation and momentum transport
- v.) particle transport and the physics of inward flows

We briefly discuss each of these problems below, and indicate critical questions which simulation could

help answer. We focus the discussion on ITER-relevant regimes, i.e. plasmas which are large, high field (small ρ_*), long pulse, have $T_e : T_i$ and $n : n_G$, the Greenwald density limit.

II.2.1 GyroBohm breakdown: physics and relevance

ITER is a huge step forward in plasma size, and will operate at relatively high field. It is thus no surprise that ρ_* scaling and the departures from the “conventional wisdom” of gyroBohm scaling in drift-ITG turbulence remain grave concerns. Scaling experiments indicate that $D : D_{GB}$, the GyroBohm diffusivity, but with small but important mismatches, which indicate GB GyroBohm scaling is broken, albeit weakly. The physics behind this is some type of dynamical non-locality mechanism due to cooperative, scale-independent interaction of localized modes, which produces a spectrum of dynamic large scale structures [Diamond and Hahm 1995]. The physics of such processes brings us in contact with ideas at the forefront of nonlinear statistical physics, such as dynamical critical phenomena, self-organized criticality [Bak, Tang and Wisenfeld 1987], statistical turbulence theory, fractional kinetics [Zaslavsky 2005], etc. Mechanisms for the breaking of gyroBohm scaling have been proposed, but each address only some aspects of the phenomenology. Specific candidate mechanisms include avalanches (ala self organized criticality [Newman et al. 1996, Carreras et al. 1996]) and turbulence propagation and spreading [Hahm et al. 2004, Gurcan, Diamond and Hahm 2006]. Avalanches are scale independent, bursty transport events resulting from sequential over-turnings of local mixing cells. Turbulence spreading results from the entrainment of neighboring regions (including stable regions) by turbulence activity localized elsewhere. It is fair to say that avalanches and turbulence spreading are ‘different sides of the same coin’, as one refers to nonlocality manifested in transport, while the other refers to nonlocality manifested in the fluctuation intensity profile. Both phenomena are observed in simulations, both are sensitive to shearing effects (by mean and zonal flows) and both break GB scaling. Other, more mundane, possibilities include the trapped ion mode [Kadomtsev and Pogutse 1970], a nearly-forgotten instability mechanism which is particularly relevant to collisionless plasmas, such as ITER.

Understanding the physics of GB breaking via dynamic nonlocality is a first rate challenge for simulation. Codes must be global, allow realistic profile evolution (i.e. fixed-flux boundary conditions), and incorporate sophisticated diagnostic and analysis packages adequate for the difficult numerical experiments (i.e. perturbative studies of transport and fluctuations) which are needed. Efficiency is required to implement the scaling studies of global simulations, which are necessary for progress. Close coupling to a vigorous theory program in parallel is a must! The rewards, both in terms

of scientific recognition for MFE physics and for ITER are great, and more than justify the effort.

ρ_* scaling is not the only issue which the adherents to the $D : D_{GB}$ dogma of simple drift-ITG wave turbulence must address. Many questions remain, including the origin of current scaling and isotope scaling, and their compatibility with drift wave theory. Recent theory and simulation studies suggest that current dependence may be lurking in the zonal flow dielectric response [Angelino et al. 2006]. The isotope scaling question remains one which is both open and important, since TFTR D-T experiments indicated a tantalizingly favorable trend in the confinement scaling with isotope mass. A robust, validated explanation of this would be good news, indeed, for ITER. Simulations have much to contribute here, too. Our understanding of zonal flow physics is a relatively recent success story for theory and simulation [Diamond et al. 2005]. The question of zonal flow impact on current scaling is already being addressed by present day gyrokinetic codes, as the somewhat related question of the parameter scaling of zonal flow shears. Aspects of the isotope scaling problem are within reach, though a definitive study will require an effort which exploits the coupling of edge and core simulations. There are important questions concerning beta scaling of confinement, as well.

II.2.2 Electron thermal transport - a persistent dilemma

Electron thermal transport is often referred to as the “great unsolved problem of tokamak transport physics”. However, there is considerable confusion as to what, precisely, the problem is! Drift-ITG (ion temperature gradient) turbulence can account for electron transport in L-mode. The difficulty becomes clearer upon consideration of ITB (internal transport barrier) discharges. In particular, studies over a period of nearly 20 years, which span the Alcator-C pellet experiments (1984-an ITB before the jargon ‘ITB’ was invented), the TFTR ERS discharges (1996), and the ρ_* scan studies on DIII-D (2002), all indicate that the ion thermal diffusivity χ_i and particle diffusivity D_n are both quenched or reduced by electric field shear, while the anomalous electron thermal diffusion often persists. This has led to a search for a ‘second transport mechanism’, which operates at small scales and so is not as susceptible to shearing. However, the issue is much more subtle, since electron barriers do exist, and because virtually any fundamentally electrostatic drift wave or trapped electron mode mechanism strongly couples the electron thermal diffusivity χ_e and the particle diffusion D_n . Thus, any model of this genre must successfully explain the apparent decoupling of χ_e and D_n , as well as the persistence of χ_e .

There are three classes of candidate models, namely electron temperature gradient (ETG) turbulence [Lee et al. 1987], collisionless trapped electron mode (CTEM) turbulence [Adam et al. 1976] and collision-

less skin depth c/ω_{pe} models [Horton et al. 1988]. The proponents of each have yet to address the critical weaknesses of their respective candidates. ETG turbulence, though interesting, is limited, at the level of dimensional analysis, by electron gyro-Bohm diffusion ($\chi = \chi_{GBE} : \rho_e \nu_{TE}/L$, where ν_{TE} is the electron thermal velocity), which is feeble. Attempts to link enhancement beyond χ_{GBE} to extended streamer structures, which have been observed in the turbulent flows of some simulations, have been highly controversial, both pro and con. Recent studies of the full dynamic range of ITG and ETG turbulence (albeit at unrealistic mass ratio) indicate that the contributions to transport from small scales ($\Delta r < \rho_i$) are weak [Candy 2006]. The role and significance of ETG-driven zonal flows are unclear, as well [Gurcan and Diamond 2004]. All this motivates the proponents of the second major candidate, the CTEM. The CTEM is basically an electron drift wave, driven by inverse dissipation due to electron drift resonances. The CTEM is active in a band of scales around $\kappa_{\perp} \rho_i : 1$, and so is thought to be less susceptible to shearing effects than longer wavelength ITG modes are. However, simulations of CTEM turbulence in regimes of strong electric field shear have not been implemented and comparative studies of thermal and particle fluxes in the simulations are not available. Thus, the burden of proof remains on the CTEM enthusiasts, who must demonstrate that their candidate can reconcile gyroBohm χ_e with strongly reduced D_n . A fluctuation-driven inward particle pinch (see below-Section II.2.5) could provide the answer [Diamond 2006]. Finally, the third class of models, which are intellectual descendants of the ideas of Kadomtsev and Okhawa, attribute the electron transport scalings to some bottleneck of energy transfer at the electromagnetic screening length c/ω_{pe} (i.e. the collisionless skin depth). These models are not firmly based on dynamics, and so do not address questions pertaining to the excitation of the fluctuations or the actual intensity at the c/ω_{pe} scale.

Electron transport is a challenge, but also a golden opportunity for simulation! Long time simulations with broad dynamic range are necessary to address questions of the importance of zonal flows to ETG dynamics and the effects of ITG-ETG coupling, respectively. Well-diagnosed CTEM simulations could address questions of the direction of spectral energy transfer and related particle pinch effects. No reliable simulation has studied the heat transport due to electromagnetic turbulence, which surely is important at higher β . In particular, resolution of the apparent disagreement between predictions of weak electromagnetic transport on account of the E_{\parallel} constraint (as in quasilinear theory), and predictions of strong electromagnetic transport due to magnetic stochasticity (as in the Rosenbluth and Rechester models [Rechester and Rosenbluth 1978]) would be a scientific coup for the MFE simulation community, and one which could also have impact in the astrophysics community, especially for the problem of cooling flows [Narayan and Medvedev 2001].

II.2.3 L-H transition and hysteresis - how big is the margin?

The story of the L-H transition and associated phenomena is a mixed one of successes and failures. On one hand, the notion of transport bifurcation and $\underline{E} \times \underline{B}$ shear suppression [Biglari, Diamond and Terry 1990, Hahm and Burrell 1995; Diamond et al. 1994, Hinton 1991, Lebedev and Diamond 1997] is physically sound and qualitatively explains nearly all of the phenomenology. On the other, quantitative understanding of the pedestal width and the threshold remains elusive. The difficulty here is due to the strong nonlinearity and inhomogeneity of the problem, the proximity in size of the scales ρ_i , ρ_{θ} , λ_N (neutral penetration depth) and the simultaneous action of sources of heat (from the core) and particle (from the edge). To solve the problem, one must describe the dynamics of an interface between a turbulent core (with $D : D_{GB}$) and a quiescent or nearly quiescent edge layer, where neoclassical transport dominates and where penetration by neutrals can be strong. It then seems obvious (though the point is lost on most), that an approach aiming to identify a single ‘‘characteristic scale’’ is doomed to failure. Rather, the problem appears to be one of coupled bifurcation front dynamics, where each transport channel has its own associated transport bifurcation [Malkov and Diamond 2006]. This is a challenging problem for theory, simulation and experiment. Empiricism (i.e. experimental scaling studies) has not succeeded, and simulations have not yet been able to contribute to our understanding. This is unfortunate, since the issue is absolutely critical to ITER because:

- a.) the pedestal height (and thus the width) sets the boundary condition for core confinement,
- b.) ITER plasmas will have much higher neutral opacity than present day plasmas do, so their pedestal structure may be quite different from present experiments, where the pedestal width seems to correlate with λ_N [Groebner et al. 2002],
- c.) the margin in power for achieving the L-H transition in ITER is tight. In ITER EDA, hysteresis was invoked as a ‘safety-valve’, with the idea the transition could be induced at low parameter values, and then hysteresis (generic to bifurcations in multi-stable systems) would maintain the H-mode during a parameter ramp up. However, hysteresis itself is poorly understood, and quite likely weaker than is commonly thought. More generally, development of a predictive, accurate model of the L-H transition power threshold is a high priority task for ITER physics studies.
- d.) the transition dynamics are intimately tied to ELM phenomena. Surely not all ELMs are due to ideal MHD instability (ala’ peeling-ballooning), and some are qualitatively well described by models which interpret them as limit cycle phenomena which appear above the bifurcation threshold [Gruzinov, Diamond and Rosenbluth 2002, Gruzinov and Diamond 2003, Beyer et al. 2005]. Indeed, it is difficult to imagine a more impor-

tant problem!

For the L-H transition, a two-pronged approach to simulations seems best. The program should focus on detailed studies of simple models and their foundations in the near term, and then switch to full simulations in the long term. It will be some time before such full simulations are possible. Once again, studies of simple simulation models should be closely coupled to analytic theory and to experiments. Critical questions include barrier initiation and hysteresis (i.e. thresholds for transition and back transition, both in heating and fueling), propagation and saturation (pedestal width), noise effects, coupling to zonal flows (dithering!?! [Kim and Diamond 2003]), and many others. It is particularly important to test the models which relate barrier propagation to Maxwell construction ideas [Lebedev and Diamond 1997, Yoshizawa, Itoh and Itoh 2003, Diamond et al. 1997], since these suggestions are the only plausible theoretical ideas now available.

II.2.4 ‘Spontaneous’ toroidal rotation and momentum transport

In contrast to most present day tokamaks, ITER will not be heated primarily by neutral beam injection. Nevertheless, toroidal rotation in ITER is desirable as a means to stabilize resistive wall modes, etc. Beams to drive the rotation in ITER are expensive. With this in mind, then, the MFE physics community has recently taken increasing note of observations of ‘spontaneous’ toroidal rotation, such as those in Alcator C-Mod [Rice et al. 2002], and previously in JFT II-M [Ida et al. 2001]. Here ‘spontaneous’ refers to rotation in the absence of external toroidal momentum input (C-Mod) or rotation profiles which are dramatically different from those expected on the basis of the popularly held idea that momentum flux is purely diffusive and that $\chi_\phi \cong \chi_i$, where χ_ϕ is the turbulent momentum diffusivity [Mattor and Diamond 1988, Scott et al. 1990]. Several authors have proposed the speculation that the total radial momentum flux or Reynolds stress $\langle \tilde{V}_r \tilde{V}_\phi \rangle$ has an additional, non-diffusive contribution, which is similar to, but not the same as, a ‘pinch’ of momentum [Diamond et al. 1996, Coppi 2002]. The energy source for this contribution to the momentum flux is the same as that which drives the turbulence. Only a few investigators have confronted the crux of the issue, namely that this effect requires some breaking of the traditionally assumed symmetry of the eigenfunctions. Such symmetry breaking is surely due to electric field shear, which is well known to shift eigenfunctions relative to their associated resonant surfaces. Note that this dependency determines the all-important net sign of the effect. This in turn suggests a feedback loop linking fluctuation intensity (driven by ∇P and regulated by electric field shear V_E') to shear in toroidal rotation (which contributes to V_E'), and electric field shear (determined by ∇P , ∇n and $\nabla \nu_\phi$). Such a loop has the necessary ingredients to explain the rotation anomaly,

its apparent dependence on plasma current and its relation to enhanced confinement. Great care must be taken prior to declaration of victory, however, since:

a.) the net sign of the effect is probably mode dependent (i.e. different for ITG and CTEM)

b.) the non-diffusive contribution maybe weak ($\langle \tau_c \tilde{\nu}_r \nabla_{||} \tilde{p} \rangle$)

c.) the effect is strongly self-limiting, in addition to weak; this is because increased shear (V_E') increases the required asymmetry, but then weakens the turbulence.

The toroidal rotation problem is a splendid opportunity for gyrokinetic simulation to make an impact on ITER now! It seems straightforward to add toroidal rotation and mean electric fields to existing codes, and do the necessary flux measurements and parameter scans. A time-dependent ‘seed momentum’ could be added, thus enabling transient experiments similar to those (i.e. transient gas puffing) which elucidated the inward particle pinch. The results might impact on, or link to, ITB studies, as well. Do not miss this opportunity!

There are other problems in momentum transport which are worthy of study. The questions of momentum transport at the edge (i.e. likely the ultimate momentum source, for C-Mod), the physics of mean poloidal momentum transport, and the relation between zonal flows and toroidal momentum are all interesting. In burning plasma, the alpha particle population will radically alter how ambipolarity is maintained, and thus the flows. Toroidal Alfvén eigenmodes can drive localized flow shear, thus coupling energetic particle modes to bulk confinement. An alpha particle population will also modify the neoclassical dielectric and thus the zonal flow response. These possibilities open the door to possible control of bulk confinement using energetic particles.

II.2.5 Particle transport and the physics of inward flows

We have, as a community, long appreciated the connection between density profile peaking and enhanced confinement. What we do not understand is the detailed physics of density profile structure. In particular, the quasi-stationary profiles achieved in experiments require some inward, non-diffusive element of the particle flux to maintain them. This missing element is called the inward particle pinch [Strachan et al. 1982]. Understanding the inward pinch is especially relevant to ITER, on account of its size, and also the issue of helium ash removal. There are two lines of thought regarding the inward pinch. The first, and traditional view is the generalized “mixing mode” idea [Coppi and Spight 1978], in which relaxation (i.e. ∇T_i , via ITG) in one channel drives a flow in another by off-diagonal terms (say, via ∇T_e) up the density gradient. This mechanism is rather delicate and model dependent, though certainly viable in some cases. The second is the “turbulent equipartition (TEP)” mechanism in which inward flows are predicted to arise from the constraints that

adiabatic invariants place on turbulent mixing in phase space [Nycander and Yankov 1995, Isichenko, Gruzinov and Diamond 1995, Isichenko et al. 1996]. The advantages of TEP over the mixing mode genre are that it is mode independent, and so insensitive to the zoology of linear instabilities in tokamaks. Also, TEP theory can explain the coupling of gradients which are not thermodynamic forces to the flows (i.e. $\nabla q(r)$), and most plausible in large, hot collisionless plasmas, such as ITER. The TEP-type models have had some success in modeling JET and DIII-D profiles, but their fundamental physics has not been explored in simulations [Garbet et al. 2005]. This is especially true of the collisionless kinetic TEP models, which are most relevant to ITER. Numerous questions must be answered. These include, but are not limited to:

a.) How robust is ‘turbulent equipartition’? Does turbulent mixing ‘homogenize’ phase space density (i.e. invariant measure) in phase space? If so, can one predict the time scale for homogenization? If not, can one understand why, and quantify the answer? In particular, how can we quantify the degree of proximity to turbulent equipartition?

b.) What effect does, say, weak breaking of an adiabatic invariant have on TEP prediction? How does a phenomenon which is localized in phase space translate into macroscopics?

c.) How strong is the anomalous electron-ion thermal coupling ($Q_{e,i}$) predicted by TEP? Is it relevant to ITER? What are the implications of TEP fluxes for helium ash removal?

d.) Can the theory be extended from electrons to ions, etc.? What might TEP have to say about toroidal momentum flux, for example?

All of the questions listed above are interesting and simulation studies, particularly gyrokinetic particle simulations, have much to contribute. More generally, a rigorous, consistent derivation of the full transport matrix from basic gyrokinetic theory, together with critical simulation tests, is required. However, to address TEP will not be trivial. Codes must be global (i.e. the pinch is a transport effect), have the capacity for lengthy runs (i.e. for weak turbulence, the approach to TEP will be slow), must be well-diagnosed, and must be fast enough to enable the multiple runs and scans needed to extract scaling dependencies. Up until now, questions of particle transport have received scant attention from, and TEP models have been ignored in the simulation community. We hope this will soon change.

II.2.6 Conclusion

This concludes our discussion of ITER transport physics issues which simulation studies can help elucidate. Our list is only partial, and there are many other interesting and important problems which should be considered. Significant progress on even a few of the topics listed here will be quite beneficial to ITER, and to plasma science in general. We hope to see exciting

contributions from new investigators in the near future.

References

- [Diamond and Hahm 1995] P. H. Diamond, T. S. Hahm. 1995, Phys. Plasmas, 2: 3640
- [Bak, Tang, Wisenfeld 1987] P. Bak, C. Tang, K. Wiesenfeld. 1987, Phys. Rev. Lett., 59: 381
- [Zaslavsky2005] G. Zaslavsky, Hamiltonian Chaos, Fractional Dynamics. (Oxford University Press, 2005), pgs. 215-314
- [Newman1996] D. Newman, et al. 1996, Phys. Plasmas, 3: 1858
- [Carreras et al. 1996] B. A. Carreras, et al. 1996, Phys. Plasmas, 3: 2903
- [Hahm et al. 2004] T. S. Hahm, et al. 2004, Plasma Phys. Controlled Fusion, 46: A323
- [Gurcan, Diamond and Hahm 2006] O. Gurcan, P. H. Diamond, T.S. Hahm. 2006, Phys. Plasma, 13: 052306
- [Kadomtsev and Pogutse 1970] B. B. Kadomtsev, O. P. Pogutse. in Reviews of Plasma Physics, edited by M.A. Leontovich (Consultants Bureau, New York, 1970), Vol. 5, pg 387
- [Angelino et al. 2006] P. Angelino, et al. 2006, Plasma Phys. Controlled Fusion, 48: 557
- [Diamond et al. 2005] P. H. Diamond, et al. 2005, Plasma Phys. Controlled Fusion, 47: R35
- [Lee et al. 1987] W. W. Lee, et al. 1987, Phys. Fluids, 30: 1331
- [Adam et al. 1976] J. C. Adam, et al. 1976, Phys. Fluids, 19: 561
- [Horton et al. 1988] W. Horton, et al. 1988, Phys. Fluids, 31: 2971
- [Candy 2006] J. Candy. 2006, “ETG-ITG Interaction”, U.S. Transport Task Force Meeting, Myrtle Beach
- [Gurcan and Diamond 2004] O. Gurcan, P. H. Diamond. 2004, Phys. Plasmas, 11: 4973
- [Diamond 2006] P. H. Diamond. 2006, Invited Overview Lecture, “Transport Physics Issues for ITER”, U.S. Transport Task Force Meeting, Myrtle Beach, SC
- [Rechester and Rosenbluth 1978] A. B. Rechester, M. N. Rosenbluth. 1978, Phys. Rev. Lett., 40: 38
- [Narayan and Medvedev 2001] R. Narayan, M. Medvedev. 2001, ApJ. 562, L129
- [Biglari and Terry 1990] H. Biglari, P. H. Diamond, P. W. Terry. 1990, Phys. Fluids B2, 1
- [Hahm and Burrell 1995] T. S. Hahm, K. Burrell. 1995, Phys. Plasmas, 2: 1648
- [Diamond et al. 1994] P. H. Diamond, et al. 1994, Phys. Rev. Lett., 72: 2565
- [Hinton 1991] F. L. Hinton. 1991, Phys. Fluids, B3: 696
- [Lebedev and Diamond 1997] V. B. Lebedev, P. H. Diamond. 1997, Phys. Plasmas, 4: 1087
- [Malkov and Diamond 2006] M. Malkov, P. H. Diamond. 2006, “Exact Solution of a Simple Model of the L-H Transition”, submitted to Phys. Plasmas
- [Groebner et al. 2002] R. T. Groebner, et al. 2002, Phys.

- Plasmas, 9: 2134
 [Gruzinov, Diamond and Rosenbluth 2002] I. Gruzinov, P. H. Diamond, M. N. Rosenbluth. 2002, Phys. Rev. Lett., 89: 255001
 [Gruzinov, Diamond and Rosenbluth 2003] I. Gruzinov, P.H. Diamond, M. N. Rosenbluth. 2003, Phys. Plasmas, 10: 569
 [Beyer et al. 2005] P. Beyer, et al. 2005, Phys. Rev. Lett., 94: 105001
 [Kim and Diamond 2003] E. Kim, P. H. Diamond. 2003, Phys. Rev. Lett., 90: 185006
 [Lebedev and Diamond 1997] V. Lebedev, P. H. Diamond. 1997, Phys. Plasmas, 4: 1087
 [Yoshizawa, Itoh and Itoh 2003] A. Yoshizawa, S.-I. Itoh, K. Itoh. 2003, Plasma and Fluid Turbulence, (IOP Publishing, Bristol), pgs. 386-431
 [Diamond et al. 1997] P.H. Diamond, et al. 1997, Phys. Rev. Lett., 78: 1472
 [Rice et al. 2002] J. Rice, et al. 2002, Nucl. Fusion, 45: 1144
 [Ida et al 2001] K. Ida, et al. 2001, Phys. Rev. Lett., 86: 3040
 [Mattor and Diamond 1988] N. Mattor, P. H. Diamond. 1988, Phys. Fluids, 31: 1180
 [Scott et al. 1990] S. D. Scott, et al. 1990, Phys. Rev. Lett., 64: 531
 [Diamond et al. 1996] P. H. Diamond, et al. 1996, "Dynamics of L→H Transition, VH-Mode Evolution, Edge Localized Modes and R.F. Driven Confinement Control in Tokamaks", in Proceedings of the 15th IAEA Conference, (Seville, 1994) pgs. 323-353
 [Coppi 2002] B. Coppi. 2002, Nucl. Fusion, 42: 1
 [Strachan et al. 1982] J. D. Strachan, et al. 1982, Nucl. Fusion, 22: 1145
 [Coppi and Spight 1978] B. Coppi, C. Spight. 1978, Phys. Rev. Lett., 41: 551
 [Nycander and Yankov 1995] J. Nycander, V. V. Yankov. 1995, Phys. Plasmas, 2: 2874
 [Isichenko, Gruzinov and Diamond 1995] M. B. Isichenko, A. V. Gruzinov, P. H. Diamond. 1995, Phys. Rev. Lett., 74: 4436
 [Isichenko et al. 1996] M. B. Isichenko, et al. 1996, Phys. Plasmas, 3: 1916
 [Garbet et al. 2005] X. Garbet, et al. 2005, Phys. Plasmas, 12: 082511

III Status of fusion simulation and modeling

III.1 Nonlinear governing equations for plasma simulations (T.S. Hahm)

Introduction

Confining hot and dense plasmas in the interior of fusion devices while keeping boundaries from being damaged by excessive heat necessarily create an inhomoge-

neous state. Such magnetically confined high temperature plasmas are not only unstable to various linear instabilities with different wavelengths and complex frequencies, but often nonlinearly self-organize themselves into a more energetically favorable state. To understand these complex nonlinear systems, systematic collaborations among theory, simulation, and experiment are highly desirable.

Despite the tremendous increase of computational power in recent years, the direct simulation of actual size fusion plasmas in realistic geometry using the primitive nonlinear plasma equations (such as the Klimontovich or Vlasov equations) is still far beyond the computational capability of even the foreseeable future. Thus, reduced equations have been employed to simplify the basic dynamical equations. The main representative models and hierarchical relations among them are summarized in Table III.1.1.

In this section, we discuss basic procedures involved in derivations from the most fundamental, Vlasov equation, to various reduced nonlinear equations which are now widely used in various turbulence and MHD stability simulations in magnetically confined plasmas including tokamaks. These include the nonlinear gyrokinetic equations and fluid equations including gyrofluid equations and magnetohydrodynamic (MHD) equations. We focus our discussion on collisionless plasmas.

Evolution of collisionless plasma can be described by the Vlasov equation for the particle distribution function for each particle species in a six-dimensional phase space,

$$d/dt f + \mathbf{V} \cdot d/d\mathbf{x} f + (q/m)(\mathbf{E} + \mathbf{v} \times \mathbf{B}) \cdot d/d\mathbf{v} f = 0, \quad (\text{III.1.1})$$

where \mathbf{E} and \mathbf{B} are the electric and magnetic fields produced by the particle motion which satisfy the Maxwell's equations. This system of equations can describe various phenomena over a wide range of spatio-temporal scales. For instance, accurate descriptions of particle dynamics in the presence of high frequency electromagnetic waves are needed for studying plasma heating by waves. This is a research area of high practical importance which will be described in detail in Sec. III.6. This is particularly true for high-density ITER plasmas where neutral beam injection (NBI) heating may not be very effective.

Nonlinear gyrokinetic equations

For turbulence and transport problems in plasmas confined by high magnetic fields, the temporal scales of collective electromagnetic fluctuations of interest are much longer than the period of a charged particle's cyclotron motion (gyro-motion), while the spatial scales of such fluctuations are much smaller than the scale length of the magnetic field inhomogeneity. In these circumstances, details of the charged particle's gyration motion are not of physical interest, and it is desirable to develop a reduced set of dynamical equations which

Table III.1.1 Hierarchy of nonlinear governing equations

Nonlinear equations: From fundamental, primitive to reduced, simplified	Steps for reduction	Physics lost due to reduction
Vlasov-Klimontovich equation [Klimontovich 67]	Remove high frequency terms ($\geq \omega_{ci}$)	High frequency phenomena
Gyrokinetic Equation: Conservative [Dubin 83, Hahm 88a,b, Brizard 89, 06]		
Gyrokinetic Equation: Conventional [Frieman 82]	Take moments in velocity space	Conservation of energy between particles and fields, of phase-space volume, nonlinear trapping of particles along \mathbf{B} .
Gyrofluid Equation [Beer 95, Dorland 93]	Expansion in finite Larmor radius terms; Ordering for collisional plasmas	Some nonlinear kinetic effects including inelastic Compton scattering [Mattor 92], accuracy in damping rates of zonal flow [Rosenbluth 96] and damped mode [Sugama97]
Fluid Equations [Yagi 94, Scott 97, Zeiler 97, Xu 02, Simakov 05]		

In this table, the hierarchy of nonlinear governing equations is explained [Diamond 05]. Steps for reduction, and physics lost due to reduction is also listed.

still captures the essential features of the low-frequency phenomena of practical relevance. By decoupling the gyro-motion, one can derive the gyrokinetic equation which describes the spatio-temporal evolution of the gyro-center distribution function, which is independent of the gyro-phase, q , defined over a five-dimensional phase space $(\mathbf{R}, \nu z, \mu)$. In simulating strongly magnetized plasmas, one can, thus, save enormous amounts of computing time by having a time step greater than the gyro-period, and by reducing the number of dynamical variables. We note that in the gyrokinetic approach, the gyro-phase is an ignorable coordinate and the magnitude of the perpendicular velocity enters as a parameter in terms of an adiabatic invariant μ which does not change in time for each particle.

Due to the broad scope of this document and space limitations, it is not appropriate to describe here the rigorous derivations of the nonlinear gyrokinetic equations in toroidal geometry. Details can be found in the literature which includes

- i) a conventional perturbative derivation with introduction of a standard nonlinear gyrokinetic ordering [Fireman82]
- ii) a derivation mainly for the purpose of particle-in-cell simulation [Lee83],
- iii) The Hamiltonian derivations of nonlinear gyroki-

netic equations for electrostatic fluctuations [Dubin83], and electromagnetic fluctuations [Hahm88a] in a uniform magnetic field, and finally,

- iv) generalizations to arbitrary geometry using phase-space LaGrange derivations (which are the most transparent and efficient to date in the author's opinion) for electrostatic fluctuations [Hahm88b], and electromagnetic fluctuations [Brizard89].

A theoretically oriented review on the subject has recently been written [Brizard06].

Both formulations and simulations traditionally focused on tokamak core turbulence in which the fluctuation amplitude is relatively small, i.e., the relative density fluctuation amplitude is less than one percent and the gradients in macroscopic parameters such as pressure are relatively mild with characteristic lengths on the order of a fraction of the minor radius. In the nonlinear gyrokinetic theory, there exist three expansion parameters; ω/Ω_i , ρ_i/L_B , and $\delta f/F_0 \sim e\phi/T_e$. The conventional gyrokinetic theory [Frieman 82] assumes that all three parameters are comparable in formal ordering, although this choice needs to be modified in some cases including plasmas with transport barriers with steep gradients in pressure and in E_r [Hahm 96]. In addition, in the nonlinear gyrokinetic ordering, the perpendicular wavelength can be comparable to the

gyroradius, while the parallel wavelength of the fluctuation is comparable to the connection length of the system $\sim qR$. Thus, the ordering is consistent with the spatial structure of the fluctuation which aligns with the equilibrium magnetic field.

Here, we simply sketch a heuristic derivation procedure in a uniform magnetic field to illustrate some key features in the nonlinear gyrokinetic equations. For more details, readers should consult the aforementioned literature.

Transforming to the guiding center variables, $\mathbf{R} = \mathbf{x} + \rho$, $\mu = v_{\perp}^2/2B$, $\mathbf{v} = v_{\parallel}b + v_{\perp}(\mathbf{e}_1 \cos \theta + \mathbf{e}_2 \sin \theta)$ we can write Eq. (III.1.2) as

$$\begin{aligned} d/dt f + v_{\parallel} \mathbf{b} \cdot d/d\mathbf{R} f + \mathbf{E} \mathbf{x} \mathbf{b} / B \cdot d/d\mathbf{R} f \\ + (q/m) E_{\parallel} d/dv_{\parallel} f - \Omega_i d/d\theta f = 0. \end{aligned} \quad (\text{III.1.2})$$

For $\omega \ll \Omega_i$, the lowest order part of Eq. (III.1.2) is $\Omega_i d/d\theta f = 0$.

Writing $f = \langle f \rangle + f_a$ (with $\langle f \rangle \gg f_a$) in which $\langle \dots \rangle$ indicates a gyro-phase average, and f_a is the gyro-phase dependent part, the next order equation is:

$$\begin{aligned} d/dt \langle f \rangle + v_{\parallel} \mathbf{b} \cdot d/d\mathbf{R} \langle f \rangle + \mathbf{E} \mathbf{x} \mathbf{b} / B \cdot d/d\mathbf{R} \langle f \rangle \\ + (q/m) E_{\parallel} d/dv_{\parallel} \langle f \rangle - \Omega_i d/d\theta f_a = 0. \end{aligned} \quad (\text{III.1.3})$$

Eq. (III.1.3) is basically a solubility condition for $\langle f \rangle$.

Gyro-averaging Eq. (III.1.3), we obtain the electrostatic gyrokinetic Vlasov equation in a uniform magnetic field,

$$\begin{aligned} d/dt \langle f \rangle + v_{\parallel} \mathbf{b} \cdot d/d\mathbf{R} \langle f \rangle + \langle \mathbf{E} \rangle \mathbf{x} \mathbf{b} / B \cdot d/d\mathbf{R} \langle f \rangle \\ + (q/m) \langle E_{\parallel} \rangle d/dv_{\parallel} \langle f \rangle = 0. \end{aligned} \quad (\text{III.1.4})$$

We emphasize that Eq. (III.1.4) is in the gyro-center coordinates, rather than in the particle coordinates (x, v) . To complete the gyrokinetic description of the influence of the particles' motion on the electromagnetic field, one need to express the charge density and the current density in Maxwell's equations in terms of the gyro-center distribution function $\langle f \rangle$. This requires the so-called "pull-back transformation" to the particle coordinates [Littlejohn 82]. We note that the effect of the polarization drift appears in the gyrokinetic Poisson's equation as the polarization density [Lee 83], rather than in the guiding center drift in the Vlasov equation. That term accounts for the difference between the particle density and the gyro-center density. That representation of the polarization drift as a shielding term has been found to be very useful computationally [Lee83].

Some simulation approaches use the particle-in-cell simulation method, which is Lagrangian in character (i.e., particles are pushed) while others use the continuum Vlasov approach which is Eulerian in character (i.e., the gyrokinetic equation is solved as a partial

differential equation). Most simulations in toroidal geometry to date ignored the parallel velocity space parallel nonlinearity (the last term on the left hand side of Eq. (III.1.4)). Although this term is formally small compared to the $\mathbf{E} \times \mathbf{B}$ nonlinearity (the third term on the LHS), it is responsible for the nonlinear exchange of energy between particles and the electromagnetic field and can affect the long term behavior of nonlinear simulations. We note that some simulations [Sydora96, Villard04] have used a fully nonlinear energy conserving form of the nonlinear gyrokinetic equation [Hahm88b].

Nonlinear fluid equations

While fluid models cannot capture all the kinetic physics described by nonlinear kinetic equations, they can be justified for many applications including macroscopic magneto-hydro-dynamic (MHD) stability (see Sec. III.2. and Sec. III.4. for details). They are also very useful for turbulence problems due to their relative simplicity and their closer connection to nonlinear theories which are primarily based on the $\mathbf{E} \times \mathbf{B}$ nonlinearity. For instance, the knowledge gained in the fluid turbulence community can serve as a useful guide for plasma turbulence problems.

Gyrofluid models are derived from the gyrokinetic equations by taking velocity moments while keeping the finite gyroradius effects. As a result, one gets a hierarchy of evolution equations for fluid moments evaluated at the gyrocenter, i.e., for density, parallel velocity, pressure, and so on. To obtain a closed set of these equations, one needs to invoke a "closure approximation". In the simulation community, the so-called "Landau closure" approach which put emphasis on accurate linear Landau damping and the linear growth rate has been mostly widely adopted [Hammett 90, Dorland 93, Waltz 94, Beer 95, Snyder 01]. In this approach, some kinetic effects, such as linear Landau damping and a limited form of nonlinear Landau damping (elastic Compton scattering), have been successfully included. However, these models do not accurately treat the strongly nonlinear wave-particle interactions (inelastic Compton scattering). Other closures for more accurate description of nonlinear kinetic effects [Mattor 92] and the treatment of damped modes [Sugama 01] have been developed, but have not been as widely used as the "Landau-closure"-based models in simulations. Gyrofluid models to date cannot describe the zonal flow damping accurately, and can overestimate the turbulence level [Rosenbluth 97]. More discussions on zonal flows can be found in Sec. I. 2. We note that there exist nonlinear gyrofluid models with an emphasis on the Hamiltonian structure and energy conservation [Brizard 92, Strinzi 05] More detailed discussions of nonlinear gyrofluid simulations are available in Sec. III. 5.

It is instructive to note that the reduced MHD equations [Strauss 76] can be derived all the way from the gyrokinetic equations [Hahm 88a]. The vorticity equation in the Hasegawa-Mima system [Hasegawa 78], Hasegawa-Wakatani system [Hasegawa 87] or in the re-

duced MHD system is nothing but the evolution of the polarization density in the gyrokinetic Poisson's equation.

There are other reduced nonlinear fluid equations, such as the four-field model [Hazeltine 85], which generalizes the MHD equations by capturing the different dynamics between ions and electrons (two fluid approach), but with less emphasis on the finite ion gyroradius effects. Roughly speaking, fluid approaches (other than Landau-closure based models for core turbulence applications) are justified with collisions [Braginskii 65]. Strong magnetic fields, however, make fluid descriptions justifiable for the dynamics across the magnetic field. Nonlinear fluid models have been extended to the long mean free path, banana collisionality regime as well [Callen 85, Connor 85]. They are called the neo-classical MHD models, and have been very useful as a starting point of the studies on neoclassical tearing modes (NTM) which are discussed in detail, in Sec. I. 2.

Useful physics discussions and derivations of MHD equations can be found in [Kulsrud 83]. Sometimes a hybrid approach in which one species is kinetically treated; while others are described with fluid models can be appropriate and useful. One of the early examples is the gyrokinetic energetic particle- bulk MHD description [Park 92]. For more recent examples and associated physics discussion, refer to Sec. III. 4. and Sec. III. 8.

References

[Beer95] M. A. Beer. 1995, Ph. D. Thesis, Princeton University
 [Braginskii 65] S.-I. Braginskii. 1965, in Review of Plasma Physics, edited by M.A. Leontovich (Consultants Bureau, NY) Vol.1. 205
 [Brizard89] A. J. Brizard. 1989, J. Plasma Phys., 41: 541 ~ 559
 [Brizard92] A. J. Brizard. 1992, Phys. Fluids B, 4: 1213
 [Brizard06] A. J. Brizard, T.S. Hahm. 2006, "Foundations of Nonlinear Gyrokinetic Theory", Rev. Mod. Phys. to appear in October-December issue.
 [Callen85] J. D. Callen, K.C. Shaing. 1985, Phys. Fluids, 28: 1845
 [Connor85] J. W. Connor, L. Chen. 1985, Phys. Fluids, 28: 2201
 [Diamond05] P. H. Diamond, K. Itoh, S.-I. Itoh, et al. 2005, Phys. Plasmas. Control. Fusion, 47: R35-R161
 [Dorland93] W. Dorland, G.W. Hammett. 1993, Phys. Fluids B, 5: 812
 [Dubin83] D. H. E. Dubin, et al. 1983, Phys. Fluids, 26: 3524 ~ 3535
 [Frieman82] E. A. Frieman, L. Chen. 1982, Phys. Fluids, 25: 502 ~ 508
 [Hahm88a] T. S. Hahm, W. W. Lee, A. J. Brizard. 1988, Phys. Fluids, 31: 1940 ~ 1948
 [Hahm88b] T. S. Hahm. 1988, Plasma Fluids, 31: 2670 ~

2673
 [Hahm96] T. S. Hahm. 1996, Phys. Plasmas, 3: 4658 ~ 4664
 [Hammett90] G. Hammett, F.W. Perkins. 1990, Phys. Rev. Lett., 64, 3019 ~ 3022
 [Hasegawa78] A. Hasegawa, K. Mima. 1978, Phys. Fluids, 21: 87
 [Hasegawa87] A. Hasegawa, M. Wakatani. 1987, Phys. Rev. Lett., 59: 1581
 [Hazeltine85] R. D. Hazeltine et al. 1985, Phys. Fluids, 28: 2466
 [Klimontovich67] Y. L. Klimontovich. 1967, "The statistical theory of Non-equilibrium processes in a Plasma" (MIT, Cambridge)
 [Kulsrud83] R. M. Kulsrud. 1983, in "Handbook of Plasma Physics" edited by M.N. Rosenbluth and R.Z. Sagdeev (North-Holland Publishing Company, Amsterdam-New York-Oxford) Vol I. 115
 [Lee83] W. W. Lee. 1983, Phys. Fluids, 26: 556-562
 [Littlejohn 82] R. G. Littlejohn. 1982, J. Math Phys., 23: 742 ~ 747
 [Mattor92] N. Mattor. 1992, Phys. Fluids B, 4: 3952 ~ 3961
 [Park92] W. Park, et al. 1992, Phys. Fluids B, 4: 2033-2037
 [Rosenbluth98] M. N. Rosenbluth, F.L. Hinton. 1998, Phys. Rev. Lett., 80: 724
 [Scott97] B. D. Scott. 1997, Plasma Phys. Control. Fusion, 39: 1635
 [Simakov05] A. N. Simakov, P. J. Catto. 2005, Phys. Plasmas, 12: 012105
 [Snyder01] P. B. Snyder, G.W. Hammett. 2001, Phys. Plasmas, 8: 744 ~ 749
 [Strauss 76] H. Strauss. 1976, Phys. Fluids, 16: 134
 [Strinzi05] D. Strinzi, B. Scott, A. Brizard. 2005, Phys. Plasmas, 12: 052517
 [Sugama 01] H. Sugama, et al. 2001, Phys. Plasmas, 8: 2617
 [Sydora96] R. D. Sydora, et al. 1996, Plasma Phys. Control. Fusion, 12: A281 ~ A294
 [Villard04] L. Villard, et al. 2004, Nucl. Fusion, 44: 172 ~ 180
 [Waltz94] R. Waltz, et al. 1994 Phys. Plasmas, 1: 2229 ~ 2244
 [Xu02] X. Q. Xu, et al. 2002, Nucl. Fusion, 42: 21
 [Yagi94] M. Yagi, W. Horton, 1994, Phys. Plasmas, 1: 2135
 [Zeiler97] A. Zeiler, et al. 1997, Phys. Plasmas, 4: 2134

III.2 Equilibrium and stability (L.L. Lao, J. Manickam)

Equilibrium Reconstruction and Equilibrium

Reconstruction of experimental axisymmetric magnetohydrodynamic (MHD) equilibria is a very important part of tokamak data analysis and plasma operation. It has contributed significantly to several major discoveries of tokamak physics such as the experimental validation of theoretically predicted β stability limit and the negative-central-shear/enhanced-

reversed-shear (NCS/ERS) operating regime. It is a critical component of plasma shape control and fundamental to transport and stability analysis.

Computational techniques and numerical tools for 2D axisymmetric tokamak equilibrium reconstruction are well developed. The amount of information that can be extracted varies with the amount of experimental data available for the reconstruction. External magnetic measurements alone only yield plasma boundary and global current and pressure profile information such as β_P and ℓ_i . Here, β_P and ℓ_i are the plasma poloidal beta and internal inductance. To fully reconstruct the current profile for applications such as current-profile analysis in discharges with lower hybrid current drive (LHCD) or electron cyclotron current drive (ECCD), internal current profile measurements must be used together with external magnetic measurements. To fully reconstruct the pressure and current profiles and the internal magnetic topology for applications such as stability analysis, internal current and kinetic profile measurements must be used in conjunction with external magnetic data. One of the most widely used tokamak equilibrium reconstruction tools is the EFIT code (Lao 2005). EFIT efficiently reconstructs the MHD equilibrium by interleaving the equilibrium and the fitting iterations with a Picard linearization scheme to find the optimum solution. The presence of toroidal plasma rotation, non-axisymmetric error or externally applied perturbation magnetic fields, or ferromagnetic inserts to reduce toroidal magnetic field ripple will increase the complexity of the equilibrium reconstruction. EFIT is used in many tokamak laboratories around the world including DIII-D, C-MOD, NSTX, MAST, TORE SUPRA and JET. Other equilibrium reconstruction tools include the VMEC code (Hirshman 1994) used for TFTR and other tokamaks, the CLISTE code (McCarthy 1999) used at AUG, and the ESC code (Zakharov 1999) sometime used for reconstruction of discharges with current hole.

New equilibrium reconstruction developments include modernizing the EFIT computational framework and architecture to improve the computational efficiency and to allow a single version for all grid sizes and for use with all tokamaks including ITER, fully integrating equilibrium reconstruction with transport and stability analyses, and 3D extension to account for non-axisymmetric error or externally applied perturbation magnetic fields, or toroidal magnetic field ripple.

In addition to experimental reconstruction tools, direct or inverse equilibrium tools are often needed to support tokamak data analysis. These include EFIT, TOQ (Miller 1998), the CORSICA equilibrium module (Crotinger 1997), ESC (Zakharov 1999), JSOLVER (DeLucia 1980), VMEC (Hirshman 1983), or CHEASE (Lutjens 1992). For stability analysis, often once an experimental equilibrium is reconstructed, an equilibrium code is then used to compute a set of equilibria perturbed around the initial experimental equilibrium for detailed stability study.

Real tokamaks usually have inherent error fields, due to a combination of non-axisymmetric structures and small displacements of coils. This introduces the need for 3D equilibrium codes, which can treat non-axisymmetric geometry. Codes such as CAS3d (Nührenberg 2003), VMEC (Hirshman 1983) and PIES (Reiman 1986) codes are available to compute 3D magnetic equilibrium. VMEC is restricted to nested magnetic surface geometry, whereas PIES can include 3D magnetic island structures and magnetic stochasticity.

Stability

The macroscopic stability of tokamaks depends on plasma features such as: plasma geometry, usually characterized by the major radius, minor radius, elongation, triangularity and boundary conditions, e. g. limited or diverted; the plasma pressure and safety factor (q) profiles, the related current profiles; plasma resistivity and the fast particle population. Plasma rotation can also play a role. The instabilities of interest include; the axisymmetric, $n = 0$, vertical instability. Here, n is the toroidal mode number. The $n = 0$ mode can be feedback stabilized. The stability limits are set by the available feedback system, which can be characterized by a limit on the allowable elongation of the plasma cross-section. The $n = 1$ current driven external kink sets a limit on the current and is often set by a limit on $q_{EDGE} > 2$. The $n = 1$ pressure driven kink sets the upper limit on the allowable β , ratio of thermal to magnetic pressure. This instability can be partially ameliorated by having a surrounding conducting shell. In practice segmented conducting plates mimic a shell and reduce the growth-rate of the instability. However, the shell acts like a resistive wall and the instability is then considered to be a resistive wall mode (RWM), and unlike the ideal kink, it has a complex frequency. The resistive wall mode can be stabilized by plasma rotation, usually driven by the momentum input of neutral beams. Theoretical models have shown that the RWMs can be stabilized by feedback coils. Experiments are filling in the details at this time.

Even before the ideal β limit is approached, other instabilities can lead to β collapse. These include sawteeth oscillations, which lead to a sharp flattening of the core temperature out to the $q = 1$ radius, and may provide the trigger for neo-classical tearing modes, NTMs, which grow more slowly, but prevent the rise in β , if there is not a collapse. Another possible trigger for NTMs is Edge localized modes, ELMs. These are increasingly being identified as current and pressure driven intermediate to high n , ($n \sim 5-30$), peeling-ballooning modes, and are observed when the plasma is in a high confinement mode, the H-mode. Other important instabilities to consider are the energetic-particle driven modes, which arise from the interaction of fast particles with resonant stable modes of the plasma, referred to as Alfvén eigenmodes. These instabilities can cause a selective loss of energetic particles, without affecting the thermal distribution. These could be of greater concern in ITER, when the alpha pressure rep-

resents a significant fraction of the total pressure. Finally, it should be noted that non-axisymmetric fields, usually due to field errors, can enhance otherwise benign modes and cause them to grow, through a process called mode locking, which usually leads to a disruption. Disruptions are catastrophic events where the plasma current is quenched in a very short time. They may be caused by a variety of plasma phenomena, including high density, loss of vertical control, mode locking or MHD instabilities. While several codes are available to model many of the ideal and resistive instabilities, see below, there are no satisfactory models for disruptions.

Ideal stability

Ideal stability limits are a useful guide to determine the stable boundaries in parameter space, and are particularly useful in machine design. In an experiment, if the boundary is violated, a fast-growing instability is likely to lead to a collapse in β or even to the quench of the discharge. The computation techniques and tools for ideal stability analysis are well developed. Various computational tools are available. These include GATO/ERATO (Bernard 1981, Gruber 1981), PEST (Grimm 1976), MISHKA (Mikhailovskii 1997, Huysmans 2001), and KINX (Degtyarev 1997) for low- n stability, the ELITE (Wilson 2002, Snyder 2002) code for intermediate to high $n \geq 5$ stability, and the BALOO (Miller 1997) and BALOON (Chance 1978) codes for high- n ballooning stability. The low- n stability codes typically compute the unstable modes using the variational energy form of the linearized ideal MHD equations with a finite element approach plus a spectral representation. It is computationally demanding to compute $n \geq 5 \sim 10$ with these low- n stability codes. The ELITE (Edge Localized Instabilities in Tokamak Experiments) code (Wilson 2002, Snyder 2002) was developed particularly to efficiently compute intermediate to high $n \geq 5$ modes to better understand edge localized mode (ELM) physics and constraints on the edge pressure pedestal. ELITE focuses on the edge plasma and vacuum regions, and uses an expansion assuming moderately high- n in order to efficiently treat edge-localized modes. Ideal stability codes have generally been well validated against experimental results as well as benchmarked against each other. Additionally, both the non-linear MHD codes NIMROD (Sovinec 2004) and M3D (Park 1999) as well as a new one JOREK (Huysmans 2006) have also been applied for investigations of non-linear aspects of ELMs.

Also available are the DCON (Glasser 1997), MARG2d (Tokuda 1999) and PEST-2 (Grimm 1983) ideal stability codes that are based on the efficient Newcomb algorithm to evaluate plasma stability. These Newcomb-based tools are computationally much faster than the conventional low- n stability tools such as GATO and provide a convenient means for between-shot stability analyses. However, they provide less information than the conventional low- n stability tools.

Energetic particles are known to interact with the

Alfvénic spectrum and cause energetic-particle driven instabilities. These are potentially an important concern for ITER, as these instabilities are often associated with energetic particle losses, which could influence the alpha-particle confinement and hence the neutron yield in fusion devices. Computational tools to analyze fast ion stability include the NOVA-K (Cheng 1992) and CASTOR-K (Borba 1997) codes for low- n modes and the HINST (Gorelenkov 1998) code for high- n modes. The non-linear MHD codes M3D-K(inetic) (Park 1999) is now addressing these instabilities as well.

New and on-going developments include adding rotational effects into ELITE, an improved algorithm to treat the plasma-vacuum region in non-linear MHD codes such as NIMROD for computing intermediate to high n edge localized modes, and applications of the low- n stability codes such as GATO together with MHD equilibrium codes that assume nested magnetic surfaces for evaluation of magnetic islands and 3D perturbed plasma equilibria (Nührenberg 2003).

Resistive stability

The computational techniques and tools for resistive stability are more challenging compared to the ideal stability codes. These include: the PEST-III (Pletzer 1994) code used to determine Δ' , the measure of the available energy for a tearing mode; the MARS (Bondeson 1992) code, and the non-linear MHD codes NIMROD (Sovinec 2004), M3D (Park 1999), and FAR (Charlton 1990). MARS has been extensively applied for investigation of resistive wall modes (RWM). MARS addresses the MHD stability as an eigenvalue problem, whereas NIMROD and M3D are initial-value codes. Various damping, rotational stabilization, and external-coil feedback models have been implemented in MARS and tested against RWM experimental results (Chu 2004). Additionally, the VALEN code (Bialek 1998) has also been developed to study detailed engineering aspects of RWM external coil feedback stabilization. Many aspects of VALEN have been tested against RWM experimental data. Both PEST-III (Pletzer 1994) and NIMROD (Sovinec 2004) have been applied for studies of resistive and neo-classical tearing modes. New and ongoing developments include construction of the TWIST-R code (Galkin 2002) to more accurately evaluate the resistive stability parameter Δ' when the Mercier index is high using a transformation technique to remove the singularity in the model equations, improvements of the MARS code to more accurately compute the eigen-function near the plasma edge for analysis of edge stability, applications of non-linear MHD codes such as NIMROD and M3D for disruption (Kruger 2005) and current hole studies (Breslau 2003), and investigations of two-fluid effects using M3D (Sugiyama 2000).

References

[Bernard1981] L. C. Bernard, et al. 1981, *Comput. Phys. Commun.*, 24: 377

[Bialek 1998] J. Bialek. 1998, *Bull. Am. Phys. Soc.*, 43: 1831

[Bondeson 1992] A. Bondeson, et al. 1992, *Phys. Fluids B*, 4 : 1889

[Borba 1999] D. Borba, W. Kerner. 1999, *J. Comput. Phys.*, 153: 101

[Breslau 2003] J. A. Breslau, et al. 2003, *Phys. Plasmas*, 10: 1665

[Chance1978] M. S. Chance.
<http://w3.pppl.gov/topdac/balloon.htm>

[Charlton 1990] L.A. Charlton, et al. 1990, *J. Comput. Phys.*, 86: 270

[Cheng 1990] C. Z. Cheng. 1990, *Phys. Fluids B*, 2: 1427

[Chu 2004] M. S. Chu, et al. 2004, *Phys. Plasmas*, 11: 2497

[Crottinger 1997] J. A. Crottinger, et al. "CORSA: A Comprehensive Simulation of Toroidal Magnetic-Fusion Devices", LLNL Report UCRL-ID-126284, Lawrence Livermore Natl. Lab., CA (1997)

[Degtyarev1997] L. Degtyarev, et al. 1997, *Comput. Phys. Commun.*, 103: 10

[DeLucia 1980] J. DeLucia, et al. 1980, *J. Comput. Phys.*, 37: 183

[Galkin 2002] S. A. Galkin, et al. 2002, *Phys. Plasmas*, 9: 3969

[Glasser 1997] A. H. Glasser, M. Chance. 1997, *Bull. Am. Phys. Soc.* 42: 1848

[Gorelenkov 1998] N. N. Gorelenkov, et al. 1998, *Phys. Plasmas*, 5: 3389

[Grimm 1976] R. C. Grimm, J. M. Greene, J. L. Johnson. 1976, *Meth. of Comp. Physics*, (Academic Press), 16: 253

[Grimm 1983] R. C. Grimm, R. L. Dewar, J. Manickam. 1983, *J. Comput. Phys.*, 49: 94

[Gruber 1981] L. E. Zakharov, A. Pletzer. 1981, *Comput. Phys. Commun.*, 21: 323

[Hirshman 1983] S. P. Hirshman and J.C. Whitson. 1983, *Phys. Fluids*, 26: 3553

[Hirshman 1994] S. P. Hirshman, et al. 1994, *Phys. Plasmas*, 1: 2277

[Huysmans 2001] G. T. A. Huysmans, et al. 2001, *Phys. Plasmas*, 8: 4292

[Huysmans 2006] G. T. A. Huysmans, et al. "MHD Stability in X-Point Geometry: Simulations of ELMs", *Fusion Energy*, (Proc. 21st Conf. Chengdu 2006) IAEA, Vienna, paper TH/P8-2

[Kruger 2005] S. E. Kruger, et al. 2005, *Phys. Plasmas*, 12: 056113

[Lao 2005] L. L. Lao, H. E. St. John, Q. Peng, et al. 2005, *Fusion Sci. Tech.*, 48: 968

[Lutjens 1992] H. Lutjens, et al. 1992, *Comput. Phys. Commun.*, 69: 287

[Mikhailovskii 1997] A. B. Mikhailovskii, et al. 1997, *Plasma Phys. Rep.*, 23: 844

[McCarthy1999] P. J. McCarthy, et al. 1999, "The CLISTE Interpretive Equilibrium Code", IPP Report 5/85, Max-Planck-Institut fur Plasmaphysik, Garching

[Miller 1997] R. L. Miller, et al. 1997, *Phys. Plasmas*, 4: 1062

[Miller 1998] R. L. Miller, et al. 1998, *Plasmas Phys. Control. Fusion*, 40: 753

[Nuhrenberg 2003] C. Nuhrenberg, A. H. Boozer. 2003, *Phys. Plasmas*, 10: 2840

[Park 1999] W. Park, et al. 1999, *Phys. Plasmas*, 6: 1796

[Pletzer 1994] A. Pletzer, et al. 1994, *J. Comput. Phys.*, 115: 530

[Reiman 1986] A. Reiman, H. Greenside. 1986, *Comput. Phys. Commun.*, 43: 157

[Snyder 2002] P. B. Snyder, et al. 2002, *Phys. Plasmas*, 9: 2037

[Sovinec 2004] C. R. Sovinec, et al. 2004, *J. Comput. Phys.*, 195: 355

[Sugiyama 2000] L. E. Sugiyama. 2000, *Phys. Plasmas*, 7: 4644

[Tokuda 1999] S. Tokuda, T. Watanabe. 1999, *Phys. Plasmas*, 6: 3012

[Wilson 2002] H. R. Wilson, P. B. Snyder, et al. 2002, *Phys. Plasmas*, 9: 1277

[Zakharov 1999] L. E. Zakharov, A. Pletzer. 1999, *Phys. Plasmas*, 6: 4693

III.3 Transport modeling (R. E. Waltz)

There has been remarkable progress during the past decade in understanding and modeling turbulent transport in tokamaks. With some exceptions the progress is derived from the huge increases in computational power and the ability to simulate tokamak turbulence with ever more fundamental and physically realistic dynamical equations, e.g. the gyrofluid and then gyrokinetic equations. Indeed transport code models are the only way to connect turbulent transport theory with experiments, and simulations have become a vital link in this path: theory, simulation, transport code model, experiment. As detailed in Section II.4, while the gyrokinetic simulations have become increasingly realistic and comprehensive, significant improvements in computation power and methods are required to bypass the transport modeling link with direct comparison with experiments...at least on a routine basis. The much faster and increasingly accurate theory based transport models will remain important in projecting and analyzing ITER performance. After a brief review of the history of turbulent transport model development from the mid-80's to the late-90's, we discuss some basic theoretical rules and recipes for developing more accurate and comprehensive transport models, the status for current development in progress, and the way forward in addressing some key issues and problems with the existing transport models.

Transport code models have historically been labeled on a continuum from empirical to theoretical. Empirical transport code models are required to fit or mathematically describe or predict the experimental plasma profiles (temperature, particle and current density, rotation, etc) given the experimentally inferred source profile. In addition to this requirement, a purely the-

oretical model is required to accurately represent the theory. As gyrofluid and then gyrokinetic simulations became more realistic and physically comprehensive after the mid-90's, the only practical measure of a model representing the theory has come to mean accurately fitting the simulations. Theoretical transport models can not be derived with mathematical rigour.

Historical background

Historically and in practice, there has been a bewildering variety of provisional empirical transport code models. They are seldom if ever purely empirical but instead the most useful such models take the form of mathematically simple analytic formulas for the local energy and particle diffusivities (χ, D) motivated by some heuristic (“back of the envelope”) reasoning from the theory. The models invariably have some theoretical content and are meant to test some possible physical approximation or dimensionless variable constraint. For example the local energy diffusivity may be broken into components with gyroBohm or Bohm scaling: $\chi_{gB} = \sum_m C_m^{gB} F_m^{gB} (c_s/a) \rho_s^2$, $\chi_B = \sum_m C_m^B F_m^B c_s \rho_s$, with F an analytic function of the local dimensionless parameters like $q, \varepsilon, \nu_*, \beta, a/R, a/L_T, a/L_n, \dots$ and more recently the magnetic shear and the $\mathbf{E} \times \mathbf{B}$ shear rate γ_E . (Models for F are rarely nonlocal, e.g. dependent on the temperature gradients a/L_T at some distance. Often but not always, the F 's are written as power laws in the dimensionless variable.) GyroBohm or Bohm scaling components differ in the single dimensionless parameter “rho-star” ($\rho_* = \rho_s/a$) which must be extrapolated (e.g. about 10-fold from DIII-D) in projecting the performance to the ITER reactor scale [Waltz 1990]. The m-index may represent components associated with a combination of well known electrostatic (no β dependence) linearly unstable drift waves [Horton 1999] like the ion temperature gradient (ITG) mode, the dissipative and collisional trapped electron modes (TEM), the collisional drift modes (CDM) or resistive g-modes at the edge which are assumed to act independently. Models before the mid-80's hoped to focus on the dominance of a single component; but it was finally recognized that the plasma core to edge spans an enormous range of collisionality and complex behavior: only a comprehensive “multi-mode” approach would suffice. The empirical coefficients (C_m) of these “multi-mode” components would have to fit a richer and ever expanding experimental database. A worldwide publicly available transport profile “ITER” database (from all tokamaks) was not assembled until the mid-90s. Before that only a patch work database of global energy confinement time was available.

In the late 80's, such gyroBohm scaling (power law) multi-mode quasi-theoretical models were used to construct “zero-dimensional” transport code models for the global energy confinement time (τ_E): $1/\tau_E = \sum_m \langle \chi_m^{gB} \rangle / a^2$ where $\langle \rangle$ represents some kind of global averaging [Waltz 1989a]. The coefficient of the dissipative TEM mode could be identified and fit with the empiri-

cal global confinement time scaling law for Ohmic heating (so-called NeoAlcator scaling); the Ohmic density saturation and beam heating scaling (so-called Goldston L-mode scaling) with the ITG and collisionless TEM [Waltz 1989b]. This provided the first evidence that electrostatic drift wave theory could provide the kernel of a comprehensive model. A persistent problem for such early models was to theoretically understand how the strong q (or current scaling) of the L-mode empirical scaling could arise from the collisionless drift scaling. Such quasi-theoretical local gyroBohm electrostatic drift wave models were considerably refined in the mid-90's with the Multi-Mode-Model (MMM95) [Kinsey 1996, Batemann 1998] for one-dimensional transport code simulation of the profiles. MMM95 was not restricted to a scaling law (power law) form for F which can't accurately describe critical ion temperature gradient (ITG) transport near threshold. In fact the core components of MMM95 are not described by analytic formulas for F . Instead at each subroutine call to the model, linear dispersion relations for simplified fluid model equations [Weiland 2000] are solved with the resulting mode frequencies and growth rates. These are substituted into quasi-linear theory relations for the transport flows which are normalized with a heuristically justified mixing length rule (as described in more detail below.)

In contrast to the empirical and quasi-theoretical models, the purely theoretical or (“first principles”) models take no information from experimental data but are fit to simulations and only then tested (not fit) against experimental data. If the test is unfavorable, something more must be added from the theory. By the mid-90's simulations of the core collisionless plasma turbulence became sufficiently realistic that they could be used to normalize (determine the strength of) the dominant (most important) ITG mode turbulence. The IFS/PPPL model [Kotchenreuther 1995] used the then state of the art gyrofluid local flux tube (gyroBohm scaled) simulations of toroidal ITG adiabatic electron (ITG-ae) turbulence [Waltz 1994, Beer 1996] to normalize a heuristic formula: roughly in the form $\chi_{gB}^{ITG-ae} = C (\rho_s^2/R) \sqrt{R/L_T - R/L_{T-crit}}$. The critical gradient R/L_{T-crit} was determined by a detailed fit to gyrokinetic linear stability. The gyrofluid (or gyro-Landau-fluid) model equations are comprised of the first 4 to 6 moments of the more fundamental gyrokinetic equations with a collisionless (Landau - wave particle resonant) dissipative closure chosen to represent gyrokinetic ballooning mode linear mode growth rate with near perfect accuracy. The corresponding nonlinear gyrofluid equations are much less expensive to simulate than gyrokinetic equations and they were used to find C . It turned out that C was much larger than expected from “back of the envelope” estimates. Given the known gyroBohm size of the experimental core values of χ , this meant that the $\sqrt{R/L_T - R/L_{T-crit}}$ factor had to be much smaller; core transport was then determined to be close to threshold and very “stiff”, i.e. sensitive to

the ion temperature gradient. Energy transport flux is poorly represented by a “Fick’s law” linear dependence on the temperature gradient $Q = -n\chi\partial T/\partial r$ if χ is not dependent on the gradient. Despite the fact that $\chi \equiv Q/(-n\partial T/\partial r)$ defines the local energy diffusivity, the IFS/PPPL model χ depends very strongly on $-\partial T/\partial r = T/L_T$ near threshold. The realization from simulations, that core transport could be stiff helped to resolve a longstanding problem for collisionless drift-wave models. Experimentally, $\chi(r)$ is known to significantly increase with radius r ; however the gyroBohm factor significantly decreases toward the cooler edge $(\rho_s^2/R)/\propto T^{3/2}$. If C is large and the core is stiff, the increase in $\chi(r)$ is easily accommodated since the local gradient R/L_T need only ride a little further above threshold to make $\sqrt{R/L_T - R/L_{T-crit}}$ increase with radius. The extreme stiffness of the IFS/PPPL model (and subsequent first principles models) proved to be a challenge to most transport codes with numerical methods designed to treat nearly diffusive (Fick’s law like) transport models. Special “D-V” transport code numerical methods have been proven adept at treating very stiff models. The IFS/PPPL ion model was accompanied by a model for the electron energy diffusivity based on the trapped electron mode quasilinear ratio with the ion energy ITG mode diffusivity. Nevertheless to construct more physically comprehensive theoretical models covering all the transport channels (electron and ion energy, plasma, impurity, momentum flows) as well as volumetric turbulent heating required a more rule based, systematic, and generalizable computational approach was needed.

The GLF23 model [Waltz1997] combined and generalized the methods used in the MMM95 and IFS/PPPL models to develop a physically comprehensive local gyroBohm which captured the q , and magnetic shear s dependence, as well as $\mathbf{E} \times \mathbf{B}$ shear stabilization documented in ITG-ae nonlinear gyrofluid simulations [Waltz 1994, Waltz1998]. The GLF23 model treated all channels equally based on per wavenumber and per branch quasilinear ratios. The mixing length rules for nonlinear saturation was based on two coefficients: one for the low-k ITG/TEM (and CDM) turbulence fit to ITG-ae simulations [Waltz1994]; and one for high-k ETG turbulence based on isomorphic ITG-ai gyrofluid simulations. (The specific forms for the quasilinear relations and mixing length rule wavenumber spectrum incorporating $\mathbf{E} \times \mathbf{B}$ shear are discussed in more detail below.) The model is based on linear ballooning mode solutions to 3-dimensional gyrofluid equations [Waltz1995]. The equations assign 4-moments to each ion species (protons and impurities): two moments to the untrapped electrons; and two to the trapped electrons. The trapped electrons are collisionally detrapped and untrapped electrons collisionally retrapped. The dimensionality is reduced from three to one, by treating only the most unstable $k_x = 0$ outward ballooning modes and representing the poloidal angle dependence with a trial wave function. A spectrum of 10 k_y modes

remains. (MMM95 uses only one k_y mode.) The moment equations are augmented with the standard finite gyroradius quasi-neutral Poisson relation for the perturbed potential ϕ_k (and Ampere’s law for $A_{||k}$). For a pure plasma, the GLF23 model requires the solution of a 8x8 dispersion relation- eigenvector matrices for each of the 10 k_y modes at each radius in the plasma. The equations and trial wave functions have about 10 parameters which were turned to fit the linear growth rates from the standard gyrokinetic ballooning mode code GKS. Many examples of the linear fits to linear gyrokinetic stability and the fit to nonlinear ITG-ai simulations (when the electron GLF equations are replaced by adiabatic electrons) have been provided [Waltz1997]. Without changing the fit coefficients, the GLF23 model with non-adiabatic electrons was found to give a good description of Beer’s ITG/TEM 6-moment gyrofluid simulations [Beer1996]. GLF23 gets the correct value for the MHD critical beta value. However GLF23 assumes the standard $s - \alpha$ infinite aspect ratio circular geometry which has a very low critical beta which is easily exceeded for real geometry elongated and shaped plasmas, thus in practice only the electrostatic version is used. For betas less than half the critical beta, $\mathbf{E} \times \mathbf{B}$ transport is weakly dependent on beta and magnetic flutter transport is small according to GLF23 and gyrokinetic simulations.

From 1995-97, the ITER Transport Working Group assembled a profile transport data base from all the major tokamak. From roughly 25 discharges, the database has grown to over one hundred. The Group defined various metrics to test various empirical and theoretical models against the database [Connor1996]. In predicting the total stored energy confinement time $\tau = W_{tot}/P_{input}$ (given the experimental boundary temperatures) from 28 discharges, GLF23 and IFS/PPPL could get RMS deviations of 22%. GLF23 had an offset of -5% and IFS/PPPL -15% (presumably because it did not include $\mathbf{E} \times \mathbf{B}$ shear stabilization) [Waltz1994, Waltz1998]. In this same “contest” [Waltz1997] the empirical global scaling laws (GSLs) ITER89P for L and ITER93H for H had 30% RMS deviation and +1% offset. A later fair contest in 1997 with 46 discharges between GLF23 and MMM95 reported RMS deviations of 27% and 15% with off-sets of +5% and -2%, respectively. (The GLF23 statistics were unchanged with 67 discharges.) A “fair contest” means same source data and transport code software was used, so that only the transport model is tested. The quasi-theoretical model MMM95 clearly did better than the purely theoretical model GLF23. However when GLF23 was allowed 2 experimentally adjusted parameters (The overall mixing rule strength and the $\mathbf{E} \times \mathbf{B}$ stabilization strength) it can compete with the impressive MMM95 statistics. However experimentally adjusted parameters is not allowed in a “first principles” model. When there is a clearly excessive deviation from experiment on a particular discharge or phenomenon, the first principles model must look for a better fit to better and more

realistic simulations, or add new detail and theoretical improvements to the model (e.g. add real geometry, nonlinear upshifted threshold, or some degree of non-locality). A “renormed GLF23” with 3.7x lower ITG and 40% less $\mathbf{E} \times \mathbf{B}$ shear stabilization gave a better fit to GYRO [Candy2003a] simulations, and a 17-fold non-isomorphy based on gyrokinetic ETG-ai simulations [Dorland 2000], produced a 8.7% RMS deviation over 50 DIII-D, JET, and C-mod discharges [Kinsey 2003]. Note the GSLs themselves have RMS deviations of at least 10% and the per discharge uncertainty is about 10%. Despite the fact that most empirical models have numerous adjustable coefficients, the empirical and other less sophisticated theoretically motivated models have somewhat poorer statistics ranging from 23 to 37% [Konings1997]. It is important to realize that predicting the total stored energy or indeed total energy confinement time is not the true figure of merit. That is reserved for fusion product $nT\tau = W_{\text{tot}}^2 / (3V_{\text{tot}} P_{\text{input}}) \propto Q$ the fusion performance. The RMS deviations and off-sets for $nT\tau$ are usually 2-fold larger than for τ . Secondly, what a core transport model really predicts is not the total stored energy W_{tot} but the incremental stored energy W_{inc} stored over the given boundary conditions of T_{ped} and n_{ped} ($W_{\text{ped}} = 3V n_{\text{ped}} T_{\text{ped}}$; $W_{\text{tot}} = W_{\text{ped}} + W_{\text{inc}}$). The RMS deviations for W_{inc} are typically 1.5-fold larger than for W_{tot} .

Predicting H-mode edge pedestal height is key challenge to transport models

This brings us to the key challenge for transport modeling and confinement theory, and ITER: How to predict the high H-mode T_{ped} . While there is a growing confidence that ITER core confinement can be predicted with increasing accuracy as theoretical transport models are improved, there is no theoretical prediction for the H-mode T_{ped} (or W_{ped}) and even a poor understanding of the mechanisms required to predict the H-mode power threshold. Due to the stiff nature of core transport the performance Q is highly dependent on T_{ped} as illustrated in Fig. III.3.1.

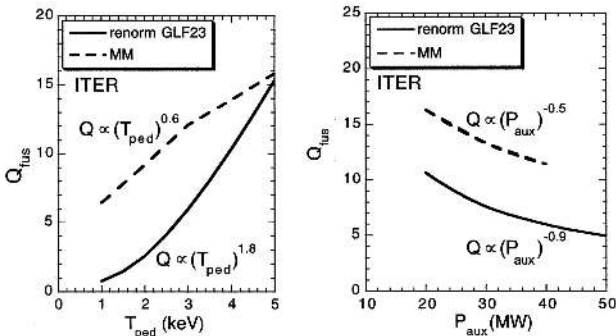


Fig. III.3.1 ITER performance Q projection vs T_{ped} at $P_{\text{aux}}=40$ M (a) and vs P_{aux} at $T_{\text{ped}}=3$ keV (b). The “renormed GLF23” model has an 8.3% RMS deviation to 50 H-mode DIII-D, JET, CMod discharges. From [Kinsey 2003]

As indicated the GLF23 model is considerably stiffer than the MMM95 model as expected. A perfectly stiff model would have $Q \propto (n_{\text{ped}} T_{\text{ped}})^2 / (P_{\text{aux}} V_{\text{tot}})$. Purely empirical scaling laws for W_{ped} or T_{ped} (typically $\propto 1/n_{\text{ped}}$) are no better than 30%. While there are fairly accurate predictions of maximum pedestal pressure given the pedestal width from ELM low- n ideal MHD stability codes [Synder 2004], there is no prediction for the width of the pedestal good confinement layer ($T_{\text{ped}} = (\Delta_{\text{ped}}) / n_{\text{ped}} dP_{\text{ped}} / dr$). To predict T_{ped} , one must average over ELM cycles (about 30% of the power flow) and account for the remaining losses from $\mathbf{E} \times \mathbf{B}$ shear suppressed turbulent transport, orbit losses, and radiation. Edge physics is discussed in Sec. III.7. There has actually been little transport code modeling work done for the H-mode edge and gyrokinetic simulations have only just begun. It is not even clear that the scale separation requirement for transport models is justified. “Full-f” gyrokinetic codes are required. We should have no illusions: ITER was designed from empirical global scaling laws (GSLs) for W_{tot} , because even the most reliable theoretical core transport model must rely on a more uncertain empirical scaling for W_{ped} . Core transport models play a only supportive role for now. The “best” of the GSLs typically sit a shallow minimum of the RMS deviation. Theoretical models favor some GSLs over others.

Recipes and rules for construction of theoretical transport models

Returning to the theoretical basis of transport models, it is useful to discuss in more detail some key ingredients of the theoretical models: the quasilinear recipe, nonlinear mixing length rules, and $\mathbf{E} \times \mathbf{B}$ shear stabilization rules. While theoretical models are allowed any number of adjustable parameters to best fit the database of nonlinear gyrokinetic simulations, experience argues that these heuristic rules are a useful guide if not inflexibly applied:

Theoretical transport models start with the assumption of scale separation (or decomposition) of the distribution $f = f_0 + \delta f$ into a dynamical equation for the turbulent perturbations δf

$$\partial \delta f / \partial t + (\vec{v}_E^0 + \delta \vec{v}_E) \cdot \vec{\nabla} \delta f + \delta \vec{v}_E \cdot \vec{\nabla} \langle f_0 \rangle + \dots = \vec{\nabla}_x \cdot \langle \delta \vec{v}_E \delta f \rangle \quad (\text{III.3.1})$$

and a radial transport equation (with a source S) for the statistical and flux surface average $\langle \rangle$ distribution f_0

$$\partial \langle f_0 \rangle / \partial t + \vec{\nabla}_x \cdot \langle \delta \vec{v}_E \delta f \rangle + \dots = S \quad (\text{III.3.2})$$

where we have ignored (...) the curvature drift and parallel motions, collisions, and have only noted the $\mathbf{E} \times \mathbf{B}$ motion from the Doppler rotation $\vec{v}_E^0 = cb \times \vec{\nabla}_r \varphi_0 / B$ perturbed electric field $\delta \vec{v}_E = cb \times \vec{\nabla} \delta \varphi / B$. (x means radial direction.) The perturbed electric field $\delta \varphi$ is obtained from the Poisson (or quasi-neutrality equation derived from the charge density associated with δf . $\delta \vec{v}_E \cdot \vec{\nabla}_x \langle f_0 \rangle = -i\omega_*(v) \langle f_0 \rangle \nabla_x (\ln \langle f_0 \rangle)$ in

Eq. (III.3.1) is the key drift wave frequency term dependent on the plasma gradients driving the linear instabilities. The radial $\mathbf{E} \times \mathbf{B}$ turbulent flux $\langle \delta v_{E_r} \delta f \rangle$ dominates the transport. This electrostatic transport can be supplemented by so called magnetic flutter transport flux $\langle v_{\parallel} (\delta B_{\perp x} / B_0) \delta f \rangle$ when the perturbed magnetic field is included. Simulations suggest this transport is important for beta values exceeding about half the critical beta. (The dominant $\mathbf{E} \times \mathbf{B}$ nonlinearity $\delta \vec{v}_E \cdot \nabla \delta f$ is similarly augmented $v_{\parallel} (\delta \vec{B}_{\perp} / B_0) \cdot \vec{\nabla} \delta f$). Turbulent transport in the ion energy transport channel can be added to the sometimes significant neoclassical losses $\nabla_x \cdot \langle v_{dr} f_0 \rangle$ in Eq. (III.3.2). There is a much smaller nonlinearity, the so called “parallel nonlinearity”, which can provide some small turbulent heating in the transport equation Eq. (III.3.2) but is otherwise ignorable in the dynamical Eq. (III.3.1). The particle, energy, and momentum moments of Eq. (III.3.2) are the transport equations, and the transport model supplies the moments of $\langle \delta v_{E_r} \delta f \rangle$ (and $\langle v_{\parallel} (\delta B_{\perp x} / B_0) \delta f \rangle$).

To proceed with a making a model of the turbulent fluxes $\langle \delta v_{E_r} \delta f \rangle$, Eq. (III.3.1) is Fourier analyzed into cross field wave number modes $[k_r, k_y]$ with linear frequency and growth rates $[\omega_k, \gamma_k]$. Linearizing Eq. (III.3.1) a linear dispersion relation gives (the eigenvalues) $[\omega_k, \gamma_k]$ and a complex linear relation for $\delta f_k = F_k(\omega_k + i\gamma_k) \delta \varphi_k$ (eigenvector) is obtained. The quasilinear fluxes follows from summing over the k-modes and branches: $\sum_k \langle \delta v_{E_r-k} \delta f_k \rangle = \sum_k \langle (i c k_y / B) F_k(\omega_k + i\gamma_k) \delta \varphi_k \rangle$. Note this quasilinear recipe is used MMM95 and GLF23, and well supported with simulations. It differs in important detail from the “quasilinear theory” often found in text books.

To obtain the strength of the turbulence a much less precise mixing length rule for the nonlinear saturation spectrum of $|\delta \varphi_k|$. One can not derive a mixing length rule. The theoretical motivation for such heuristic rules have changed little from Kadomtsev’s 1965 Plasma Turbulence except now we can test them against simulations. Balancing the $\mathbf{E} \times \mathbf{B}$ nonlinearity against the time derivative: $\partial \delta f / \partial t \sim \delta \vec{v}_E \cdot \vec{\nabla} \delta f \Rightarrow [\omega_k, \gamma_k] \sim (c k_y / B) k_x \delta \varphi_k$. If the balance is against frequency given by the drift wave frequency $\omega_k \sim \omega_{*k}$, the “strong rule” results. This equivalent is to balancing the nonlinear term against $\delta v_{E_r} \cdot \nabla_r \langle f_0 \rangle$. Since the electrons are nearly adiabatic, this takes the familiar form $e \delta \phi_k / T_0 \sim \delta n_k / n_0 \sim 1 / k_x L$ where $1/L$ is a the inverse gradient length driving the instabilities. This is really an upper bound saying that the turbulence can do no more than wipe out a driving gradient. It does not account for the generally observed linear threshold of the turbulence which can only be obtained by balancing against the growth rate: the “weak rule” results in $e \delta \varphi_k / T_0 \sim (\gamma_k / \omega_{*k}) (1 / k_x L)$. Typically $k_x \propto k_y$ is used with $k_y \propto \rho_s^{-1}$ required to preserve gyroBohm scaling. The weak rule is used in most of MMM95. An intermediate rule like $e \delta \varphi_k / T_0 \sim (\gamma_k / \omega_{*k})^{1/2} \omega_{*k} (1 / k_x L)$ seems to give better agreement with the scaling of actual sim-

ulations. Note that only $k_y > 0$ drift-ballooning modes produce turbulent transport, so the mixing rule refers only to $|\varphi_k|^2$ in the quasilinear flux with $k_y > 0$. These mixing rules seem at odds with the modern understanding of nonlinear drift mode saturation: saturation is due almost entirely to $\mathbf{E} \times \mathbf{B}$ shearing from the $k_y = 0$ and $k_x > 0$ neutrally stable zonal flows [Diamond2005] or radial modes [Waltz 1994] nonlinear pumped by the unstable $k_y > 0$ drift modes. GLF23 [Waltz1997] used $e \delta \varphi_k / T_0 \sim [(\gamma_k \omega_{dk})^{1/2} / \omega_{*k}] (1 / k_x L)$ to reflect the fact that excited radial modes algebraically decay to a residual zonal flow at the a curvature drift rate ω_{dk} . Faster decay should result in increased transport. In the end any dimensionally consistent form preserving gyroBohm scaling and best fitting all parametric variations of the simulations is chosen. Finally it is crucially important to account for $\mathbf{E} \times \mathbf{B}$ shear stabilization in the mixing rule. (This is shear in the Doppler rotation term of Eq. (III.3.1). In GLF23 this was done with by replacing γ_k with $\gamma_{net,k} = \gamma_k - \alpha_E \gamma_E$ in the mixing rule. α_E is adjusted to match the $\mathbf{E} \times \mathbf{B}$ shear quench point of gyrofluid or gyrokinetic simulations where $\gamma_{E-quench} = \gamma_{k,max} / \alpha_E$. Recent gyrokinetic simulations [Kinsey2005] including kinetic electrons set $\alpha_E \sim 0.5(s - \alpha \text{ circle})$ and 0.8 ($\kappa = 2$ real geometry). Only low-k ITG/TEM transport can be quenched. Some ETG transport always remains for the highest attainable levels of γ_E .

If a fast dispersion theoretic δf linear gyrokinetic code were available, it would be preferable to use that for Eq. (III.3.1). Most gyrokinetic codes are initial value codes and linear mode convergence is problematic near thresholds. So gyrofluid moments of Eq. (III.3.1) are used. The latest most elaborate gyrofluid models (discussed below) can produce linear mode growth rates and frequency spectra, eigenfunctions more than 10,000x faster than initial value gyrokinetic codes to within an accuracy of 10-15% over some 30 parameter scans. This level of difference is comparable to that between various gyrokinetic code. Gyrofluid equations are just moments of the gyrokinetic equation. The moment hierarchy relies on a collisionless but dissipative closures to model Landau damping or curvature drift resonance broadening [Waltz1992]. For example, ignoring finite gyroradius and curvature drift, a three moment model has plasma response function similar to the famous 3-pole approximation to the Z-function.

Way forward to improved theoretical transport models

Work is in progress to develop a much more advanced and physically comprehensive gyrofluid transport model. Once again the goal is to find the best and most accurate fit to a broad spectrum of the most physically comprehensive gyrokinetic simulations available. A transport database is available on the GYRO [Candy2003a] website <http://fusion.gat.com/comp/parallel/>. Kinsey has assembled over 350 nonlinear flux tube (gyroBohm) simulation scanning a wide parameter space. Many “full

physics” global GYRO simulations of Bohm scaled L-mode and gyroBohm scaled H-mode simulations of DIII-D discharges are also available. An improved model must fit all these. Here we discuss some of the directions being taken and issues to be addressed by the improved models.

Staebler et al. [Staebler 2005] has developed a much more accurate gyrofluid closure equations to be incorporated in a replacement for GLF23. The model will be called TGLF because the gyrofluid equations more naturally include the trapped particles.

15 electron gyrofluid moments replace 2 passing fluid moments and 2 trapped fluid moments. This allows the TEM low-k modes and the ETG high-k modes to be spanned seamlessly. Trapped ions are likely unimportant so a 6-moment [Beer1996] ion gyrofluid model can stand in for the equivalent 15-moment model. In addition, whereas GLF23 has a single poloidal trial Gaussian wave function, the new model will have as many as 4 Hermite polynomials to represent the extended poloidal ballooning angle. Thus for a pure plasma of ions and electrons (impurities are easily added), the GLF23 8×8 matrix solutions (per mode) are replaced by 96×96 $[(15+9) \times 4 = 96]$. It is still only about 10x slower than the GLF23 linear solve, but cluster computers are much faster a decade later. Real shaped geometry via the Miller-Waltz formulation [Waltz1999] have been added to collisions, finite-beta. These have all tested well against the GYRO gyrokinetic code. Accuracy in linear rates over 30 parameter scans is 10-15% compared to 10-60% for GLF23. (GLF23 can be worse for some pedestal of negative central shear scans.) The 4 Hermite polynomials are needed to describe the real geometry distortions and should provide a better treatment of viscosity (broken wave function parity). Presently only the most unstable $k_x = k_y s \sqrt{0} = 0$ (i.e. outward ballooning modes $\theta_0 = 0$) are included in the quasilinear spectrum. $\mathbf{E} \times \mathbf{B}$ shear linearly couples modes with the same $k_y = nq/r$ but different θ_0 s. There is some speculation that expanding the dispersion matrix to include many θ_0 s, a linear “quasi-ballooning” eigenmode (with an average $\langle \theta_0 \rangle \neq 0$) could be found. Its growth rate could replace $\gamma_{k.net}$ in the mixing length rule and the approximate $\mathbf{E} \times \mathbf{B}$ shear stabilization quench rule could be replaced with a more precise linear growth rate calculation. It also appears possible to build in a nonlinear upshift in the ITG threshold (i.e. the low-q Dimits shift.) by a simple k-independent subtraction in $\gamma_{k.net}$.

A variety of local mixing length rules are being tested with the TGLF model using automated fit routines. Perhaps the most challenging issue to be addressed by an improved model is how to quantify the nonlocality and broken gyroBohm scaling found in physically comprehensive GYRO simulations of DIII-D. Up to now all models discussed are local (dependent only on local gradients) and have exact gyroBohm scaling. These are approximations strictly valid only in the limit of vanishing ρ_* . While core experimental transport lev-

els are always gyroBohm sized and ITER will have ρ_* values less than 0.1%, precisely dimensionally similar DIII-D L-mode discharges and corresponding GYRO simulations show clear evidence of Bohm scaling at ρ_* less than 1%. Note precision measurement and profile similarity [Waltz2006] is important in quantifying broken gyroBohm scaling because single machine experiments can only vary ρ_* by 1.60fold (in DIII-D). The experimental separation between Bohm and gyroBohm scaling with this variation corresponds to just a 17% difference in the temperature (i.e. just outside 10% error bars)[Waltz2005c]. Normed to gyroBohm, a Bohm scaled diffusivity is just 1.6-fold smaller than a gyroBohm scaled diffusivity on increasing ρ_* by 1.6-fold. GYRO simulations show that this is easily compensated by a 10% decrease in the ion temperature gradient. This is a simple measure of core stiffness. It is now well understood from recent global gyrokinetic simulations [Lin2002, Waltz2002, Candy2003b, Waltz2005b, Waltz2006] that Bohm scaling results from local profile shearing over the local ballooning modes or more importantly nonlocal profile variation in the local mode growth rates. It has been speculated [Waltz2005a] that nonlocality and broken gyroBohm scaling can be accurately incorporated into theoretical transport models by replacing $\gamma_{k.net}$ in the local mixing rule with a locally averaged $\langle \gamma_{k.net} \rangle$. The local averaging extends over a nonlocality length $L_{nonlocal}/a \propto \rho_*$. Regression to locality and gyroBohm scaling at vanishing ρ_* is guaranteed.

It may be instructive to end this discussion contrasting the empirical approach to model building based on fits to experiments with the theoretical approach based on fits to simulations in regard to how gyroBohm scaling is broken. Theory and simulation [Garbet1996, Waltz2006] have demonstrated this paradigm: $\chi = \chi(0)\chi_{gB}[1 - \rho_*/\rho_{*crit}]$. The minus sign indicates a stabilization process at work. As ρ_* becomes sufficiently small, the local gyroBohm diffusivity $\chi = \chi(0)\chi_{gB}$ results. At an intermediate $\rho_* = 2\rho_{*crit}$, the local diffusivity near this ρ_* is half its local gyroBohm scaled value and has the Bohm ρ_* -scaling: $\chi/[\chi(0)\chi_{gB}] = (1/2)(\rho_{*crit}/\rho_*)$. This is precisely the same as $\chi = [(1/2)\rho_{*crit}]\chi(0)\chi_B$ which is much smaller in size than in size than $\chi(0)\chi_B$. Here $\chi_{gB} \equiv [c_s/a]\rho_s^2$ and $\chi_B \equiv c_s\rho_s \equiv \chi_{gB}/\rho_*$. This theoretical paradigm has the happy result that ITER is guaranteed gyroBohm scaling. In contrast a well know “mixed Bohm-gyroBohm” empirical model [Erba1998] with poor theoretical motivation, counts Bohm and gyroBohm as separate processes: $\chi = \chi(0)\chi_B[1 + \rho_*/\rho_{*norm}]$. The empirical paradigm unfortunately suggests that reactor (ITER) scale tokamaks will tend to Bohm scaling rather than gyroBohm going to very small ρ_* .

References

- [Bateman 1998] G. Bateman, A. H. Kritz, J. E. Kinsey, et al. 1998, Phys. Plasmas, 5: 1793
- [Beer 1996] M. A. Beer, G. W. Hammett. 1996, Phys. Plasmas, 3: 4018
- [Candy 2003a] J. Candy, R.E. Waltz. 2003, J. Comp. Phys., 186: 545
- [Candy 2003b] J. Candy, R.E. Waltz. 2003, Phys. Rev. Lett., 91: 45001
- [Connor 1996] J. W. Connor, et al. 1996, Fusion Energy 16th IAEA, Montreal 2: 935 IAEA-CN-64/FP-21
- [Dorland 2000] W. Dorland, F. Jenko, M. Kotschenreuther, et al. 2000, Phys. Rev Lett., 85: 5579
- [Diamond 2005] P. H. Diamond, S.-I. Itoh, K. Itoh, et al. 2005, Plasma Phys. Control. Fusion, 47: (2005)
- [Erba 1998] M. Erba, T. Aniel, V. Basiuk, et al. 1998, Nucl. Fusion, 38: 1013
- [Garbet 1996] X. Garbet, R. E. Waltz. 1996, Phys. Plasmas, 3: 1898
- [Horton 1999] W. Horton. 1999, Rev. Mod. Phys., 71: 735
- [Kadomtsev 1965] B. B. Kadomtsev. 1965, Plasma Turbulence. New York: Academic Press
- [Kinsey 1996] J. E. Kinsey, G. Bateman. 1996, Phys. Plasmas, 3: 3344
- [Kinsey 2003] J. E. Kinsey, G. M. Staebler, R. E. Waltz. 2003, Fus. Sci. & Tech., 44: 763
- [Kinsey 2005] J. E. Kinsey, R.E. Waltz. J. Candy. 2005, Phys. Plasmas, 12: 62302
- [Kinsey 2006] J. E. Kinsey, R.E. Waltz. J. 2006, Candy. Phys. Plasmas, 13: 22305
- [Konings 1997] J. A. Konings, R. E. Waltz. 1997, Nucl. Fusion, 37: 863.
- [Kotschenreuther 1995] M. Kotschenreuther, W. Dorland, M. A. Beer, et al. 1995, Phys. Plasmas, 2: 2381
- [Lin 2002] Z. Lin, S. Ethier, T. S. Halm, W. Tang. 2002, Phys. Rev. Lett., 88: 195004
- [Snyder 2004] P. B. Snyder, H. R. Wilson, et al. 2004, Nucl. Fusion, 44: 320
- [Staebler 2005] G. M. Staebler, J. E. Kinsey, R. E. Waltz. 2005, Phys. Plasmas, 12: 102508
- [Waltz 1989a] R. E. Waltz, R. R. Dominguez, F. W. Perkins. 1989, Nuclear Fusion, 29: 351
- [Waltz 1989b] R. E. Waltz. 1989, Nagoya Lectures in Plasma Physics and Controlled Fusion, Tokai University Press, p. 357 (Tokyo)
- [Waltz 1990] R. E. Waltz, J. C. DeBoo, M. N. Rosenbluth. 1990, Phys. Rev. Lett., 65: 2390
- [Waltz 1992] R. E. Waltz, R. R. Dominguez, G. W. Hammett. 1992, Phys. Fluids B, 4: 3138
- [Waltz 1994] R. E. Waltz, G. D. Kerbel, J. Milovich. 1994, Phys. of Plasmas, 1: 2229
- [Waltz 1995] R. E. Waltz, G. D. Kerbel, J. Milovich, et al. 1995, Phys. of Plasmas, 2: 2408
- [Waltz 1997] R. E. Waltz, G. M. Staebler, G.W. Hammett, et al. 1997, Phys. Plasmas, 4: 2482
- [Waltz 1998] Waltz, R. E. Dewar, R. L. Garbet, X. 1998, Phys. Plasmas, 5: 1784
- [Waltz 1999] R. E. Waltz, R. M. Miller. 1999, Phys. Plasmas, 6: 4265
- [Waltz 2002] R. E. Waltz, J. Candy, M. N. Rosenbluth.

2002, Physics of Plasmas, 9: 1938

[Waltz 2005a] R. E. Waltz, J. Candy. 2005, Phys. Plasmas 12, 072303

[Waltz 2005b] R. E. Waltz, J. Candy, F. L. Hinton, et al. 2005, Nucl. Fusion, 45: 741

[Waltz 2005c] R. E. Waltz. 2005, Fus. Sci. and Tech., 48: 1051

[Waltz 2006] R. E. Waltz, J. Candy, C. C. Petty. 2006, Phys. Plasmas, 13: 072304

[Weiland 2000] J. Weiland. 2000, Institute of Physics Publishing Ltd (Bristol and Philadelphia)

III.4 Nonlinear MHD simulations (G. Y. Fu)

III.4.1 Introduction

Understanding MHD instability dynamics is a key issue for burning plasmas. Important MHD modes ranging from the plasma center to the edge include sawtooth oscillations and fishbone (center), ballooning modes and neoclassical tearing modes (core), external kink-ballooning modes (core/edge), and peeling-ballooning modes or edge localized modes (edge). In particular, sawtooth oscillations affect the central plasma profiles and can seed neoclassical tearing modes. Neoclassical tearing modes, ideal ballooning modes and kink modes all set a limit to the plasma beta, above which the plasma is vulnerable to disruptions. ELM dynamics determines the H-mode pedestal's height and width, which in turn determines the core plasma confinement.

In the past decade, significant progress has been made in MHD and extended MHD simulations of fusion plasmas. Many modern 3D nonlinear MHD and extended MHD codes [Park99, Sovinec04, Popov01, Xu02, Lutjens01, Huysmans05, Schnack06] have been developed with advanced numerical methods such as high order finite elements, implicit time advance, unstructured mesh, field aligned coordinates and domain decompositions for parallel computing. State of the art extended MHD models have been developed [Schnack06], including simplified two fluid models with drift ordering [Sugiyama00], heuristic closures for neoclassical tearing modes [Giannakon02] and kinetic closures for energetic particles [Park99]. Simulations of sawtooth and fishbone oscillations [Breslau05, Fu06], major disruptions [Kruger05], neoclassical tearing modes [Popov02, Giannakon02], and edge localized modes [Snyder05, Brennan05] in tokamaks have been made possible through massively parallel computations. Here we present a review of a selection of recent work in nonlinear MHD simulations and suggest important problems for future work.

III.4.2 MHD and extend MHD models

MHD and extended MHD equations can be derived from the general plasma kinetic equation and are writ-

ten as follows:

$$\frac{d\mathbf{n}_\alpha}{dt} = \mathbf{n}_\alpha \nabla \cdot \mathbf{V}_\alpha \quad (\text{III.4.2.1})$$

$$\rho_i \frac{d\mathbf{V}_i}{dt} = -\nabla p - \nabla \cdot \Pi_i - \nabla \cdot \mathbf{P}_h + \mathbf{J} \times \mathbf{B} \quad (\text{III.4.2.2})$$

$$\mathbf{E} + \mathbf{V}_i \times \mathbf{B} = \eta \mathbf{J} - \frac{1}{n_e} [\mathbf{J} \times \mathbf{B} - \nabla p_e - \nabla \cdot \Pi_i] \quad (\text{III.4.2.3})$$

$$\frac{n_\alpha}{\Gamma - 1} [\partial \mathbf{T}_\alpha / \partial t + \mathbf{V}_\alpha \cdot \nabla \mathbf{T}_\alpha] = -\mathbf{T}_\alpha \cdot \nabla \cdot \mathbf{V}_\alpha - \nabla \cdot \mathbf{q}_\alpha + Q_\alpha \quad (\text{III.4.2.4})$$

$$\mathbf{J} = \nabla \times \mathbf{B}, \quad \frac{\partial \mathbf{B}}{\partial t} = -\nabla \times \mathbf{E} \quad (\text{III.4.2.5})$$

where n_α , T , and Q are the density, temperature, heat flux and heating term respectively of the species α . In addition, ρ_i is the thermal ion mass density, p is the thermal pressure, P_h is the energetic particle pressure tensor, Π_i and Π_e are the ion and electron stress tensors respectively, p_e is the electron pressure.

In deriving this set of extended MHD equations, we have assumed zero electron mass and neglected the electron stress tensor in the momentum equation. Also we have neglected the inertial term for fast ions, appropriate for a low fast ion density. To close this set of equations, we still need to specify P_h , Π_i , Π_e and q . For a collisional plasma, the electron and ion stress tensors and heat flux are given in Braginskii's equations with recent corrections by Catto and Symakov [Catto05, Symakov05]. In collisionless plasmas, a general form of ion stress tensor has been recently derived by [Ramos05]. The fast ion pressure tensor can be calculated kinetically using the drift-kinetic or gyrokinetic equation [Fu06].

Solving the system of equations above for a magnetically confined fusion plasma is an extremely challenging problem because many different time and spatial scales are present [Schnack06]. This is true even for the resistive MHD model. For example, to evolve a slowly growing tearing mode, one has to resolve the small radial scale length associated with plasma resistivity. One also needs to deal with stiffness of the equations due to compressional Alfvén waves and shear Alfvén waves. Recently this difficult problem has been solved [Sovinec04] by using a semi-implicit scheme, a high order finite element method, and parallel computing. The semi-implicit scheme allows a time step much larger than the CFL criterion would permit. High order finite element methods with radial mesh packing can resolve efficiently the very small scales associated with tearing modes. Finally parallel computing enables simulations with high resolutions and many Fourier modes.

III.4.3 Recent results of MHD and extended MHD simulations

Here we highlight some recent 3D nonlinear simulations in tokamak plasmas. The modes simulated are sawtooth, fishbone, disruption, Neoclassical tearing

modes and ELMs. This is a very brief review of selected topics, meant to illustrate major recent advance in 3D nonlinear MHD and extended MHD simulations.

A. Sawtooth oscillations in CDX-U

Sawtooth oscillations in the CDX-U spherical tokamak have recently been simulated [Breslau06] using the multi-level 3D extended MHD code M3D [Park99]. Initial studies were conducted with a relatively simple resistive MHD physics model. Using an on-axis Lundquist number $S = 2 \times 10^4$, consistent with the experiment, sawtooth oscillations of a few cycles were successfully reproduced. The sawtooth period for a case that retained 10 toroidal modes was found to be approximately 100 μs ; consistent with the experimental value of 125 μs . A follow-up study was conducted in which the ion diamagnetic term from the two-fluid model was turned on. The most significant effect of this change is the induced rotation of the plasma. The sheared plasma rotation notably suppresses the island growth so that the magnetic field no longer passes through a stochastic state.

B. Nonlinear dynamics of fishbone instability in tokamaks

The fishbone [McGuire83] is an $(n, m) = (1, 1)$ kink mode driven resonantly by the precession of energetic trapped particles. Extensive simulations of the fishbone have been carried out using the MHD/particle hybrid model of M3D [Fu06]. In the model, the thermal electrons and ions are treated as an ideal fluid while the energetic species is described by the drift-kinetic equation. The effects of energetic particles are coupled to the MHD equations via the stress tensor term in the momentum equation. Nonlinear simulations showed mode saturation and strong mode frequency due to nonlinear flattening of the energetic particle distribution. The saturation level is reduced by the MHD nonlinearity.

C. Tokamak major disruptions

Nonlinear simulations of a major disruption in a DIII-D plasma were carried out [Kruger05] using the NIMROD code [Sovinec04]. The full resistive MHD model is used with thermal conduction and free boundary condition. The model is justified because the disruption is much faster than other time scales. The simulation started from an $n = 1$ ideal MHD mode and the nonlinear evolution of this mode leads to a stochastic magnetic field. The corresponding parallel heat transport leads to a localization of the heat flux that is deposited on the wall. This calculated heat flux localization is consistent with experimental measurements.

D. Neoclassical tearing modes

Neoclassical tearing modes in the DIII-D tokamak have been investigated using the nonlinear full toroidal code, NFTC [Popov01, Popov02], which is based on the 3D MHD equations including transport effects and neoclassical effects. An effective fully implicit numerical scheme allows the transport profile to evolve self-consistently with the nonlinear MHD instabilities and externally applied sources. Simulation results showed [Popov02] that the seed island from a sawtooth crash is

big enough to exceed the threshold size for excitation of neoclassical tearing modes with $(m, n)=(3, 2)$. Simulations in reversed shear plasmas showed that the seed island can also be generated from conventional tearing modes through nonlinear mode coupling.

NTMs have also been simulated successfully using the NIMROD code with poloidal flow damping closure [Giannakon02]. The numerical results compared well with theory in term of poloidal flow damping, growth rate reduction due to the neoclassical enhancement of the polarization current, and amplification of neoclassical tearing modes due to perturbed bootstrap currents.

E. Edge localized modes

Edge localized modes (ELM) are extremely important for ITER since they can cause a large outgoing energy flux to the wall. Recently there are many nonlinear simulations carried out to investigate their nonlinear behaviors. Here we mention a few of them. A relatively earlier work was from the BOUT code[Xu02], which was used to simulate the dynamics of edge localized modes (ELMs) driven by intermediate wavelength peeling-ballooning modes. It was found that the early behavior of the modes is similar to expectations from linear, ideal peeling-ballooning mode theory, with the modes growing linearly at a fraction of the Alfvén frequency. In the nonlinear phase, the modes grow explosively, forming a number of extended filaments which propagate rapidly from the outer closed flux region into the open flux region toward the outboard wall. The results of explosive instability agree qualitatively with theory of Wilson and Cowley [Wilson 02].

More recent nonlinear simulations have been carried out using extended MHD codes including M3D [Strauss 06], NIMROD [Sovinec 06], and JOEAK [Huysmans 06]. Simulations of ELMs in DIII-D using M3D [Strauss 06] showed a full cycle of ELM clash and subsequent relaxation of the pressure pedestal. The density perturbations were large relative to temperature perturbations. NIMROD simulations of ELMs in DIII-D [Sovinec06] showed that the linear growth rate and mode structure are similar to those from the ELITE code [Wilson02]. Nonlinear simulation results showed complex mode structures with a high temperature region flowing outward. With flow shear, the radial propagation of the mode structure is limited. However, the energy loss remains large.

III.4.4 Future challenges

In the past decade, significant advances have been made in simulating key MHD modes in tokamak plasmas using advanced numerical methods and massively parallel computation. However, challenging problems remain to be solved in the future for an integrated, long time, comprehensive simulation of MHD modes in fusion plasmas such as ITER. In the numerical method area, there is still open question on the most efficient finite element method. Is it regular Lagrangian element or spectral element? Is it low continuity element or

high continuity element [Jardin05]? Another question deals with optimal mesh distribution. There is question whether field aligned meshes can be used effectively for both global modes as well as localized modes. In the area of closures, it is still debated whether we can find good fluid closures for high temperature future plasmas. If not, are kinetic closures feasible for slow MHD modes such as NTM? Even more uncertain is the feasibility of pure kinetic simulations of global MHD modes. Finally, in the integrated simulation area, work has just begun to do integrated simulations of MHD modes together with energetic particles, RF heating and plasma turbulence. This requires multiscale simulation which is one of greatest challenges in fusion plasma simulations.

References

- [Breslau 06] J. Breslau, et al. Proceedings of 2006 American Physical Society Division of Plasma Physics Meeting, Denver, Colorado, paper GI2.
- [Catto 05] P. J. Catto, A. N. Symakov. 2005, Phys. Plasmas, 12: 114503
- [Fu 06] G. Y. Fu, W. Park, H. R. Strauss, et al. 2006, Phys. Plasmas, 13: 052517
- [Giannakon 02] T. A. Giannakon, S.E. Kruger, C.C. Hegna. 2002, Phys. Plasmas, 9: 536
- [Huysmans 05] G. T. A. Huysmans, et al. 2005, Plasmas Phys. Cont. Fusion, 47: 2107
- [Huysmans 06] G. T. A. Huysmans, et al. Proceeding of 2006 IAEA Fusion Energy Conference, Chengdu, China, paper TH/P8-2.
- [Jardin 05] S. C. Jardin, J. A. Breslau. 2005, Phys. Plasmas, 12: 056101
- [Kruger 05] S. E. Kruger, D. D. Schnack, C. R. Sovinec, et al. 2005, Phys. Plasmas, 12: 056113
- [Lutjens 01] H. Lutjens, J. F. Luciani, X. Garbet. 2001, Plasma Phys. Control. Fusion, 43: A339
- [McGuire 83] K. McGuire, R. Goldston, M. Bell, et al. 1983, Phys. Rev. Lett., 667 50, 891
- [Park 99] W. Park, E. V. Belova, G.Y. Fu, et al. 1999, Phys. Plasmas, 6: 1796
- [Popov 01] A. M. Popov, V. S. Chan, M. S. Chu, et al. 2001, Phys. Plasmas, 8: 3605
- [Popov 02] A. M. Popov, R.J. La Haye, Y.Q. Liu, et al. 2002, Phys. Plasmas, 9: 4205
- [Ramos 05] J. J. Ramos. 2005, Phys. Plasmas, 12: 112301
- [Schnack 06] D. D. Schnack, D. C. Barnes, D. P. Brennan, et al. 2006, Phys. Plasmas, 13, 058103
- [Snyder 05] P. B. Snyder, H. R. Wilson, X. Q. Xu. 2005, Phys. Plasmas, 12: 056115
- [Sovinec 04] C. Sovinec, et al. 2004, J. Comput. Phys., 195: 355
- [Sovinec 06] C. Sovinec, et al. proceeding of 2006 IAEA Fusion Energy Conference, Chengdu, China, paper TH/P8-3
- [Strauss 06] G. T. A. Huysmans, et al. Proceeding of 2006 IAEA Fusion Energy Conference, Chengdu, China, paper TH/P8-6

- [Sugiyama 00] L. E. Sugiyama, W. Park. 2000, Phys. Plasmas, 7: 4644
 [Symkov 05] A. N. Symakov, P. J. Catto. 2005, Phys. Plasmas, 12: 012105
 [Wilson 02] H. R. Wilson, P. B. Snyder, G. T. A. Huysmans, et al. 2002, Phys. Plasmas, 9: 1277
 [Wilson 04] H. R. Wilson, S. Cowley. 2004, Phys. Rev. Lett., 92: 175006
 [Xu 02] X. Q. Xu, R. H. Cohen, W. M. Nevins, et al. 2002, Nucl. Fusion, 42: 21

III.5 Turbulence (Z. Lin and R. E. Waltz)

Turbulent transport driven by plasma pressure gradients [Tang1978] is one of the most important scientific challenges in burning plasma experiments since the balance between turbulent transport and the self-heating by the fusion products (α -particles) determines the performance of a fusion reactor like ITER. The high plasma temperature often hinders detailed measurements of fluctuation characteristics in experiments. The highly nonlinear and chaotic dynamics render an analytic treatment intractable in most situations. Direct numerical simulation of the gyrokinetic equation [Frieman1982, Hahm1988a, Hahm1988b, Brizard1989] suitable for low frequency phenomena has therefore emerged as an important tool to study plasma turbulence and transport. The nonlinear gyrokinetic equation can be solved either in Lagrangian (particle-in-cell or PIC simulation) or in Eulerian phase space (continuum or Vlasov simulation). PIC and continuum methods have complementary strengths and weaknesses [Idomura2006]. Therefore, both methods should be well supported as a cross check given the many pitfalls in each method. PIC codes are efficient for massively parallel computer and relatively straightforward to program, but must fight against discrete particle noise. Continuum codes are difficult to program and must fight numerical instability. In terms of simulation geometry, there are both global (full torus) and local (flux-tube) nonlinear simulations. Flux-tube simulations are regarded as the local limit of global simulations as $\rho_* \rightarrow 0$. Here, $\rho_* \equiv \rho_s/a$ is the ratio of gyroradius to system size, with ρ_s the ion-sound Larmor radius, and the plasma minor radius. The simulation code validation should proceed at three levels: code-code benchmarks as the initial step, then rigorous simulation-analytic theory cross-checks, and finally simulation-experimental comparisons with predictive capability.

III.5.1 Gyrokinetic particle simulation (Z. Lin)

In the gyrokinetic particle simulation [Lee1983; Lee1987, Dubin1983] of low frequency turbulence in magnetized plasmas, the gyromotion of a charged particle is averaged out [Antonsen1980, Qin1999] and the

resulting polarization drift appears in the quasineutrality condition. This method leads to a larger time step, bigger spatial grid, and lower discrete particle noise, which enables the simulation of fusion plasmas with realistic parameters [Lee1988]. Using a parallel computer, the first toroidal gyrokinetic particle simulation [Parker1993b] was able to demonstrate the spectral correlations between ion temperature gradient (ITG) modes and the fluctuation measurements in TFTR [Fonck1993]. The conjecture of the gyro-Bohm transport scaling as $\rho_* \rightarrow 0$ was confirmed in a flux-tube simulation [Dimits1996] of the ITG turbulence. However, the global simulation [Sydora1996] found a Bohm-like scaling for the ITG turbulent transport. Subsequently, the effects of zonal flow on ITG modes [Lin1998] and the role of collisional damping of zonal flows [Lin1999, Lin2000] were studied using the global Gyrokinetic Toroidal Code (GTC). These simulations have shown that the meso-scale zonal flow, nonlinearly generated by the turbulence itself, can substantially reduce the saturation level of ITG turbulence and the resulting ion heat transport. With the introduction of collisions, the GTC code has also shown an interesting bursting behavior in the turbulent steady state arising from the interplay between the turbulent fluctuations, zonal flow, and collisions similar to the experimental observations in TFTR [Mazzucato1996]. Furthermore, the ion thermal transport level exhibits significant dependence on the ion-ion collision frequency even in regimes where the collisional effects on linear growth rate is negligible. The GTC simulations of turbulence self-regulation by zonal flows have inspired intense theoretical study of the generation of zonal flows through the modulational instability [Diamond2000; Chen2000; Guzdar2001; Chen2001b, Diamond2001]. Motivated by the trends observed in simulations [Hahm2000], experimental searches for the signatures of zonal flows [Diamond2005] have been pursued on most of existing tokamaks in the world fusion program. Zonal flows have also been studied in reversed magnetic shear plasmas [Kishimoto2000] and with parallel nonlinearity [Villard2004, Angelino2006].

The transition from the Bohm scaling for existing tokamaks to the gyroBohm scaling for reactor size tokamaks [Lin2002] has been found in GTC simulations of ITG turbulence. These simulations found an intriguing phenomenon, consistent with measurements in magnetically confined tokamak plasma experiments, that the fluctuations are microscopic, while the resulting turbulent transport depends on macroscopic scales, e.g., device sizes. A resolution to this apparent contradiction has been identified as turbulence spreading to linearly stable region [Lin2004]. The GTC simulations of turbulence spreading have stimulated the development of dynamical theories based on radial diffusion resulting from nonlinear mode coupling [Hahm2004, Hahm2005, Gurcan2005] and on radial propagation of dispersive waves nonlinearly enhanced by the drift wave-zonal flow interaction [Chen2004; Zonca2004, White2005].

Concentrated efforts in the last decade have led to

much improved understanding of the ITG turbulence, and thus the ion transport is better controlled in fusion experiments. Therefore, the interest of studying the electron transport has become a new priority in fusion research, especially for ITER since the heating of electron by α -particle is important in burning plasmas. A possible candidate for the electron heat transport is the electron temperature gradient (ETG) turbulence [Idomura2005] with a short scale length of the electron gyroradius. GTC simulation [Lin2005] and associated nonlinear gyrokinetic theory [Chen2005] find that the ETG instability saturates via nonlinear toroidal coupling, which transfers energy successively from unstable modes to damped modes preferentially with longer poloidal wavelengths. The electrostatic ETG turbulence is dominated by nonlinearly generated radial streamers with a nonlinear decorrelation time much longer than the linear growth time. An outstanding issue in tokamak confinement studies is the origin of the anomalous electron thermal transport in internal transport barriers (ITB), where the ion transport is reduced to the neoclassical level. As the density gradient steepens in barrier regions, the electrostatic trapped electron mode (TEM) is often driven unstable, e.g., in ASDEX Upgrade [Bottino2004] and JT-60U [Nazikian2005] experiments. The key issue to be addressed by nonlinear simulation is whether short wavelength TEM turbulence is capable of driving a large electron heat flux without driving significant ion heat and particle flux.

Discrete particle noise, which has been studied extensively [Dimits2000; Hatzky2002; Allfrey2003, Idomura2003, Lee2004], needs to be carefully managed to the level that the underlying physics is not contaminated in the particle simulations. After the invention of PIC simulation using finite-size particles, it was found, through the use of the fluctuation-dissipation theorem, that the numerical noise is greatly reduced for the short wavelength modes [Langdon1970], while the long wavelength modes is intact. This noise suppression also renders the simulation plasma collisionless, and one needs Monte-Carlo schemes to account for the collisions as a subgrid phenomena [Shanny1967]. Therefore, as long as the physics is dominated by long wavelength modes, particle codes are useful. For a gyrokinetic plasma, the numerical noise is further reduced by a factor of $(\lambda_D/\rho_i)^2$ according to the fluctuation-dissipation theorem [Lee1987]. Furthermore, the development of perturbative (δf) schemes [Dimits1993, Parker1993a] for microturbulence and neoclassical transport [Lin1995a, Lin1997], based on the concept of a multi-spatial-scale expansion, has provided further noise reduction by another factor of $(\delta f/f_0)^2$ [Hu1994]. The small electron mass presents a numerical difficulty in simultaneously treating the dynamics of ions and electrons in simulations of electromagnetic microturbulence and Alfvénic instabilities in high pressure plasmas. To reduce the particle noise and to increase the time step, a “split-weight” scheme [Manuilskiy2000,

Lee2001, Lewandowski2003] was developed by separating the adiabatic and non-adiabatic electron response, and subsequently, a fluid-kinetic hybrid electron model [Lin2001] was proposed based on an expansion of the electron response using the electron-ion mass ratio as a small parameter. These advanced algorithms have enabled the implementation of the electron dynamics in several gyrokinetic codes including GEM [Chen2001b, Chen2003, Parker2004] and GTC.

The GTC code, which is the a production code of the US DOE fusion Scientific Discovery through Advanced Computing (SciDAC) [Tang2005], has been optimized to achieve high efficiency on a single computing node and nearly perfect scalability on both massively parallel computers (MPP) such as the IBM SP and parallel vector computers such as the Earth Simulator Computer [Ethier2004], two complementary architectures for the next generation of high performance computers. Transmitting a tera-byte dataset over the network is often a daunting task. A threaded parallel data streaming approach using Globus has been developed for concurrent transfer of GTC data [Klasky2003]. The large device simulations only became feasible with the implementation of an efficient global field-aligned mesh using magnetic coordinates to take advantage of the quasi-2D structure of toroidal drift wave eigenmodes. Global electromagnetic simulations were enabled by implementing two complementary methods in the GTC code for solving the gyrokinetic Poisson equation and Ampere’s law. A FEM elliptic solver [Nishimura2006] is fully optimized using multi-grid methods [HYPRE], and could efficiently handle one million mesh points per poloidal plane, which is the typical size for simulations of the International Thermonuclear Experimental Reactor (ITER). Another global solver casts the original integral form of the gyrokinetic Poisson equation in a sparse matrix [Lin1995a] to be solved by the state-of-the-art parallel solver PETSc [PETSc].

Most of the existing gyrokinetic particle codes utilize a perturbative method suitable for small amplitude fluctuations and treat collisionless dynamics of the turbulence. This approach has not addressed key aspects of turbulent transport at long time scales, such as the plasma profile evolution, formation of phase space structure, collisional dissipation, and interaction between neoclassical and turbulent transport. Properly addressing these long time behaviors is critical for simulation with multiple time scales ranging from the turbulence dynamical time to the plasma profile relaxation time, which is needed in an integrated modeling of fusion plasmas such as the core-edge coupling and the whole discharge simulation. The full-f method that could address some of these issues in long time simulations has recently been used [Heikkinen2004] for the ITG turbulence simulation with realistic plasma parameters.

References

- [Allfrey2003]S. J. Allfrey, R. Hatzky. 2003, *Comput. Phys. Comm.*, 154: 98
- [Angelino]P. Angelino et al. 2006, *Plasma Phys. Controlled Fusion*, 48: 557
- [Antonsen1980]T. M. Antonsen, B. Lane. 1980, *Phys. Fluids*, 23: 1205
- [Bottino2004]A. Bottino, et al. 2004, *Phys. Plasmas*, 11: 198
- [Brizard1989]A. Brizard. 1989, *J. Plasma Phys.*, 41: 541
- [Chen2000]L. Chen, Z. H. Lin, R. White. 2000, *Phys. Plasmas*, 7: 3129
- [Chen2001a]L. Chen, et al. 2001, *Nuclear Fusion*, 41: 747
- [Chen2004]L. Chen, R. B. White, and F. Zonca. 2004, *Phys. Rev. Lett.*, 92: 075004
- [Chen2005]L. Chen, F. Zonca, Z. Lin. 2005, *Plasma Phys. Controlled Fusion*, 47: B71
- [Chen2001b]Y. Chen, S. E. Parker. 2001b, *Phys. Plasmas*, 8: 2095
- [Chen2003]Y. Chen, et al. 2003, *Nuclear Fusion*, 43: 1121
- [Diamond2000]P. H. Diamond, et al. 2000, *Phys. Rev. Lett.*, 84: 4842
- [Diamond2001]P. H. Diamond, et al. 2001, *Nucl. Fusion*, 41: 1067
- [Diamond2005]P. H. Diamond, et al. 2005, *PLASMA PHYSICS AND CONTROLLED FUSION*, 47: R35
- [Dimits1993]A. M. Dimits, W. W. Lee. 1993, *J. Comp. Phys.*, 107: 309
- [Dimits1996]A. M. Dimits, et al. 1996, *Phys. Rev. Lett.*, 77: 71
- [Dimits2000]A. M. Dimits, et al. 2000, *Phys. Plasmas*, 7: 969
- [Dubin1983]D. H. E. Dubin, et al. 1983, *Phys Fluids*, 26: 3524
- [Ethier2004]S. Ethier, Z. Lin. 2004, *Comput. Phys. Comm.*, 164: 456
- [Fonck1993]R. J. Fonck, et al. 1993, *Phys. Rev. Lett.*, 70: 3736
- [Frieman1982]E. A. Frieman, L. Chen. 1982, *Phys. Fluids*, 25: 502
- [Gurcan2005]O. D. Gurcan et al. 2005, *Phys. Plasmas*, 12: 032303
- [Guzdar2001]P. N. Guzdar, et al. 2001, *Phys. Rev. Lett.*, 87: 015001
- [Hahm1988a]T. S. Hahm. 1988a, *Phys. Fluids* 31: 2670
- [Hahm1988b]T. S. Hahm, W. W. Lee, A. Brizard. 1988b, *Phys. Fluids*, 31: 1940
- [Hahm2000]T. S. Hahm, et al. 2000, *Plasma Phys. Controlled Fusion*, 42: A205
- [Hahm2004]T. S. Hahm, et al. 2004, *Plasma Phys. Controlled Fusion*, 46: A323
- [Hahm2005]T. S. Hahm et al. 2005, *Phys Plasmas*, 12: 090903
- [Hatzky2002]R. Hatzky, et al. 2002, *Phys. Plasmas*, 9: 898
- [Heikkinen2004]J. A. Heikkinen, et al. 2004, *Contrib. Plasma Phys.*, 44: 13
- [Hu1994]G. Hu, J. A. Krommes. 1994, *Phys. Plasmas*, 1: 863
- [HYPRE]HYPRE: high performance preconditioners; Scalable Algorithms Group, Center for Applied Scientific Computing, <http://www.llnl.gov/CASC/hypre>.
- [Idomura2003]Y. Idomura, S. Tokuda, Y. Kishimoto. 2003, *Nucl. Fusion*, 43: 234
- [Idomura2005]Y. Idomura, S. Tokuda, Y. Kishimoto. 2005, *Nucl. Fusion*, 45: 1571
- [Idomura2006]Y. Idomura, T. H. Watanabe, H. Sugama. 2006, *COMPTES RENDUS PHYSIQUE* 7: 650
- [Kishimoto2000]Y. Kishimoto, J. Y. Kim, W. Horton, et al. 2000, *Nucl. Fusion*, 40: 667
- [Klasky2003]S. Klasky et al. 2003, SC2003 technical paper,
- [Krommes1993]J. A. Krommes. 1993, *Phys. Fluids B*, 5: 2405
- [Langdon1970]A. B. Langdon and C. K. Birdsall. 1970, *Phys. Fluids*, 13, 2115
- [Lee1983]W. W. Lee. 1983, *Phys. Fluids* 26: 556
- [Lee1987]W. W. Lee. 1987, *J. Comput. Phys.* 72: 243
- [Lee1988]W. W. Lee, W. M. Tang. 1988, *Phys. Fluids*, 31: 612
- [Lee2001]W. W. Lee, et al. 2001, *Phys. Plasmas*, 8: 4435
- [Lee2004]W. W. Lee. 2004, *Comput. Phys. Comm.*, 164: 244
- [Lewandowski2003]J. L.V. Lewandowski. 2003, *Plasma Phys. Controlled Fusion*, 45: L39
- [Lin1995a]Z. Lin, W. M. Tang, W. W. Lee. 1995a, *Phys. Plasmas*, 2: 2975
- [Lin1995b]Z. Lin, W. W. Lee. 1995b, *Phys. Rev. E*, 52: 5646
- [Lin1997]Z. Lin, et al. 1997, *Phys. Rev. Lett.*, 78: 456
- [Lin1998]Z. Lin, et al. 1998, *Science*, 281: 1835
- [Lin1999]Z. Lin, et al. 1999, *Phys. Rev. Lett.*, 83: 3645
- [Lin2000]Z. Lin et al. 2000, *Phys. Plasmas*, 7: 1857
- [Lin2001]Z. Lin, L. Chen. *Phys. Plasmas*, 8: 1447
- [Lin2002]Z. Lin, et al. 2002, *Phys. Rev. Lett.*, 88: 195004
- [Lin2004]Z. Lin, T. S. Hahm. 2004, *Phys. Plasmas*, 11: 1099
- [Lin2005]Z. Lin, L. Chen, F. Zonca. 2005, *Phys. Plasmas*, 12: 056125
- [Manuilskiy2000]I. Manuilskiy, W. W. Lee. *Phys. Plasmas*, 7: 1381
- [Mazzucato1996]E. Mazzucato, et al. 1996, *Phys. Rev. Lett.*, 77: 3145
- [Nazikian2005]R. Nazikian, et al. 2005, *Phys. Rev. Lett.*, 94: 135002
- [Nishimura2006]Y. Nishimura, et al. 2006, *J. Comput. Phys.*, 214: 657
- [Parker1993a]S. E. Parker, W. W. Lee. 1993a, *Phys. Fluids*, B5: 77
- [Parker1993b]S. E. Parker, et al. 1993b, *Phys. Rev. Lett.*, 71: 2042
- [Parker2004]S. E. Parker, et al. 2004, *PHYSICS OF PLASMAS*, 11: 2594
- [PETSc]PETSc: Portable, Extensible Toolkit for Scientific Computation, Mathematics and Computer Science Division, Argonne National Laboratory; <http://www-unix.mcs.anl.gov/petsc/petsc-2>.
- [Qin1999]H. Qin, et al. 1999, *Physics of plasma*, 6: 1575

- [Shanny1967]R. Shanny, et al. 1967, Phys. Fluids, 10: 1281
 [Sydora1996]R. D. Sydora, V. K. Decyk, J. M. Dawson. 1996, Plasma Phys. Controlled Fusion, 38: A281
 [Tang1978]W. M. Tang. 1978, Nucl. Fusion, 18: 1089
 [Tang2005]W. M. Tang, V. S. Chan. 2005, Plasma physics and controlled fusion, 47, R1
 [Villard2004]L. Villard, et al. 2004, Nucl. Fusion, 44: 172
 [White2005]White, et al. Physics of plasma, 12: 057304 (2005)
 [Zonca2004]Zonca F, White R B, Chen L. 2004, Physics of plasma, 11: 2488

III.5.2 Continuum gyrokinetic and gyrofluid codes(R. E. Waltz)

While historically the Particle-In-Cell (PIC) codes initiated nonlinear gyrokinetic simulation of turbulence, the so called “continuum” codes have proven remarkable efficient. Continuum refers to the use of velocity space grids in addition to the three space grids common to the PIC codes. Continuum codes are usually Eulerian (rather than Lagrangian like PIC) and picture the plasma as a 5D phase-space fluid. Such codes grew out a long history of simple fluid turbulence codes (e.g. collisional two fluid edge codes) and the gyrofluid codes. Gyrofluid equations are dissipative closed moments of the gyrokinetic equation.

Work on continuum gyrokinetics started in 1992 with Kotschenreuther linear continuum gyrokinetic stability GSTOTAL code [Kotschenreuther1988]. The GSTOTAL code had ions and electron, trapped and passing, as well as collisional and electromagnetic physics. The main advance in GSTOTAL was that implicit numerical methods could pass over the fast electron transit frequency in an initial value code...the first step to a nonlinear code with electron physics. With reformatting and the addition of plot packages, real Miller geometry and δB_{\parallel} [Waltz1999], GSTOTAL was further developed into the GKS linear stability code at GA for routine DIII-D experimental analysis. GKS is still in use today. Combined with nonlinear flux tube gyrofluid code simulations [Waltz1994, Waltz1995], GKS was crucial in the development of the GLF23 transport model [6] which is the transport model of choice at numerous tokamak labs worldwide.

Nonlinear gyrofluid flux-tube simulations by Beer, Dorland, Hammett, Snyder, Waltz and others provided key physics discoveries in the mid-1990s. These gyrofluid simulation demonstrated: (1) that nonlinear, self-generated (zonal) flows control the nonlinear saturation of transport [Dorland1993,Waltz1994,Waltz1995]; and (2) equilibrium $\mathbf{E} \times \mathbf{B}$ shear can quench toroidal transport if the shearing rates are comparable to the maximum linear growth rates [Waltz1994, Waltz1995]. Nonlinear gyrofluid simulation codes treated trapped electron [Beer1996], and electromagnetic [Snyder2001] turbulence.

The first major contribution from nonlinear gyroki-

netic codes was the verification of the importance of the Rosenbluth-Hinton[Rosenbluth1998] gyrokinetic “residual” zonal flows made by the PIC δf flux tube code PG3EQ [Dimits1996]. These persistent zonal flows apparently give rise to a so called Dimits shift [Dimits 2000] or upshift in the linear threshold in adiabatic electron ITG (ITG-ae) turbulence. The inaccuracy of the residual and the difficulty of formulating finite- ρ_* (or nonlocal) effects in gyrofluid models, motivated a redirection to gyrokinetics. Dorland first went beyond these adiabatic electrons nonlinear gyrokinetic simulations by converting GSTOTAL to the now widely used nonlinear flux tube gyrokinetic simulation code GS2. By 2000, the continuum flux tube code GS2 was operational in full generality including electron physics with finite beta, and real shaped geometry. This allows physically accurate treatment of the low-k ITG/TEM turbulence in the local gyroBohm limit [Ross2003]. Dorland’s GS2 and Jenko’s GENE continuum code also first treated the high-k ETG modes with adiabatic ions (ETG-ai) [Dorland 2000]. (see the GS2 website: <http://gs2.sourceforge.net/>).

Candy and Waltz began development of the global continuum code GYRO in 1999 and completed major design goals by APS 2002[Candy2003a, Candy2003b]. (see the GYRO website: <http://fusion.gat.com/comp/parallel/>) The primary design target was to include all physics relevant to simulating microturbulence in the core plasma (excluding the H-mode edge pedestal). This meant retaining the finite- ρ_* which would in principle allow: (1) local stabilization from the profile variation (mainly in the driving plasma gradients); (2) nonlocal transport and the draining of turbulence in regions of high drive and spreading into low; and (3) deviations from gyroBohm scaling all the way to Bohm scaling or finite- ρ_* stabilization. By 2001, GYRO ITG-ai simulations had the possibility of operating either locally as a flux-tube with cyclic boundary conditions, or globally with zero-value boundary conditions on a large radial slice with profile variation. The boundary conditions were shown to be benign, i.e. without profile variation global and flux tubes of the same size produce the identical gyroBohm scaled result no matter the value of ρ_* [Waltz2002]. When profile variation is included, the diffusivity in global simulations approaches the local gyroBohm limiting value found in flux tubes from below as ρ_* gets very small [Candy2004]. Bohm scaling in ITG-ai simulations could result for $\rho_* \sim 1\%$ [Waltz2002, Lin2002]. It has been emphasized that there is no universal ρ_* value for transition from Bohm to gyroBohm scaling. Bohm scaling results from large enough profile variation when sufficiently close to threshold [Waltz2002,Waltz2006] and thus to quantify and match Bohm scaling found in experiments requires physically comprehensive simulations with “full physics”.

The essential “full physics” required to match the core experimental transport and Bohm scaling in DIII-

D L-mode pairs [Candy 2003b] and gyroBohm scaled H-mode pairs [Waltz2006a] include: (1) the ITG-ai kernel; (2) trapped and passing electrons for ITG/TEM physics; (3) electron-ion pitch-angle scattering; (4) finite beta fluctuations and transport; (5) shaped real geometry; (6) equilibrium parallel velocity shear for Kelvin-Helmholtz drive; (7) equilibrium $\mathbf{E} \times \mathbf{B}$ shear (strongly stabilizing in DIII-D); (8) finite- ρ_* ; (9) input of actual experimental profiles; (10) particle, momentum, and energy flow diagnostics. With given experimental profiles, GYRO typically gives a 2-fold larger transport flows than DIII-D. But the experimental transport is easily matched by lowering either the experimental ion temperature gradient or raising the $\mathbf{E} \times \mathbf{B}$ shear by 10~15%. The profile similarity of the DIII-D L-mode ρ_* -pair is excellent and GYRO has verified the Bohm scaling is real by simulations a ρ_* -pair constructed with perfect similarity numerically. The gyroBohm scaling of the H-mode pair (at larger ρ_* !) was also matched but found to be due to poor similarity [Waltz2006b]. GYRO has developed a feedback technique to make small adjustments in the experimental plasma gradients in temperature and density to match the given flows [Waltz2005]. It is hoped that this technique for turbulence simulation on transport time scales will lead to a steady state gyrokinetic core transport code for simulating ITER fusion performance (given an H-mode pedestal height !).

The numerical methods in GYRO were patterned after GS2 where possible, but an efficient electromagnetic global code required significant advances in numerical methods. (The flux-tube code GS2 lacks only (7) and (8) above, but $\delta B_{||}$ is still lacking in GYRO.) The completely implicit linear plus split step GS2 method was replaced with a state of the art mixed-implicit-explicit (IMEX-RK) method. The GYRO methods to solve the dread ‘‘Ampere-cancellation’’ problem in finite- β simulations were later adopted by the GEM PIC code [Chen2003]. The most difficult numerical problem in global continuum codes has been to find numerically stable algorithms to evolve the neutrally stable $n = 0$ zonal flows (when ion-ion collisions are negligible)

Plasma and impurity flows, as well as neoclassical flows embedded in turbulence have been treated with GYRO simulations [Waltz2005]. It was found that there was no practically significant coupling between $n = 0$ neoclassical flows and $n > 0$ (low-k ITG/TEM: $0 < k_y \rho_{s,i} < 1$) turbulent flows and they can be superposed to good approximation. There is some preliminary and tentative indication from GYRO that coupling between low-k ITG/TEM and the smaller higher-k ETG transport is also weak, and ITG/TEM and ETG can also so be superposed to good approximation.

The most unexpected feature of global gyrokinetic simulations in GYRO has been the presence of time averaged (small scale quasi-equilibrium) radial profile corrugations in plasma gradients and current density [Hinton2003] at low order singular surfaces like 3/1, 5/2, 2/1, 3/2. These are components of zonal flow fluc-

tuations which do not time average to zero near low order surfaces where the density of singular surfaces dips. These would be difficult to measure in monotonic-q profiles. However recent DIII-D ECC measurements of a large bump-dip-bump in the electron temperature gradient as $q\text{-min} = 2/1$ enters the plasma of a reversed central shear discharge, matches GYRO simulated 2/1 corrugations very well [Waltz2006b]. There is a huge ‘‘gap’’ in singular surface density at $q\text{-min}=2$ ($s = 0$). GYRO simulations show a huge $\mathbf{E} \times \mathbf{B}$ shear layer just interior to the 2/1, which seems to explain the formation of an ITB often found at $q\text{-min} = 2/1$.

Code development of both flux-tube and global δf continuum gyrokinetic codes is nearly ended. Many productive years of application to analysis of experiments and development of transport models remain. One can expect that full physics δf continuum gyrokinetic steady state transport codes (operating at fixed input flows rather than fixed input gradient profiles) will soon be in common use for comparison with experiments and even for projection of ITER Q-performance and core confinement given an H-mode edge pedestal height. The way forward for simulating the edge pedestal and the dynamics of internal transport barrier (ITB) formation is in the development of ‘‘full- f ’’ global gyrokinetic codes which make no scale separation between dynamical δf turbulence and f_0 transport ($f = f_0 + \delta f$).

References

- [Beer 1996] M. A. Beer, G. W. Hammett. 1996, Phys. Plasmas, 3: 4018
- [Candy 2003a] J. Candy, R. E. Waltz. 2003, J. Comp. Phys., 186: 545
- [Candy 2003b] J. Candy, R. E. Waltz. 2003, Phys. Rev. Lett., 91: 45001
- [Candy 2004] J. Candy, R. E. Waltz, W. Dorland. 2004, Phys. Plasmas, 11: L25
- [Dimits 1996] A. M. Dimits, T. J. Williams, J. A. Byers, et al. 1996, Phys. Rev. Lett., 77: 71
- [Dimits 2000] A. M. Dimits, et al. 2000, Phys. Plasmas, 7: 969
- [Dorland 1993] W. Dorland, G. W. Hammett. 1993, Phys. Fluids B, 5: 812
- [Dorland 2000] W. Dorland, F. Jenko, M. Kotschenreuther, B. N. Rogers. 2000, Phys. Rev. Lett., 85: 5579
- [Hinton 2003] F.L. Hinton, R.E. Waltz, J. Candy. 2004, Phys. Plasmas, 11: 2433 ~ 2440
- [Kotschenreuther 1995] M. Kotschenreuther, G. Rewoldt, G. W. Tang. 1995, Comput. Phys. Comm., 88: 128
- [Kotschenreuther 1988] M. Kotschenreuther. 1988, BAPS 33 DPP APS 1988 invited talk 9I4 p.2107 or in a proceeding format This is standard format for Bulletin of the APS?
- [Lin2002] Z. Lin, S. Ethier, T. S. Hahm, W. M. Tang. 2002, Phys. Rev. Lett., 88: 195004
- [Rosenbluth1998] M. N. Rosenbluth, F. L. Hinton. 1998,

- Phys. Rev. Lett., 80: 724
 [Ross2003] R. W. Ross, W. Dorland. 2003, Phys. Plasmas, 9: 5031
 [Snyder 2001] P.B. Snyder, G. W. Hammett. 2001, Phys. Plasmas, 3: 4046
 [Waltz 1994] R. E. Waltz, G. D. Kerbel, J. Milovich. 1994, Phys. of Plasmas, 1: 2229
 [Waltz 1995] R. E. Waltz, G. D. Kerbel, J. Milovich, et al. 1995, Phys. of Plasmas, 2: 2408
 [Waltz 1999] R. E. Waltz, R. M. Miller. 1999, Phys. Plasmas, 6: 4265
 [Waltz 2002] R. E. Waltz, J. Candy, M. N. Rosenbluth. 2002, Physics of Plasmas, 9: 1938
 [Waltz 2005] R. E. Waltz, J. Candy, F. L. Hinton, et al. 2005, Nucl. Fusion, 45: 741
 [Waltz 2006a] R. E. Waltz, J. Candy, C. C. Petty. 2006, Phys. Plasmas, 13: 072304
 [Waltz 2006b] R. E. Waltz, M. E. Austin, K. H. Burrell, J. Candy. 2006, Phys. Plasmas, 13: 052301

III.6 RF heating and current drive (D. B. Batchelor)

Foundations of RF simulation

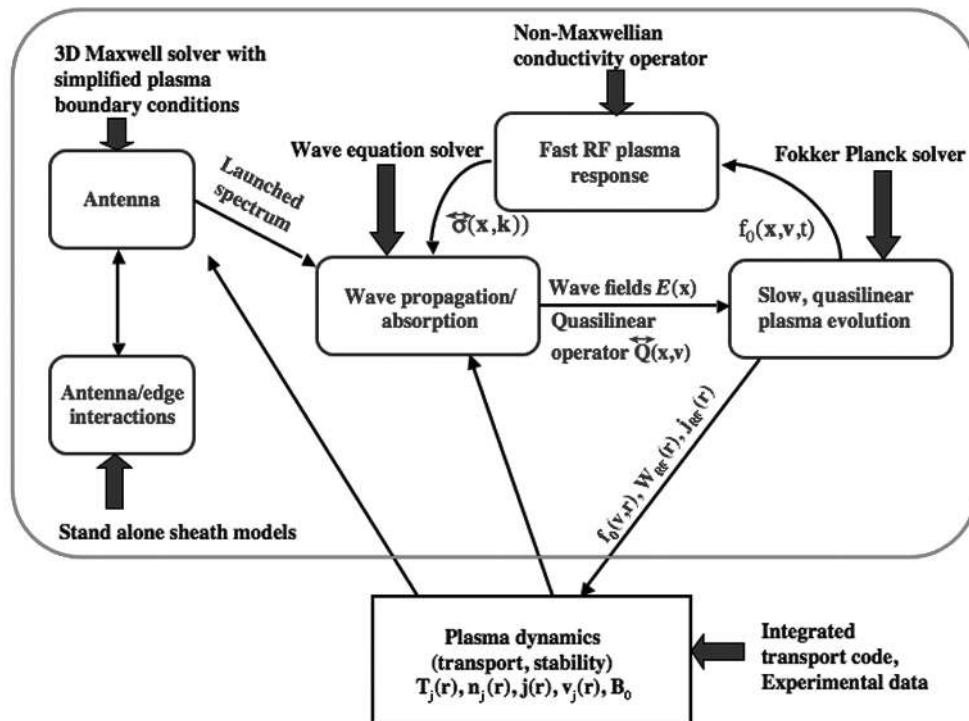


Fig. III.6.1 The elements of an integrated simulation of wave interactions with fusion plasmas

The starting point for the theory of waves in hot magnetized plasmas is the kinetic equation describing the evolution in time of the distribution of plasma particles of species j in a six dimensional phase space of position and velocity. The electric charge, $q(\mathbf{x}, t)$, and current, $\mathbf{J}(\mathbf{x}, t)$, that act as sources for the electromagnetic field in Maxwell's equations are obtained by tak-

A complete simulation for the interaction of RF waves with plasma can be divided into separate but interacting pieces as indicated schematically in Fig. III.6.1 First, the 3D launching structure and the coupling of this structure to the plasma must be modeled with sufficient realism and detail to reliably predict the spectrum of the launched waves, the intense fields near the antenna, and the interaction of these fields with the edge plasma. Next, the wave equation must be solved within the plasma to predict the field structure and the ultimate absorption of the waves by the plasma particles. The wave fields induce local macroscopic sources of deposited power, driven current, and plasma flow, all of which are quadratic operators on the electric field. These must be calculated using the full detail of the wave field solution and the necessary structure of the underlying plasma equilibrium and including the possibly non-Maxwellian particle velocity distribution. Finally, the long time evolution of the plasma distribution function must be obtained from a time-averaged form of the Fokker-Planck equation. Although these pieces interact, these interactions are only now beginning to be modeled in numerical simulations.

ing velocity moments of $f_j(\mathbf{x}, \mathbf{v}, t)$ to yield the charge and current densities, $q(\mathbf{x}, t)$ and $\mathbf{J}(\mathbf{x}, t)$.

Since the RF wave period is by far the fastest timescale in the system, the fields and distribution function can be separated into a time-average, or equilibrium, part $(\mathbf{E}_0, \mathbf{B}_0, f_j^0)$ that is slowly varying, and a rapidly oscillating part, $(\mathbf{E}_1(\mathbf{x})e^{-i\omega t}, \mathbf{B}_1(\mathbf{x})e^{-i\omega t},$

$f_j^1(\mathbf{x}, \mathbf{v})e^{-i\omega t}$ where ω is the frequency of the RF power source. For most heating and current drive applications, the time-harmonic wave fields are small compared to the equilibrium fields and we may linearize the kinetic equation with respect to these amplitudes. Solving the linearized equation gives the rapidly varying part $f_j^1(\mathbf{x}, \mathbf{v})$ in terms of the equilibrium distribution, $f_j^0(\mathbf{x}, \mathbf{v})$, and the rapidly varying component of the electromagnetic field. This solution then allows us to relate the plasma current induced by the wave fields, \mathbf{J}_p^1 to the fields through a nonlocal, integral conductivity operator acting on the wave field.

$$\mathbf{J}_p^1(\mathbf{x}) = \sigma \circ \mathbf{E}_1 = \sum_j \int dx' dt' \mathbf{K}(f_j^0, \mathbf{x}, t, \mathbf{x}', t') \circ \mathbf{E}_1(\mathbf{x}', t') \quad (\text{III.6.1})$$

The Maxwell's wave equation that must be solved reduces to a generalization of the Helmholtz equation,

$$\nabla \times \nabla \times \mathbf{E} = \mathbf{J}_p + \mathbf{J}_{\text{ant}} + \text{boundary conditions} \quad (\text{III.6.2})$$

The source for the waves is an externally driven antenna current, \mathbf{J}_{ant} , localized near the plasma edge. The interaction takes place in a bounded domain, on which are imposed appropriate boundary conditions determined by the shape of the fusion device.

Three wave frequency regimes are important for ITER applications [Gomezano 06]. The waves in the ion cyclotron range of frequencies (ICRF) resonate with the ions at the ion cyclotron frequency or its harmonics, and can also interact with the motion of the electrons parallel to B through Landau damping and transit time magnetic pumping. ITER plans to use 20 MW at ~ 50 MHz in ITER phase I. Because of their long wavelength, an accurate calculation of ICRF waves requires solution of the full-wave equation, Eq. (III.6.3), which in 2D or 3D is a terascale computing problem. Lower hybrid waves can interact with both ions and electrons but are used primarily to drive electron current. Lower hybrid is still being considered for ITER. If employed the frequency would be about 5 GHz. None is planned for installation in phase I. A geometrical optics approximation to the wave equation is usually adequate for calculation of lower hybrid wave propagation, although full wave solutions at very high resolution have recently been obtained [Wright 05]. Waves in the electron cyclotron range of frequencies (ECRF) resonate at the electron cyclotron frequency or its harmonics (20 MW at 170 GHz in ITER phase I). Propagation of electron cyclotron frequency waves is well described by geometrical optics with ray tracing algorithms. Ray tracing, as required for lower hybrid or ECRF is considerably less computationally intensive since it only necessary to solve a set of ordinary differential equations that describe the ray trajectory and power absorption along the ray.

Fokker Planck theory

The response of the plasma distribution function, $f_0(\mathbf{x}, \mathbf{v}, t)$, on timescales much slower than the RF period is obtained from a time-averaged form of the kinetic equation, referred to as the quasilinear Fokker-Planck equation,

$$\frac{df_0}{dt} = Q(\mathbf{E}, f_0) + C(f_0) + S(\mathbf{x}, \mathbf{v}) \quad (\text{III.6.3})$$

Here, the time derivative includes particle drift motion, and the RF quasilinear operator, $Q(\mathbf{E}^1, f_0)$, [Kennel 66] is quadratic in the RF field $\mathbf{E}(\mathbf{x}, t)$ and describes wave-induced velocity-space diffusion of f_0 . Velocity moments of the quasilinear operator can also be calculated to give instantaneous macroscopic plasma responses such as local power deposition, $W_{\text{rf}}(\mathbf{x})$, momentum sources, $\mathbf{R}_{\text{rf}}(\mathbf{x})$, or ponderomotive force, $\mathbf{F}_{\text{rf}}(\mathbf{x})$. In the absence of sources, the collision operator relaxes f_0 to a local Maxwellian distribution. However, quasilinear diffusion, particle or energy sources, or gradients in macroscopic plasma quantities drive f_0 away from Maxwellian.

To obtain self-consistency of the wave fields with the distribution, and to follow the time evolution of the plasma, a procedure of iteration of Eqs. (III.6.2-III.6.3) is necessary. This iteration greatly compounds the computational demands of the RF calculation. This loop has now been closed using full wave fields from the AORSA code to generate the quasilinear operator and the CQL3D Fokker Planck code to calculate the distribution function [Jaeger 06].

To achieve any of the objectives of high-power waves for plasma heating or control it is necessary to launch the desired spectrum of waves into the plasma from some type of antenna. Existing plans for ITER call for RF core heating, and possible advanced tokamak scenarios may require special tailoring of the RF-launched spectrum for current profile or sawtooth control. The power levels and spectra of launched waves depend very sensitively on details of the plasma properties at the edge near the antenna and on geometric details of the antenna structure and nearby materials. In turn, the RF fields near the antenna can have strong nonlinear interactions with the edge plasma, thereby modifying the plasma properties and dissipating substantial power in RF-driven sheaths or wave modes localized near the plasma edge. An example of concern in present experimental observations is that antenna voltage-handling limits are lower with plasma than can be achieved in vacuum. Another observation, thought to result from sheath physics is that antennas must typically operate with restrictions on relative phasing or must utilize ceramic limiting structures to mitigate impurity generation. Furthermore, for some experiments, a power balance in the plasma core cannot account for all of the launched power, possibly because of edge absorption by sheaths or wave-wave parametric decay. A failure to understand the reasons for these technological difficulties could strongly affect RF performance in ITER. Thus,

it is vital that a better understanding be obtained by implementing better physics in the models used for antenna design and analysis in order to maximize ITER performance and flexibility.

Modeling the interaction of RF power with the plasma edge is an extremely complex problem. It combines all the complications of existing edge models (transport, atomic physics, plasma-material interactions, turbulence, neutral particle dynamics) with the nonlinear interactions of strong wave fields (e.g., RF-driven sheaths, ponderomotive effects, edge wave modes). Simplified models for several of these processes have been developed and have had some success in explaining antenna/edge plasma interactions. Sheath interactions are qualitatively understood [Perkins 89, Myra 90, D'Ippolito 91] but quantitative analysis is not possible.

When the edge plasma properties are known from experiment or can be reliably assumed, good calculations of the wave spectrum are now possibly absent the non-linear edge interactions described above. Three-dimensional antenna models coupled to 1D models for the plasma with outgoing wave boundary conditions have been successfully compared with loading measurements in many experiments, including Tore Supra [Carter 95], TFTR [Carter 96], and DIII-D [Swain 97]. However, these models do not account for the actual shape of the plasma, which in many cases does not conform well to the shape of the antenna, they do not account for the bounded domain with power reflecting from distant walls back to the antenna or for power dissipated nonlinearly by plasma sheaths, nor can they represent the full level of geometric detail of the antennas.

Key codes for RF simulation and development issues

The solution of Eqs.(III.6.1) through (3) must be carried out with sufficient dimensionality, resolution, and detail in the conductivity operator to represent all of the important physics involved in the wave-particle interaction. Considerable simplification can be achieved by assuming that $(k_{\perp}\rho_I)^2 \ll 1$ [Brambilla 99]. In this limit, finite Larmor radius (FLR) effects are included by expanding the conductivity operator to second order in $k_{\perp}\rho_I$. The integral operator perpendicular to the magnetic field can thus be reduced to a second order differential operator whose finite element representation yields a sparse matrix. This type of full-wave ICRF field solver is commonly referred to as an FLR model. Such an approach works well for minority ion heating in the ion-cyclotron range of frequencies (ICRF) where mode conversion to the short wavelength ion Bernstein and slow ion cyclotron waves is negligible. If mode conversion becomes significant however, or if energetic particles with large Larmor radii are present in the plasma, higher order terms in $k_{\perp}\rho_I$ must be included in the conductivity. All-orders spectral wave solvers have now been developed [Jaeger 01, Jaeger 02] and used to carry out studies of mode conversion in 2D as well as minor-

ity ion heating in 3D. AORSA takes advantage of new computational techniques for very large parallel computers to solve the complete integral form of the wave equation in 2D and 3D without any restriction on wavelength relative to orbit size, and with no limit on the number of cyclotron harmonics. This capability has been exploited to elucidate mode conversion physics in 2D and to provide valuable guidance as to the range of validity of the FLR solvers.

There are two approaches to solving the Fokker Planck equation, Eq. (III.6.3), presently being used in RF applications- finite difference or finite element solution of the continuum equation and direct simulation using Monte Carlo particle methods. These employ different numerical techniques and different time or orbit averages to reduce the dimensionality. The primary research issues for the wave solver codes are to understand the limits of validity of the quasi-local approximations employed in constructing the RF conductivity operator, and to improve the treatment of 3D antenna geometries including possible non-linear edge effects.

There are several codes which solve a time dependent bounce averaged form of Eq. (III.6.3) by finite difference methods in a 2D velocity space with a 1D radial spatial coordinate and have the capability to include radial derivatives of the bounce averaged distribution functions [Harvey 92, O'Brien 95]. The existing models for the radial diffusion which remains after bounce-averaging are somewhat ad hoc and need to be improved to give a physics-based model for radial diffusive transport and RF modifications of the bootstrap current. Recently the CQL3D code has been directly coupled to the AORSA2D wave solver to yield converged self-consistent solutions for minority tail formation in Alcator C-Mod and fast wave coupling to alpha particles in ITER.

Monte Carlo methods allow solutions in high dimensional phase space and correctly model the drift of particle orbits across flux surfaces [Choi 05, Kwon 06]. This method can straightforwardly include both Coulomb pitch angle and energy scattering as well as RF quasi-linear diffusion. In addition, RF heating effects on the distribution, non-local closures, radial transport effects and unclosed flux surfaces can be taken into account. The Monte Carlo approach is scalable to massively parallel systems but there are challenges related to the computational performance. First, there is the need to run with a sufficiently large number of particles to resolve narrow boundary layers important for calculating plasma current that may be present in the distribution function, especially for the collisionalities of ITER. Next, a number of self-consistency relations (e.g., momentum conservation, equivalency between test particle and background plasmas, ambipolar transport, etc.) need to be prescribed. These may require higher-level iterations outside the main particle stepping loop. Finally there is little experience in using the somewhat noisy distribution functions obtained from Monte Carlo methods as inputs to the wave solvers, which require

velocity space derivatives to calculate the plasma conductivity.

Objectives of RF simulation for ITER

The key role of wave-plasma interaction studies for ITER is to answer questions such as: Are the RF systems capable of producing and controlling a particular desired plasma state, and if so how should these systems be operated to achieve that state? In a specific experiment that has been performed, what role did the RF waves play in the measurements that were actually made? To what extent can RF waves be used to stabilize or otherwise control instabilities, such as sawtooth oscillations or neoclassical tearing modes, and what are the RF system requirements for this purpose? Such studies require interfacing with models of other plasma processes such as transport, extended MHD and microstability. In particular, the RF models must provide to the other codes macroscopic RF plasma responses - local power deposition, the driven current, the RF force or flow profile, and for some applications they must provide the detailed plasma distribution function. In turn, the RF models must receive the magnetic equilibrium, the macroscopic variables describing the state of each plasma species, such as density and temperature, and any non-RF sources of non-Maxwellian particles such as from neutral injection or fusion reactions. In addition a fully predictive capability will require the coupling of the edge/antenna phenomena to the core wave propagation and Fokker-Planck solutions. A complete solution to this problem is the very long-term goal of a global integrated simulation effort.

References

- [Brambilla 99] M. Brambilla. 1999, Plasma Phys. Cont. Fusion, 41: 1
- [Carter 95] M. D. Carter, et al. 1995, AIP Conf. Proc 355, RF Power in Plasmas, 364
- [Carter 96] M. D. Carter, et al. 1996, Nucl. Fusion, 36: 209
- [Choi 05] M. Choi, et al. Proc. of the 16th Topical Conf., Park City, Utah (2005)
- [D'Ippolito 91] D. A. D'Ippolito, et al. 1991, Plasma Phys. and Controlled Fusion, 33: 607
- [Gormezano 06] ITER Tokamak Physics Basis, Chapter 6, to be published in Nuclear Fusion
- [Harvey 92] R. W. Harvey, M. G. McCoy. "The CQL3D Fokker-Planck Code" in Proceedings of the IAEA Technical Committee Meeting on Advances in Simulation and Modeling of Thermonuclear Plasmas (IAEA, Montreal, 1992), available through USDOC, NTIS No. DE9300962
- [Jaeger 01] E. F. Jaeger, et al. 2001, Phys. Plasmas, 8: 1573
- [Jaeger 02] E. F. Jaeger, et al. 2002, Phys. Plasmas, 9: 1873
- [Jaeger 06] E. F. Jaeger, et al. 2006, Phys. Plasmas, 13: 056101
- [Kennel 66] C. F. Kennel, F. Engelmann. 1966, Phys. Flu-

ids, 9: 2377

[Kwon 06] J-M Kwon, et al. 2006, Bull. Am. Phys. Soc., VP1.00115

[Myra 90] J. R. Myra, D. A. D'Ippolito, M. Gerver. 1990, Nucl. Fusion, 30: 845

[O'Brien 96] O'Brien M. R, Cox M, Gardner C. A, Zaitsev F. S. 22nd European Conference on Controlled Fusion and Plasma Physics. July, 1995

[Perkins 89] F. W. Perkins. 1989, Nucl. Fusion, 29: 583

[Swain 97] D. W. Swain, et al. 1997, Nucl. Fusion, 37: 211

[Wright 05] J. C. Wright, et al. 2005, Nucl. Fusion, 45: 1411

III.7 Edge physics simulation (X. Q. Xu and C. S. Chang)

The plasma edge includes the pedestal, scrape-off, and divertor regions. A complete edge physics should deal with the plasma, atomic, and the plasma-wall interaction phenomena. The edge provides the source of plasma through ionization of the incoming neutral particles and source of impurity through the wall sputtering. Edge plasma sets a boundary condition for the core confinement physics. Importance of the edge plasma has been elevated to the top list of the ITER physics research needs due to the necessity of the self-organized plasma pedestal and its destruction by edge localized mode activities. Extrapolation of the present tokamak data base predicts that a sufficient pedestal height is a necessary condition for the success of ITER.

Plasma turbulence and the resulting anomalous cross-field plasma transport, integrated with the strong neoclassical transport, are crucial physics processes in the boundary region, affecting both core plasma confinement and plasma-wall interactions. Reduction of anomalous plasma transport at the boundary, associated with the transition to the H-mode operating regime, leads to sharp pedestal-like structures in the temperature and density profiles. The continuing buildup of the sharp pressure gradients in the pedestal region can drive edge localized modes (ELMs). The large bursting events due to ELMs not only destroy the edge pedestal, force the discharge back to low confinement regime, and therefore strongly impact global confinement and fusion performance; they also cause the large power from the collapse of the edge pedestal to move across the separatrix into the Scrape-Off Layer (SOL), with the power either flowing into divertor plates along the field-line or to the main chamber wall. The large outward heat flux resulting from ELM bursting puts serious constraints on the lifetime of ITER divertor plates and first wall.

The edge physics is a mix of plasma physics, atomic physics, and chemistry and material science. The important issues associated with the edge physics are instabilities, turbulence, transport, plasma sources and sinks, and impurity generations. There are many sources of instabilities and turbulence, such as gradients of density, temperature, current, flow, radiation and

ionization. The most popular instabilities for the edge are ideal and resistive ballooning modes, peeling modes, drift waves and drift Alfvén modes, Kelvin-Helmholtz modes, and sheath-driven modes. However, these are not really all independent modes, but rather are co-existing for destabilizing drift-wave type instabilities. In fact, since typical edge plasmas have low densities and temperatures, and steep radial gradients, the diamagnetic drift time scale, collision time scale, Alfvén time scale, and electron transit time scale are all on the same order, with no clear distinction between them. They are all drift-wave type instabilities with full electromagnetic perturbations.

Over the last two decades, there has been rapid development of edge modeling and simulations around the world. The characteristics of this stage is that each code addresses each specific physics, such as the fluid transport codes SOLPS [Coster 2006] and UEDGE [Rognien 2005], 3D fluid turbulence code BOUT [Xu 1998], DBM [Rogers 1998] and DALF3 /GEM [Scott 2006], the reduced MHD code JOEK [Huysmans 2005], kinetic Monte Carlo neutral models DEGAS [Strotler 2006] and Eirene [Reiter 2002], neoclassical particle-in-cell kinetic codes XGC-0 [Chang 2004] and ASCOTT [Heikkinen 2001]. The XGC-0 code has just been converted into a particle-in-cell kinetic (electrostatic) turbulence code XGC-1 in the US SciDAC Fusion Simulation Project Center for Plasma Edge Simulation (CPES) headquartered at New York University. A 4D kinetic neoclassical continuum code TEMPEST [Xu 2006] is under development the U.S. Edge Simulation Laboratory (ESL) headquartered at Lawrence Livermore National Laboratory. A new particle-in-cell kinetic (electrostatic) turbulence code ELMFIRE [Heikkinen 2006] is in operation in Europe. A complete review of each code around the world is beyond the scope of this paper.

III.7.1 Fluid simulation (X. Q. Xu)

In this section we will give a narrative description of BOUT code: arguably representative current state of art for nonlinear edge turbulence and ELM simulation. The goal of the BOUT project is the development and deployment of a user-friendly, state-of-art, nonlinear fluid turbulence capability for the analysis of boundary turbulence in a general geometry on a routine basis. BOUT models the 3D electromagnetic boundary plasma turbulence that spans the separatrix using a set of fluid moment equations with the neoclassical closures for plasma vorticity, density, ion and electron temperature and parallel momentum, and with proper sheath boundary conditions in the SOL [Xu 1998, Xu 2000]. The BOUT code solves these equations in a 3D toroidal segment (toroidal wedge), including the region somewhat inside the separatrix and extending into the SOL; the private flux region is also included. With poloidal flux, ψ , normalized to unity on the separatrix, BOUT typically sets the inner simulation boundary condition to be $\psi_c=0.9$ and the outer boundary at

$\psi_w=1.1$. The boundary conditions are homogeneous Neumann at ψ_c and at $\psi = \psi_w$, sheath boundaries in the SOL and the private flux regions, shifted periodic in the poloidal direction in the “edge” (inside of separatrix), and periodic in toroidal direction. A finite difference method is used, and the resulting difference equations are solved with a fully implicit, parallelized, Newton-Krylov solver PVOE/PVOE. In order to investigate boundary turbulence, BOUT is able to couple to the edge plasma transport code UEDGE, and MHD equilibrium code EFIT/Corsica to get realistic X-point divertor magnetic geometry and plasma profiles.

BOUT contains much of the relevant physics for the pedestal barrier problem for the experimentally relevant X-point divertor geometry. Encouraging results have been obtained when using measured plasma profiles in the current generation of major US fusion devices such as DIII-D, C-Mod and NSTX. The resistive X-point mode has been identified in an X-point divertor geometry [Xu 2000nf, Myra 2000]. Comparison of the shifted-circle vs. X-point geometry shows the different dominant modes and turbulence fluctuation levels [Xu 2000]. The poloidal fluctuation phase velocity shows the experimentally observed structure across the separatrix in many fusion devices [Xu 2002]. The fluctuation phase velocity is larger than the velocity. The Quasi-Coherent mode is believed to be responsible for the high energy confinement (H-mode), yet acceptably low particle (impurity) confinement in the Alcator C-Mod high density plasma regime. The experimentally measured dispersion and mode stability is in good agreement with the resistive ballooning X-point mode predicted by the BOUT code [Mazurenko 2002]. A strong poloidal asymmetry of particle flux in the proximity of the separatrix may explain the paradox of the JET probe measurements of the particle flux when comparisons of the limiter vs. divertor experiments had been made [Xu 2002]. Other studies highly relevant to pedestal physics have been performed with BOUT, including one with fixed H-mode-like temperature and density profiles showing generation of Er profiles and turbulence consistent with experimental results [Xu 2000], and another, in which all profiles are evolved, showing a plausible L-H transition [Xu 2000, Xu 2002]. Other recent physics results from BOUT include a study of the effects of variable density on edge turbulence, leading to a more definitive picture of the tokamak density limit [Xu 2003, Xu 2004], the formation and propagation of large-amplitude convective structures (blobs) [Russell04], and simulations [Umansky04] and theory [Xu 2004fec] indicating the possibility of divertor-leg turbulence which is independent of turbulence in the main edge plasma.

In H-mode discharges, the sharp pressure gradients in the pedestal region can drive large bootstrap currents which provide an additional source of free energy to drive MHD instabilities. This current drives “peeling” or edge-localized external kink, modes [Connor 1998, Snyder 2002cpp], due to the expected sharp current gradient near the separatrix, and can be unstable even at

relatively high values of the toroidal mode number (n). In addition to driving peeling modes, the large bootstrap current in the edge region also lowers the local magnetic shear, and in shaped discharges this can allow second stability access to high- n ballooning modes. The stability physics is further complicated by the coupling of peeling modes to pressure driven ballooning-type instabilities which occurs at finite n [Connor 1998, Snyder 2002]. As a result, intermediate $3 < n < 40$ coupled peeling-ballooning modes are often the limiting ideal MHD instability in the pedestal. It has been proposed that these peeling-ballooning modes are responsible for edge localized modes (ELMs), and that they provide constraints on the height of the H-mode pedestal. Predictions from linear peeling-ballooning stability calculations have yielded encouraging agreement with observed ELM onset times and penetration depth, and variation in pedestal characteristics with plasma shape [Snyder 2002]. A number of characteristics of the BOUT simulation results, including poloidal extent and filamentary structure, are consistent with fast ELM observations on multiple experimental devices. Several characteristics of the BOUT simulation results are also qualitatively consistent with nonlinear ballooning theory [Wilson 2004, Snyder 2005], including explosive growth of the filaments, with perturbations growing roughly as $1/(t-t_0)^\gamma$, and a growth rate increasing with time.

References

- [Coster 2006] D P Coster, X Bonmin, M Warrier. 2006, Phys. Scr., no. T124: 9-12
- [Rognlien 2005] T D Rognlien, M V Umansky, X Q Xu, et al. 2005, Journal of Nuclear Materials, 337-39(1-3): 327-331
- [Xu 1998] X. Q. Xu, R. H. Cohen. 1998, Contributions to Plasma Physics, 38(1-2): 158-170
- [Rogers 1998] B. N. Rogers, J. F. Drake, A. Zeiler. 1998, Physical Review Letter, 81: 4396-4399
- [Scott 2006] B. D. Scott. 2006, Contributions to Plasma Physics, 46(7-9): 714-725
- [Huysmans 2005] G T A Huysmans. 2005, ELMs: Plasma Physics and Controlled Fusion, 47: B165-B178
- [Stotler 2006] D P Stotler. 2006, PHYS SCRIPTA, T124: 23-26
- [Reiter 2002] D Reiter, S Wiesen, M Born. 2002, Plasma Physics and Controlled Fusion, 44: 1723
- [Chang 2002] C. S. Chang, S. Ku, H. Weitzner. 2002, Phys. Plasmas, 9: 3884
- [Heikkinen 2001] J.A.Heikkinen, et al. 2001, Journal of Computational Physics, 173: 527-548
- [Xu 2006] X. Q. Xu, et al. 2006, 21th IAEA Fusion Energy Conference/(Chengdu, China, 2006), TH/P6-23; http://www-pub.iaea.org/MTCD/Meetings/FEC2006/th_p6-23.pdf.
- [Heikkinen 2006] J A Heikkinen, Heikkinen J A, Henriksson S, et al. 2006, Contributions to Plasma Physics, 46 (7-9):

490-495

- [Xu 2000] X. Q. Xu, R. H. Cohen, T. D. Rognlien, et al. Phys. of Plasmas, 7: 1951-1958
- [Myra 2000] J. R. Myra, D. A. D'Ippolito, X. Q. Xu, et al. 2000, Physics of Plasma, 7: 4622-4631
- [Xu 2000nf] X. Q. Xu, R. H. Cohen, G. D. Porter, et al. 2000, Nuclear Fusion, 40(3Y): 731-736
- [Xu 2002] X. Q. Xu, R. H. Cohen, W. M. Nevins, et al. 2002, Nucl. Fusion, 42: 21-27
- [Mazurenko 2002] A. Mazurenko, M. Porkolab, X. Q. Xu, W. M. Nevins. 2002, Physics of Review Letter, 89: 225004-1-225004-4
- [Xu 2003] X. Q. Xu, W. M. Nevins, T. D. Rognlien, et al. 2003, Physics of Plasma, 10(5): 1773-1781
- [Xu 2004] X. Q. Xu, W. M. Nevins, R. H. Cohen, et al. 2004, Plasma Physics, 44: 105-110
- [Russel 2004] D. A. Russell, D. A. D Ippolito, J. R. Myra, et al. Physical Review letters, 93: 265001-4
- [Umansky 2004] M. V. Umansky, T. D. Rognlien, X. Q. Xu, et al. 2004, Plasma Physics, 44: 182-187
- [Xu 2004fec] X. Q. Xu, R.H. Cohen, W.M. Nevins, et al. 2004, 20th IAEA Fusion Energy Conference Vilamoura, Portugal, 1-6 November 2004, IAEA-CN-116/TH/1-5
- [Connor 1998] J. W. Connor, R. J. Hastie, H. R. Wilson, et al. 1998, Phys. Plasmas, 5: 2687
- [Snyder 2002cpp] Snyder, P. B., Wilson, H. R. 2002, Contributions to Plasma Physics, 42: 258. (this citation should be distinguished from the next one)
- [Snyder 2002] P. B. Snyder, H. R. Wilson, J. R. Ferron, et al. 2002, Phys. Plasmas, 9: 2037
- [Wilson 2004] H. R. Wilson, S. C. Cowley, 2004, Phys. Rev. Lett., 92: 175006
- [Snyder 2005] P. B. Snyder, H. R. Wilson, X. Q. Xu. 2005, Physics of Plasmas, 12: 056115

III.7.2 Kinetic simulation (C. S. Chang)

The ITER relevant edge plasmas in the present day experiments are in the kinetic regime, with the pedestal ions in the long-mean-free-path banana collisionality regime and the pedestal electrons in the banana-plateau regime. Ions experience significant orbit loss due to the existence of the divertor X-point [Chang2002]. There is a kinetic nonlinear interaction between the radial orbit excursions and pedestal width, which breaks the ordering assumptions in the analytic neoclassical theories. These phenomena are completely kinetic, not to be described by a fluid modeling, and the kinetic interplay generate self-consistent radial electric field. The radial electric field in turn determines the pedestal width. In other words, the conventional fluid or neoclassical modeling cannot determine the radial electric field and the pedestal width. More details will be described shortly. There is another reason why a kinetic description is necessary for edge plasma. It has been verified by experiment [Burrell 2003] and simulation [Chang 2005] that the ion distribution function in the scrape-off layer are not Maxwellian.

There are two kinetic simulation efforts in the USA. One is the continuum effort at the Edge Simulation Laboratory (ESL), a multiple institutional efforts funded by DOE, and the other is the particle-in-cell effort within the US SciDAC Fusion Simulation Project Center for Plasma Edge Simulation (CPES). The particle-in-cell XGC code in CPES has been successful in producing the neoclassical solutions self-consistently with the 2D electric field solutions, neutral kinetics and atomic physics, and wall recycling physics (XGC-0) [Chang2004]. XGC is also beginning to produce the electrostatic turbulence solutions (XGC-1). Even though XGC contains an atomic neutral Monte Carlo simulation package, US has a stand-alone Monte Carlo neutral particle code DEGAS2, which has a more complete atomic physics package. The atomic physics package in XGC is currently being replaced by the more complete routines from DEGAS2 as part of the CPES activity.

Despite all the advantages of a particle-in-cell code to study the edge plasma, it may suffer from the discrete particle noise problem if not handled properly (see the discussions in the core turbulence section). The best method to reduce the discrete particle noise without increasing the number of particle number is to use a physical Coulomb scattering in the simulation. The XGC-code will be using such a physical collision scheme to dissipate the discrete particle noise. An advanced physical collision scheme may also improve the simulation time of a particle code by allowing a more advanced particle push algorithm.

Just inside the magnetic separatrix (H-mode layer), ion orbits can easily drift out of the closed flux surface region into the open field lines. Without the X-point, the collisionless orbits come back to the closed field lines. However, the X-point geometry directs many of such orbits to the divertor plates, instead of allowing them to come back into the closed flux surface region [Hahn 2005, Weitzner 2004]. This creates velocity-space holes in the H-mode layer. The worst of such velocity-space hole exists near the X-point, as shown in Fig. (II.7.2.1)[Chang 2002]. This type of orbit loss is an important source of the edge radial electric field and, thus, the flow shear in the H-mode layer. The orbit loss becomes stronger as the edge ion temperature gets stronger, raising the radial electric field strength. The pedestal pressure gradient then rises in accordance with the radial force balance. Fast rise of the pedestal gradient is accomplished by the particle source from neutral ionization. An edge code must be able to describe these kinetic phenomena in order to obtain a reliable radial electric field and its effect on the neoclassical and turbulence transport.

The narrowing of the pedestal width caused by the steepening of pedestal gradient causes another kinetic complication which cannot be described by a fluid modeling. As the pedestal width becomes comparable to the ion banana width, radial orbital mixing of the ions become strong and the nonlinear neoclassical saturation

of the pedestal slope occurs. At the same time, radial charge separation tendency of the ion orbits from the electrons forces the radial electric field to build up in such a way to keep the plasma quasi-neutral by way of orbit squeezing. The pedestal width and shape will thus have to be consistent with the self-generated orbit-squeezing electric field. A reliable edge simulation code must include these inter-connected nonlinear kinetic effects self-consistently. We refer the interested readers to Ref. [Chang2004, Heikkinen 2004] for further details.



Fig.III.7.2.1 A loss orbit near X-point

The plasma confinement time in the open field line region is much shorter than that of the closed field line region. Hence, the particle density and temperature of the scrape-off plasma is much lower than those of the core plasma. Plasma particles bombarding the wall are neutralized and captured in the material surface to undergo quantum mechanical scatterings and relaxations with the material atomic crystals. Many of them are thermalized to the wall temperature, and, released back into the scrape-off region as neutral molecules at much lower energy than the original plasma energy. The accurate energy and angular distribution of the released neutral particles, as well as the sputtering of the material surface, are best studied with a surface molecular dynamics code. Such results are to be incorporated into the XGC edge code in the SciDAC CPES project. The number of the particles absorbed in the material surface is usually significant compared to the total number of particles in the plasma. Its release rate does not have a one-to-one correspondence with the impinging plasma particles at a given time and can become a significant unknown factor in the edge physics.

Plasma interaction with the neutrals can provide a different source of physics from the usual plasma-plasma Coulomb interactions. Unlike the plasma-plasma interactions, they do not have to satisfy momentum and energy conservation in the plasma. They are known to influence the plasma rotation physics and H-mode transition power threshold [Maingi2004, Helander2003]. It is also known that the plasma rotation in the scrape-off can have a strong non-local influence on the core rotation which is related to the core plasma stability and transport (counter rotation usually yields a worse confinement) [Rice 2005]. The physics behind

these phenomena is beginning to be understood, but is still largely unknown at this moment.

The XGC code may soon begin to unveil the electrostatic kinetic turbulence physics in the edge region, self-consistently with the neoclassical physics. However, the simulation capability of the kinetic electromagnetic turbulence physics in XGC is still to be developed.

As the edge pedestal builds up, the edge plasma can become MHD unstable and induces the so called edge localized modes (ELMs), which can significantly reduce the pedestal width and the core confinement. Another serious consequence of ELM is the intolerable amount of heat load on the divertor plates. At the present time, the ELMs are best studied with MHD/fluid modeling codes. There are several linear ideal MHD codes in the world which can evaluate the linear instability boundary of the peeling-ballooning modes. There are a few codes which can evaluate the nonlinear evolution of the ELMs: the MHD two fluid codes M3D and NIMROD as described elsewhere in this report, and the Braginskii two fluid code BOUT and Huysmans's recent work [Huysmans 2005] as described in the previous section.

References

- [Burrell 2003] K. H. Burrell, R. J. Groebner, P. Gohil, W. M. Solomon. 2003, the 45th Annual Meeting of the Division of Plasma Physics, October 27-31, 2003, Albuquerque, New Mexico, Bulletin of the American Physical Society, KP1.029.
- [Chang 2005] C. S. Chang. 2005, Transport Task Force Meeting, April 6: 2005 - April 9, 2005, Napa, California, USA
- [Chang 2002] C. S. Chang, S. Ku, H. Weitzner. 2002, Phys. Plasmas, 9: 3884
- [Chang 2004] C. S. Chang, S. Ku, H. Weitzner. 2004, Phys. Plasmas, 11: 2649
- [Hahn 2005] S. H. Hahn, Seunghoe Ku, C. S. Chang. 2005, Physics of Plasmas, 12: 102501
- [Heikkinen 2004] J. A. Heikkinen, et al. 2004, Contr. Plasma Phys., 44: 13
- [Helander 2003] P. Helander, T. Fulop, P. J. Catto. 2003, Phys. Plasma, 10: 4396
- [Huysmans 2005] G T A Huysmans. 2005, Plasma Physics and Controlled Fusion, 47: B165 ~ B178
- [Ku 2004] S. Ku, H. Baek, C. S. Chang. 2004, Phys. Plasmas, 11: 5626
- [Rice 2005] J. Rice, M. Greenwald, et al. to appear in Phys. Plasmas APS Special Issue
- [Maingi 2004] R. Maingi, C. S. Chang, Seunghoe Ku, et al. 2004, Plasma Phys. Cont. Fusion, 46: A305 ~ A313
- [Weitzner 2004] H. Weitzner, C. S. Chang. 2004, Phys. Plasmas, 11: 3060

III.8 Energetic particle physics (F. Zonca, G.Y. Fu, S.J. Wang)

The confinement properties of energetic ($E \approx 1$ MeV) ions are a crucial aspect of burning plasmas since they are present both as fast particles generated via additional heating and current drive systems as well as charged fusion products. In the first case, successful plasma operations rely on the possibility of controlling plasma current and flow profiles via neutral beam injection (NBI) and plasma temperature profiles by both NBI and ion cyclotron resonant heating (ICRH). In the second case, fusion alpha particles must provide a significant fraction of the local power density, which is ultimately necessary for the sustainment of the plasma burn.

The possible detrimental effects of collective shear Alfvén (s.A.) fluctuations [Rosenbluth 75, Mikhailovskii 75] as well as of lower frequency MHD modes [McGuire 83, Chen 84, Coppi 86] on energetic (fast) ion confinement properties were recognized in the early 1970's and ever since the stability properties of Alfvénic and MHD fluctuations have been an important subject of the field. The nonlinear behaviors of these modes was also investigated [Berk 90] at the time of the first systematic experimental studies of collective s.A. oscillations [Wong 91, Heidbrink 91] and together with the first numerical simulations of fast ion transport in the presence of these modes [Sigmar 92]. In this respect, the studies of energetic ion physics in burning plasmas are good examples of the positive and fruitful feedbacks between theory, experiment and numerical simulations, producing significant advances in the understanding of fundamental aspects as well as in the predictability of actual plasma behaviors in present and future machines, like ITER.

III.8.1 Linear stability analyses

The various s.A. modes that can be excited in the presence of the energetic ion free energy source are strongly influenced by the presence of the s. A. continuous spectrum, which is characterized by gaps. The frequency gap at $\nu_A/(2qR_0)$ (ν_A being the Alfvén speed, q the safety factor and R_0 the plasma major radius) is due to the finite toroidicity of the system [Kieras 82], but other gaps generally exist at $\omega = \ell\nu_A/(2qR_0)$, due to either non-circularity of the magnetic flux surfaces ($\ell=2,3,\dots$) [Betti 91], to anisotropic trapped energetic ion population ($\ell=1,2,3,\dots$) [Van Dam 98] or to finite-b (mainly $\ell=2$, with $\beta = 8\pi P/B^2$, the ratio of kinetic with magnetic pressure) [Zheng 98]. A low-frequency gap also exists because of finite plasma compressibility [Turnbull 93] and is located at $\omega \cong \beta_i^{1/2}(7/4 + T_e/T_i)^{1/2}\nu_A/R_0$ [Zonca 96], with β_i the thermal (core) ion β and $T_e(T_i)$ the core electron (ion) temperature. Discrete s.A. modes, or Alfvén Eigenmodes (AEs) exist in all these frequency gaps and have been given different names accordingly, e.g. Beta induced AE (BAE) [Turnbull 93, Heidbrink 93] for

$\omega \cong \beta_i^{1/2}(7/4 + T_e/T_i)^{1/2}\nu_A/R_0$, Toroidal AE (TAE) [Cheng 85] for $\omega \cong \nu_A/(2qR_0)$, Ellipticity induced AE (EAE) [Betti 91] for $\omega \cong \nu_A/(qR_0)$, etc. Global AEs (GAE) [Appert 82] may also exist in a non-uniform cylindrical plasma equilibrium and are localized in both frequency and radial position near an extremum of the s.A. continuous spectrum. In addition, a variety of kinetic counterparts of the corresponding ideal AE also exists when, e.g. finite resistivity [Cheng 85] or finite Larmor radius (FLR) are accounted for, as in [Mett 92] for the Kinetic TAE (KTAE). A unified picture of all these modes was recently proposed in [Zonca 06], where it was demonstrated that all AE from the BAE to the TAE frequency can be consistently described by the fishbone-like dispersion relation

$$-i\Omega + \delta W_f + \delta W_k = 0, \quad (\text{III.8.1})$$

where δW_f and δW_k play the role of fluid (core component) and kinetic (fast ion) contribution to the potential energy, while Ω represents a generalized inertia term, which reduces to $\Omega = qR_0\omega/\nu_A$ in the ideal MHD limit [Zonca 06]. Equation (1) shows the existence of two types of modes; i.e., a discrete AE, for $\Re\Omega^2 < 0$; and an energetic particle continuum mode (EPM) [Chen 94] for $\Re\Omega^2 > 0$. For the AE, the combined effect of δW_f and the non-resonant fast ion response provides a real frequency shift, which removes the degeneracy with the s.A. continuum accumulation point and makes the mode weakly damped [Cheng 85]. Meanwhile, the resonant wave-particle interaction gives the mode drive, which is necessary to overcome the small but finite damping due to the core component. In the case of the EPM, ω is set by the relevant energetic ion characteristic frequency and mode excitation requires the drive to exceed a threshold due to continuum damping [Hasegawa 74, Chen 74, Zonca 92, Rosenbluth 92]. However, the non-resonant fast ion response is crucially important for EPM excitation as well, since it provides the compression effect that is necessary for balancing the generally positive MHD potential energy of the wave [Chen 84, Chen 94].

The combined effect of δW_f and $\Re\delta W_k$, which determines the existence conditions of AE by removing the degeneracy with the s.A. accumulation point, depends on the plasma equilibrium profiles. For example, TAE mode structure and existence condition are modified at low magnetic shear values typical of the plasma near the magnetic axis and have been dubbed core-localized TAE [Fu 95a]. Similar considerations apply for hollow-q plasma equilibria, where an AE can be excited in the local s.A. frequency gap which is spontaneously formed at the minimum-q surface [Berk 01], yielding the so called Alfvén cascade (AC) [Sharapov 01] or reversed shear AE (RSAE) [Takechi 02], satisfying Eq. (1). The effect of plasma compressibility on ACs was also analysed recently [Breizman 05], when the mode frequency becomes comparable with that of the low-frequency s.A. accumulation point $\omega \cong \beta_i^{1/2}(7/4 + T_e/T_i)^{1/2}\nu_A/R_0$ [Turnbull 93, Zonca

96].

In summary, the s.A. fluctuation spectrum in toroidal system is well understood. Considerable progress has been also made in the quantitative comparison of numerical predictions with experimental data, e.g. by comparing active measurements of global damping rates of long wavelength modes in JET with numerical simulation results from global codes [Jaun 98, Borba 02], built as kinetic extensions of MHD codes, such as NOVA-K [Cheng 92] or Castor-K [Borba 02], or based on kinetic models, as in the case of PENN [Jaun 95]. Calculated damping rates using non-perturbative kinetic models agree qualitatively with experiments, although details of damping mechanisms are still being debated [Jaun 98, Borba 02, Fu 05, Lauber 05]. Precise comparisons with measured damping rates depend on plasma edge boundary conditions [Fu 05], as was recently confirmed by the global gyrokinetic code LIGKA [Lauber 05]. This suggests that future developments in numerical stability analyses of burning plasmas in realistic conditions will need to incorporate accurate models of the scrape-off Layer (SOL) and of the mode structure outside the last closed magnetic surface in divertor configurations. Another critical aspect is the accurate modeling of the mode conversion of long wavelength MHD-like modes to shorter wavelengths, typical of kinetic Alfvén Waves (KAW) [Chen 74]. Differences in the wave propagation properties are the explanation of different predictions of the AE kinetic damping rates in the plasma interior, which still require some effort in code benchmarking among themselves and vs. known analytical results. The coupling of AE to the drift Alfvén branch has also been partly investigated [Zonca 99, Jaun 00] and needs to be further explored. Finally, reliable numerical stability calculations for EPMs must account for self-consistent energetic ion physics, since the fast ion free energy source may modify the wave field structure itself [Chen 94]. Another important aspect is the detailed modeling of the fast ion distribution function, as recently shown in stability analyses of the internal kink modes excited by energetic passing ions [Betti 93, Wang 01, Wang 02]. The most recent systematic stability analyses of proposed burning plasma experiments are summarized in [Gorelenkov 03].

III.8.2 Nonlinear physics and fast ion transport

The fundamental problem to be addressed in studies of collective mode excitation by energetic ions in burning plasmas is to assess whether or not significant degradation in the plasma performance can be expected in the presence of Alfvénic fluctuations and, if so, what level of wall loading and damage of plasma facing materials can be caused by energy and momentum fluxes due to collective fast ion losses. For obvious reasons, this problem requires a solution before ITER operation and, therefore, only numerical simulations can provide the necessary information with the appropriate level of

confidence and accuracy. On the other hand, continuous and positive feedback is necessary between theory, computer simulation and existing as well as future experimental evidences for reliable modeling verification and validation.

Energetic particle losses up to 70% of the entire fast particle population have been predicted theoretically and found experimentally. The particle loss mechanism is essentially of two types [Sigmar 92, Hsu 92]: (1) transient losses, which scale linearly with the mode amplitude ($\approx \delta B_r/B$, δB_r being the radial magnetic field perturbation), due to resonant drift motion across the orbit-loss boundaries in the particle phase space of energetic particles which are born near those boundaries; (2) diffusive losses above a stochastic threshold, which scale as $\approx (\delta B_r/B)^2$, due to energetic particle stochastic diffusion in phase space and eventually across the orbit-loss boundaries. Due to the large system size, mainly stochastic losses are expected to play a significant role in ITER. The stochastic threshold for a single mode is $(\delta B_r/B) \approx 10^{-3}$, although that may be greatly reduced ($(\delta B_r/B) \leq 10^{-4}$) in the multiple mode case [Sigmar 92, Hsu 92].

For weakly unstable AEs, a possible nonlinear saturation mechanism is via phase-space nonlinearities (wave-particle trapping) [Berk 90, Berk 92]. This fact has been confirmed by many numerical simulations [Wu 94, Todo 95, Fu 95b, Candy 97]. Another possible saturation scenario is by ion Compton scattering off the thermal ions [Hahm 95], which locally enhance the mode damping via nonlinear wave-particle resonances, or by mode-mode couplings which may cause poloidal flows [Spong 94] or generate a nonlinear frequency shift and locally enhance the interaction with the s.A. continuum [Zonca 95, Chen 98]. Recently, numerical simulations confirmed that mode-mode couplings give an estimate for AE saturation amplitudes on TFTR that are closer to experimentally measured levels than if they were not included in the simulation model [Todo 05]. While the role of nonlinear wave-particle and wave-wave interactions is generally important in determining the AE saturation level [Hahm 95, Spong 94, Zonca 95, Chen 98], nonlinear evolution of the energetic ion distribution function is affected by formation of phase space-structures. Noticeable examples of such structures are the pitchfork splitting of TAE spectral lines observed on JET [Fasoli 98] and explained in terms of hole-clump pair formations in phase space, near marginal stability [Berk 97]. Still, the nonlinear dynamics of AEs discussed so far, refer to single wave-particle resonances or to local saturation mechanisms. It is then not surprising that AE yield negligible energetic particle losses, unless phase-space stochasticity is reached, possibly via a phase-space explosion (“domino effect” [Berk 96]). This fact has been confirmed also by numerical simulations of alpha particle driven Alfvén gap modes in ITER [Candy 97]. For this reason, the dominant loss mechanism below the stochastic threshold is expected to be that of scattering of barely counter-passing par-

ticles into unconfined “fat” banana orbits [Sigmar 92, Hsu 92]. Once again, this loss mechanism is expected to be weak in ITER, due to the small ratio of banana orbit width to system size.

Numerical simulations of collective excitations of MHD and Alfvén modes by energetic ions and of fast ion transport in burning plasmas mostly rely on global hybrid MHD-gyrokinetic codes, such as M3D [Park 92], HMGC [Briguglio 95] and MEGA [Todo 98], which solve the hybrid MHD-gyrokinetic model equations [Park 92], where the thermal (core) component of the plasma is described by nonlinear MHD and the energetic ion dynamics enter only via the divergence of the fast ion pressure tensor, $\nabla \cdot \mathbf{P}_E$, in the momentum balance equation. The nonlinear gyrokinetic equation [Frieman 82] is solved, generally via particle-in-cell (PIC) techniques, for the direct computation of $\nabla \cdot \mathbf{P}_E$ in the self-consistent wave fields. Generally, the hybrid MHD-gyrokinetic model [Park 92] is sufficiently accurate for the adequate description of those modes that are most relevant for both stability and fast ion transport [Zonca 06], although more accurate kinetic models based on the Vlasov-Maxwell system are required for analyzing energetic ion redistributions at shorter wavelengths [Vlad 05, Estrada-Mila 06], typical of Alfvénic turbulence. For weakly unstable AEs, the use of global hybrid MHD-Gyrokinetic codes provides the most promising route to exploring the issue of fast ion transport in burning plasmas. Along this path, two issues remain to be solved: (1) the multi-mode simulation in realistic equilibria, for adequate treatment of possible phase-space stochasticity effects; (2) the coupling of global wave-field solvers to evolution (transport) codes for the energetic particle equilibrium distribution function on long time scales. The first point is mostly demanding on numerical computation efficiency and memory, and eventually requires accurate SOL models and realistic X-point geometry (see also III.8.1). The second aspect also requires the development of physics models for the simultaneous treatment of very disparate time scales, possibly involving additional phenomena such as nonlocal behaviors due to finite size orbits and canonical invariant breaking due to non-axisymmetry, e.g. toroidal field ripple or strong non-linear equilibrium distortions.

The picture of nonlinear fast ion dynamics is further complicated if the plasma is significantly above marginal stability. Simulation results indicate that, above threshold for the onset of the resonant EPM [Chen 94], strong fast ion transport occurs in “avalanches” [Zonca 05]. Such strong transport events occur on time scales of a few inverse linear growth rates (generally 100-200 Alfvén times, $\tau_A = R_0/\nu_A$) and have a ballistic character [White 83] that basically differentiates them from the diffusive and local nature of weak transport. Experimental observations on the JT-60U tokamak have also confirmed macroscopic and rapid energetic particle radial redistributions in connection with the so-called abrupt large amplitude events

(ALE) [Shinohara 01]. Therefore, it is crucial to theoretically assess the potential impact of fusion product avalanches due to the hard limit that these may impose on burning plasma operations. Recent numerical simulations of burning plasma operations proposed for ITER indicate that significant fusion- α losses ($\approx 5\%$) may occur due to a rapid broadening of α -particle profiles in the hollow- q “advanced”-tokamak scenario [Vlad 06]. Meanwhile, only moderate internal energetic ion relaxation is expected for “conventional” q -profiles, whereas strong EPM excitation and significant convective fusion- α losses are predicted in the “hybrid” centrally flat- q -profile case only if the volume averaged fast ion density is increased by a factor 1.6 [Vlad 06]. These results are obtained assuming an initial given fusion- α profile. In the EPM case, the coupling of global field solvers to evolution codes for the energetic particle reference distribution function on long time scales is even more demanding than for weakly unstable AEs, due to the bigger separation of time scales and the self-consistent evolution of the wave-field with the fast ion free energy source profiles. Similar considerations can be made for the non-linear energetic ion dynamics in the presence of low-frequency MHD modes (see also II.4). Convective losses with ballistic character [White 83], similar to those of EPM avalanches, were originally proposed for explaining experimental observations of the fishbone mode [McGuire 83]. Recent numerical simulations of both kink and fishbone instability confirm the fact that rapid fast ion transport is expected when the system is significantly above marginal stability [Fu 06]. Simulation results also elucidate the complex interplay between mode structure and fast ion source, showing that saturation is reached because of the rapid broadening of the energetic ion radial profile, even if fluid nonlinearities are important as well [Fu 06].

These results suggest that energetic ion transport in burning plasmas has two components: one identified by slow diffusive processes due to weakly unstable AEs and a residual component possibly due to plasma turbulence; another one characterized by rapid transport processes with ballistic or secular nature due to coherent nonlinear interactions with EPM and/or low-frequency long-wavelength MHD modes.

III.8.3 Outlook and open problems

One crucial aspect that needs attention is the integration of global simulation codes for collective modes with fast ion transport codes (see also III.8.2). This problem poses a number of fundamental physics issues, due to the extremely disparate space and time scales involved and due to the different nature of the processes to be accounted for: external (see II.6) and internal (fusion- α 's) fast ion sources need to be treated self-consistently in the presence of fluctuations and their nonlinear dynamic evolution. Furthermore, the transition of the system through marginal stability and its further nonlinear behavior and evolution must be ad-

ressed consequently. As discussed in III.8.2, numerical simulations of collective excitations of MHD and Alfvén modes by energetic ions and of fast ion transport in burning plasmas mostly rely on global hybrid MHD-Gyrokinetic codes, such as M3D [Park 92], HMGC [Briguglio 95] and MEGA [Todo 98]. The gyrokinetic solvers in these codes are being modified in order to include fast ion sources and collision operators in the gyrokinetic Boltzmann equation. The most challenging task is obviously posed by the large separation of scales between the nonlinear Alfvén mode time and the collision as well as the source characteristic times. A complementary approach is based on Fokker-Planck solvers for numerical simulations of fast ion dynamics, where the effect of AE fluctuations are accounted for by ad-hoc quasi-linear operators, obtained assuming that AE mode structures are given by those in the linear limit; thus, AEs evolve only in amplitude and frequency. This method is adequate for exploring AE nonlinear dynamics near marginal stability, but is obviously invalid for analyzing EPMs. Such efforts are important parts of integrated tokamak modeling research projects worldwide. The investigation of nonlinear AE dynamics will then provide a useful and natural test-bed for comparing and benchmarking the results obtained via complementary methods. Future developments of global simulation codes will also require the inclusion of realistic boundary conditions and thermal plasma kinetic effects (see III.8.1) for numerical stability and fast ion transport analyses of practical relevance for burning plasmas.

Another fundamental aspect, which still remains essentially unexplored, is the issue of whether mutual interactions between collective modes and energetic ion dynamics on the one side and drift wave turbulence and turbulent transport on the other side, may decrease, on long time scales, the thermonuclear efficiency. Theory predicts that Alfvénic fluctuations near the low-frequency s.A. accumulation point can be excited for a wide range of mode number by fast ions (for long wavelengths) as well as by thermal ion temperature gradients (for short wavelengths). The fast ion driven modes were originally observed in DIII-D as BAE modes [Heidbrink 93], while the Alfvénic ITG (AITG) [Zonca 96, Zonca 99] remained a theoretical prediction until recent experimental measurements on DIII-D [Nazikian 06], confirmed the broad wave-number spectrum of Alfvén fluctuations excited by both energetic and thermal ions. This nice example of positive feedback between theory and experiment shows the profound relationship between Alfvénic turbulence and AEs.

On the long-time scale, AE and EPM nonlinear evolutions, as well as those of AITG or strongly driven MHD modes, can be predominantly affected by either spontaneous generation of zonal flows and fields [Chen 01, Guzdar 01] or by radial modulations in the fast ion profiles [Zonca 05, Fu 06], depending on the proximity to marginal stability. Zonal flows generated by MHD and/or AE/EPM and AITG have higher intrinsic frequency with respect to similar flows generated by

electrostatic drift turbulence: thus the possible nonlinear interplay between zonal structures, drift wave turbulence and collective modes excited by energetic ions remains to be assessed [Hahm 99].

A new perspective on the study of fast ion transport by low-frequency MHD modes is given by the recent interest in the excitations of fishbone-like modes by energetic trapped electrons [Sun 05]. Their relevance to burning plasmas arises from the fact that the bounce averaged dynamics of trapped electrons depends on energy (not mass): thus, their effect on low frequency MHD modes can be used to simulate/analyze the analogous effect of charged fusion products, which, unlike fast ions in present day experiments, are characterized by small orbits. Thus, numerical simulations of these modes may offer a simple way for investigating the behavior of trapped fusion-as without introducing additional complications in the physics due to nonlocal behaviors.

References

- [Rosenbluth 75] M. N. Rosenbluth, P.H. Rutherford. 1975, Phys. Rev. Lett., 34: 1428
- [Mikhailovskii 75] A. B. Mikhailovskii. 1975, Zh. Eksp. Teor. Fiz. 68: 1772
- [McGuire 83] K. McGuire, R. Goldston, M. Bell, et al. 1983, Phys. Rev. Lett., 50: 891
- [Chen 84] L. Chen, R. B. White, M. N. Rosenbluth. 1984, Phys. Rev. Lett., 52: 1122
- [Coppi 86] B. Coppi, F. Porcelli. 1986, Phys. Rev. Lett., 57: 2272
- [Berk 90] H. L. Berk, B. N. Breizman. 1990, Phys. Fluids B, 2: 2235
- [Wong 91] K. L. Wong, R. J. Fonck, S.F. Paul, et al. 1991, Phys. Rev. Lett., 66: 1874
- [Heidbrink 91] W. W. Heidbrink, E. J. Strait, E. Doyle, et al. 1991, Nucl. Fusion, 31: 1635
- [Sigmar 92] D. J. Sigmar, C. T. Hsu, R. B. White, C. Z. Cheng. 1992, Phys. Fluids B, 4: 1506
- [Kieras 82] C. E. Kieras, J. A. Tataronis. 1982, J. Plasma Phys., 28: 395
- [Betti 91] R. Betti, J.P. Freidberg. 1991, Phys. Fluids B, 3: 1865
- [Van Dam 98] J. W. Van Dam, M. N. Rosenbluth. 1998, Bull. Am. Phys. Soc., 43: 1753
- [Zheng 98] L.-J. Zheng, L. Chen. 1998, Phys. Plasmas, 5: 444, 1056
- [Turnbull 93] A. D. Turnbull, E. J. Strait, W. W. Heidbrink, et al. 1993, Phys. Fluids B, 5: 2546
- [Zonca 96] F. Zonca, L. Chen, R. A. Santoro. 1996, Plasma Phys. Control. Fusion, 38: 2011
- [Heidbrink 93] W. W. Heidbrink, E. J. Strait, M. S. Chu, et al. 1993, Phys. Rev. Lett., 71: 855
- [Cheng 85] C. Z. Cheng, L. Chen, M.S. Chance. 1985, Ann. Phys., (N.Y.) 161: 21
- [Appert 82] K. Appert, R. Gruber, F. Troyon, et al. 1982, Plasma Phys., 24: 1147
- [Mett 92] R. R. Mett, S. M. Mahajan. 1992, Phys. Fluids B, 4: 2885
- [Zonca 06] F. Zonca, L. Chen. 2006, Plasma Phys. Control. Fusion, 48: 537
- [Chen 94] L. Chen. 1994, Phys. Plasmas, 1: 1519
- [Hasegawa 74] A. Hasegawa, L. Chen. 1974, Phys. Rev. Lett., 32: 454
- [Chen 74] L. Chen, A. Hasegawa. 1974, Phys. Fluids, 17: 1399
- [Zonca 92] F. Zonca, L. Chen. 1992, Phys. Rev. Lett., 68: 592
- [Rosenbluth 92] M. N. Rosenbluth, H. L. Berk, J. W. Van Dam, et al. 1992, Phys. Rev. Lett., 68: 596
- [Fu 95a] G.Y. Fu 1995, Phys. Plasmas, 2: 1029
- [Berk 01] H. L. Berk, D. N. Borba, B. N. Breizman, et al. 2001, Phys. Rev. Lett., 87: 185002
- [Sharapov 01] S. E. Sharapov, et al. 2001, Phys. Lett. A, 289: 127
- [Takechi 02] M. Takechi, et al. 2002, Fusion Energy 2002, (Proc. 19th Int. Conf. Lyon, 2002) (Vienna: IAEA) CD-ROM file EX/W-6
<http://www.iaea.org/programmes/ripc/physics/fec2002/html/fec2002.htm>
- [Breizman 05] B. N. Breizman, M. S. Pekker, S. E. Sharapov, et al. 2005, Phys. Plasmas, 12: 112506
- [Jaun 98] A. Jaun, A. Fasoli, W. W. Heidbrink. 1998, Phys. Plasmas, 5: 2952
- [Borba 02] D. Borba, H. L. Berk, B. N. Breizman, et al. 2002, Nucl. Fusion, 42: 1029
- [Cheng 92] C. Z. Cheng. 1992, Phys. Rep., 211: 1
- [Jaun 95] A. Jaun, K. Appert, J. Vaclavik, et al. 1995, Comput. Phys. Commun., 92: 153
- [Fu 05] G. Y. Fu, H. L. Berk, A. Pletzer. 2005, Phys. Plasmas, 12: 082505
- [Lauber 05] Ph. Lauber, S. Günter, S.D. Pinches. 2005, Phys. Plasmas, 12: 122501
- [Zonca 99] F. Zonca, L. Chen, J.Q. Dong, et al. 1999, Phys. Plasmas, 6: 1917
- [Jaun 00] A. Jaun, A. Fasoli, J. Vaclavik, et al. 2000, Nucl. Fusion, 40: 1343
- [Betti 93] R. Betti, J. P. Freidberg. 1993, Phys. Rev. Lett., 70: 3428
- [Wang 01] S. Wang. 2001, Phys. Rev. Lett., 86: 5286
- [Wang 02] S. Wang, T. Ozeki, K. Tobita. 2002, Phys. Rev. Lett., 88: 105004
- [Gorelenkov 03] N. N. Gorelenkov, H. L. Berk, R. Budny, et al. 2003, Nucl. Fusion, 43: 594
- [Hsu 92] C. T. Hsu, D. J. Sigmar. 1992, Phys. Fluids B, 4: 1492
- [Berk 92] H. L. Berk, B. N. Breizman, H. Ye. 1992, Phys. Rev. Lett., 68: 3563
- [Wu 94] Y. Wu, R. B. White. 1994, Phys. Plasmas, 1: 2733
- [Todo 95] Y. Todo, T. Sato, K. Watanabe, et al. 1995, Phys. Plasmas, 2: 2711
- [Fu 95b] G. Y. Fu, W. Park. 1995, Phys. Rev. Lett., 74: 1594
- [Candy 97] J. Candy, D. Borba, H. L. Berk, et al. 1997,

- Phys. Plasmas, 4: 2597
 [Hahm 95] T. S. Hahm, L. Chen. 1995, Phys. Rev. Lett., 74: 266
 [Spong 94] D.A. Spong, B.A. Carreras and C.L. Hedrick. 1994, Phys. Plasmas, 1: 1503
 [Zonca 95] F. Zonca, F. Romanelli, G. Vlad, et al. 1995, Phys. Rev. Lett., 74: 698
 [Chen 98] L. Chen, F. Zonca, R.A. Santoro, et al. 1998, Plasma Phys. Control. Fusion, 40: 1823
 [Todo 05] Y. Todo, H. L. Berk, B.N. Breizman. 2005, Proceedings of the IAEA TCM 9th IAEA Technical Meeting on Energetic Particles, (9th IAEA TCM-EP, Takayama, 2005) paper OT09
<http://http.lhd.nifs.ac.jp/IAEATM-EP2005/index.html>
 [Berk 97] H. L. Berk, B. N. Breizman, N. V. Petviashvili. 1997, Phys. Lett. A, 234: 213
 [Fasoli 98] A. Fasoli, et al. 1998, Phys. Rev. Lett., 81: 5564
 [Berk 96] H. L. Berk, B. N. Breizman, J. Fitzpatrick, et al. 1996, Phys. Plasmas 3: 1827
 [Park 92] W. Park, S. Parker, H. Biglari, et al. 1992, Phys. Fluids B, 4: 2033
 [Briguglio 95] S. Briguglio, G. Vlad, F. Zonca, et al. 1995, Phys. Plasmas, 2: 3711
 [Todo 98] Y. Todo, T. Sato. 1998, Phys. Plasmas, 5: 1321
 [Frieman 82] E. A. Frieman, L. Chen. 1982, Phys. Fluids, 25: 502
 [Vlad 05] M. Vlad, F. Spineanu, S.-I. Itoh, et al. 2005, Plasma Phys. Control. Fusion, 47: 1015
 [Estrada-Mila 06] C. Estrada-Mila, J. Candy, R. E. Waltz. 2006 Turbulent transport of alpha particles in reactor plasmas submitted to Nucl. Fusion
 [Zonca 05] F. Zonca, S. Briguglio, L. Chen, et al. 2005, Nucl. Fusion, 45: 477
 [White 83] R. B. White, R. J. Goldston, K. McGuire, et al. 1983, Phys. Fluids, 26: 2958
 [Shinohara 01] K. Shinohara, et al. 2001, Nucl. Fusion, 41: 603
 [Vlad 06] G. Vlad, S. Briguglio, G. Fogaccia, et al. 2006, Nucl. Fusion, 46: 1
 [Fu 06] G. Y. Fu, W. Park, H. R. Strauss, et al. 2006, Phys. Plasmas, 13: 052517
 [Nazikian 06] R. Nazikian, H. L. Berk, R. V. Budny, et al. 2006, Phys. Rev. Lett., 96: 105006
 [Chen 01] L. Chen, Z. Lin, R. B. Whit. 2001, Nucl. Fusion, 41: 747
 [Guzdar 01] P. N. Guzdar, R. G. Kleva, A. Das, et al. 2001, Phys. Rev. Lett., 87: 015001
 [Hahm 99] T. S. Hahm, M. A. Beer, Z. Lin, et al. 1999, Phys. Plasmas, 6: 922
 [Sun 05] Y. Sun, B. Wan, S. Wang, et al. 2005, Phys. Plasmas, 12: 092507

III.9 Time-dependent integrated predictive modeling of ITER plasmas (R.V. Budny)

Introduction

Modeling burning plasmas is important for speeding

progress toward practical Tokamak energy production. Examples of issues that can be elucidated by modeling include requirements for heating, fueling, torque, and current drive systems, design of diagnostics, and estimates of the plasma performance (e.g., fusion power production) in various plasma scenarios. The modeling should be time-dependent to demonstrate that burning plasmas can be created, maintained (controlled), and terminated successfully. The modeling also should be integrated to treat self-consistently the nonlinearities and strong coupling between the plasma, heating, current drive, confinement, and control systems.

The state of the art for time-dependent integrated Tokamak modeling uses “1.5 D” transport-timescale evolution codes. The 1.5 D refers to the mix of 1 D and 2 D techniques. Calculations for the thermal plasma are generally performed in one spacial dimension assuming that the profiles depend only on magnetic flux surfaces. These surfaces are typically allowed to have shaping (as planned for ITER), i.e., to depend on poloidal angle, but not on toroidal angle. Calculations for the fast ions often use two spatial dimensions, and sometimes two phase space dimensions, such as, energy and pitch angle.

Various modules are used to predict and evolve the plasma profiles. Examples are GLF23 [Waltz, 1997], Weiland [Strand, 1998], and Multimode [Bateman, 1998]). Also, various modules are used in these codes to describe the MHD equilibria, and the energy, momentum, and particle flows. Typically these modules are not the most advanced available, and are chosen to achieve a compromise between physics accuracy and computational speed. The modeling is generally of a more pragmatic, expedient than basic, fundamental nature.

This section describes progress and results using pTRANSP, a combination of the TRANSP plasma analysis code [Goldston, 1981], [Budny, 1995] and TSC (Tokamak Simulation Code) [Jardin, 1986], [Kessel, 2006] for time-dependent integrated modeling of ITER burning plasmas. The p in pTRANSP refers to predictive. There are alternative time-dependent integrated modeling efforts with similar goals. Some are discussed in other sections of this white paper.

Special features of TRANSP and TSC are:

- 1) Extensive international use (including China, e.g., [Gao, 2000] and [Gao, 2003]) for analysis and simulation of Tokamak experiments;
- 2) Extensive results for burning plasmas (e.g., [Budny, 2002]);
- 3) Choice of many modules for equilibrium solution, heating, current drive, etc;
- 4) Results for phase space distributions of fast ion species;
- 5) Easy coupling to other “down-stream” codes for more detailed analysis of issues such as turbulence, MHD, TAE instability (e.g., [Fu, 1993] and [Gorelenkov, 1998]), and diagnostic design (e.g., [Mazzucato, 1998] and [Kramer, 2006]).

Modeling Techniques

The TSC code is used to simulate the startup and control of the plasma boundary adjusting the shaping and control coils. Typically the electron density profile is assumed and the GLF23 module is used to predict and evolve the temperature profiles from the heating and plasma current profiles. The outputs of the time-dependent boundary and plasma profiles are input to TRANSP for a more detailed analysis. TRANSP has more comprehensive and self-consistent methods for computing the equilibrium, heating, and current drive. The TRANSP results for heating, current drive, and rotation profiles can be input back into TSC for further iteration to converge on a more accurate model. Iteration is necessary since the temperatures depend on the heating and the heating depends on the temperatures, etc.

TRANSP uses Monte Carlo techniques (NUBEAM, [Pankin, 2004]) to model alpha heating and neutral beam heating, torque, and current drive, the SPRUCE [Evrard, 1995] and TORIC [Brambilla, 1999] full-wave,

reduced order codes for minority ICRH, LSC [Ignat, 1994] for LHCD, and TORRAY [Batchelor, 1980] for ECH/ECCD. The outputs from TRANSP are being used in other codes to assess the MHD stability, TAE stability, and microturbulence (such as GS2 and GYRO). Electronic files of the MHD equilibria and of the phase space distributions of the fast ions are available.

Applications

The pTRANSP combination is being used to model ELMy H-mode and advanced plasmas for ITER. The H-mode plasma regime is considered to be a baseline scenario for achieving $Q_{DT} = P_{DT}/P_{aux} = 10$ [Campbell, 2001]. Two classes of advanced plasmas are being modeled: 1) The Hybrid regime is considered to be a path to similar Q_{DT} but requiring less inductive current with the safety factor q_{MHD} profile maintained close to, or above unity; 2) the steady state regime aims at longer pulse durations with close to zero inductive current drive. Examples of a few parameters for these ITER plasma regimes are given in Table III.9.1.

Table III.9.1. Representative values for ITER plasmas in the three standard regimes. f_{OH} is I_p/I_{boot} and f_{GW} is the Greenwald fraction

Regime	I_p MA	I_{boot} MA	I_{NNBI} MA	f_{OH}	$n_e(0)$ $10^{20}/m^3$	f_{GW}	$T_e(0)$ keV	P_{DT} MW	β_n
ELMY H-mode	15	2.7	1.1	0.7	1.1	0.8	22	400	1.8
Hybrid	12	2.8	4.5	0.3	0.7	0.5	33	300	2.8
Steady state	9	4.3	4.3	0.0	0.6	0.6	35	300	4.0

The auxiliary heating powers are assumed to be 16.5 MW in each of the two planned negative ion neutral beam injectors (NNBI at 1 MeV), and up to 20 MW of ICRH at 40-53 MHz (tuned to the He³ minority resonance near the plasma center). For the advanced plasmas, ECH/ECCD and LHCD are also assumed, and varied to control the current profiles.

Results of the modeling are being submitted to the ITPA (International Tokamak Physics Activity) profile database maintained by the Core Modeling and Database Working Group and the Transport Working Group. The intended uses of the databases submissions are for code benchmarking and for inputs for downstream analysis.

The figures show results from an H-mode and a hybrid plasma which have been submitted to the ITPA profile database. Fig. III.9.1 shows the assumed n_e profile and the temperature profiles computed using GLF23 in TSC. The electron density and the temperature at the top of the pedestal ($x=0.9$) are assumed. The temperatures further in are calculated using the GLF23 model in TSC. A modified Kadomstev mixing of sawteeth is assumed with a period of 50 s. This simulation achieves a predicted flattop fusion power of P_{DT} 495 MW with an input power of 33 MW NNBI and 12MW ICRH so the Q_{DT} is near 10.

Fig. III.9.2 shows an example of the heating power

waveforms and the total plasma current assumed, along with the Ohmic, beam, and bootstrap currents computed by TRANSP. Examples of effects of sawtooth mixing on the total plasma current and q are shown in Fig. III.9.3 Significant mixing of fast ions is predicted.

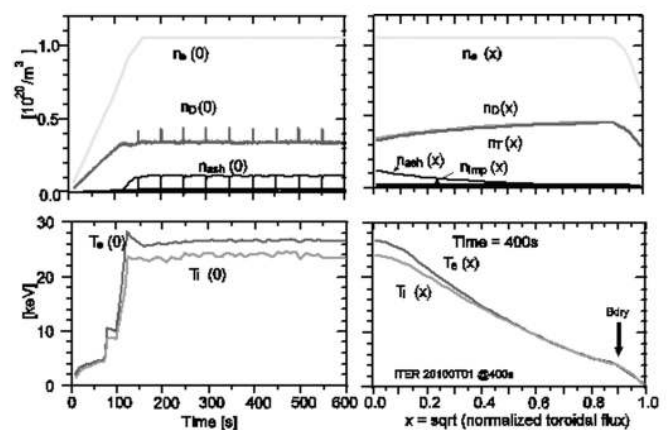


Fig.III.9.1 (a, b) Temperatures and (c, d) densities in an ITER H-mode plasma

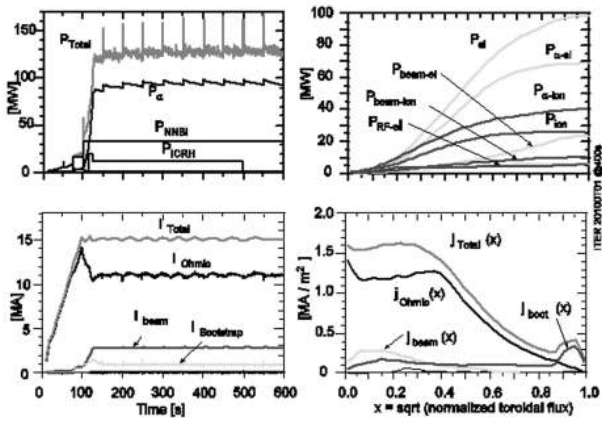


Fig.III.9.2 (a, b) Heating powers from fusion alpha particles, N_{NBI} , and I_{CRH} , (c, d) Currents in the ITER H-mode plasma

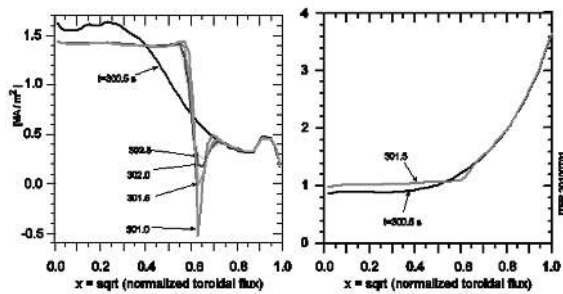


Fig.III.9.3 - Profiles of a) current and b) q_{MHD} just before and after a sawtooth crash

It is important to estimate the plasma rotation in ITER for several reasons:

- 1) deleterious resistive wall modes may be avoided if the rotation speed near the edge is sufficiently fast;
- 2) turbulent transport may be reduced if the radial flow has sufficient shear.

Fig. III.9.4 shows an estimation of $v_{toroidal}$. The radial electric field E_r (calculated from force balance) can cause sheared flow, and the toroidal velocity contribution could be significant. The toroidal velocity generated by the NNBI torque in ITER can be estimated by momentum balance assuming, for instance, a fixed relation between $\chi_{cmomentum}$ and χ_{cion} .

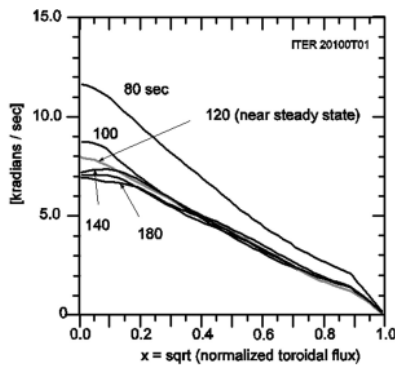


Fig.III.9.4 - Profile of toroidal rotation in an ITER H-mode resulting from the NNBI torque and the transport assumption $\chi_{cmomentum} = \chi_{cion}$

ITER is expected to contain Be, C, and W impurities recycled from the walls and divertor targets, and Ar from gas puffing to increase the energy radiated in the divertor scrape-off flow region. These impurities can be modeled in TRANSP. Also, the thermalized He ash profile will evolve in time. The effects of depletion of the D and T fuel are modeled. The accumulation of ash can also be simulated assuming a form for the transport such as:

$$\Gamma_{ash} = -D_{ash} \text{grad}(n_{ash}) + V_{ash} n_{ash} A_{surf}, \quad (\text{III.9.1})$$

where A_{surf} is the area of the flux surface and D_{ash} and V_{ash} are flux surface variables. The ash density, n_{ash} , is calculated from the local source rate of thermalizing fusion alphas and recycling influx from the wall. The recycling coefficient of the ash, R , defined as the ratio of the fluxes entering and exiting the plasma boundary, Γ_{in}/Γ_{out} , needs to be assumed as well. At fixed electron density the fusion rate would decrease to low values if R is close to unity.

Predictions of the ash profiles and of the total number of ash atoms are given in Fig. III.9.5. Three values of the ash recycling coefficient R were assumed and the values of D and V in Eq. III.9.1 were assumed to be $1^2/\text{s}$ and 1 m/s . The case $R = 0.7$ achieves $P_{DT} = 495 \text{ MW}$. The P_{DT} is reduced to 100 MW if R is increased to $R = 0.85$ due to dilution of the D and T fuel (assuming fixed n_e); b) shows computed profiles for the case $R = 0.7$. The resulting ash confinement times are $\tau_p = 3.6 \text{ s}$ and $\tau_p^* = \tau_p/(1 - R) = 12 \text{ s}$.

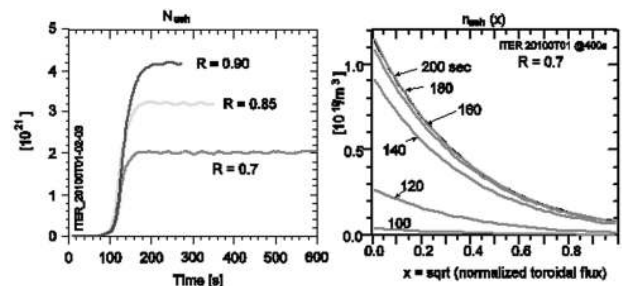


Fig.III.9.5 - Simulation of ash from thermalized fusion alpha particles. a) Total number of He ash atoms with assumed values for D and V and three choices of the recycling coefficient; b) ash profiles for 0.7

The ITER design for the NNBI sources allows for a rotation in the vertical plane allowing the footprint of the beam in the plasma to vary by approximately 50 cm vertically from shot to shot. The modeling of the hybrid scenario indicates that the below-axis aiming can maintain the q_{MHD} profile above unity. Details are shown in Fig. III.9.6.

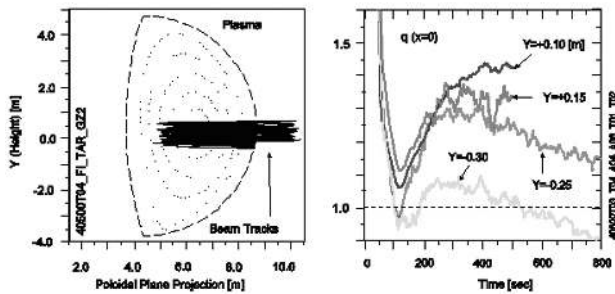


Fig.III.9.6 - a) Samples of NNBI neutral 3D trajectories into sections at their toroidal angle; b) calculated $q(0)$ in a ITER hybrid plasma (with high β_n), indicating that $q(0)$ can be maintained above unity for long durations

One use of these results is in designing experiments to study alpha parameters in burning plasmas. The fast ions from auxiliary heating can mask or complicate the measurement of fast alpha effects. Figure 3.9.7 shows results for TAE stability with NNBI and alpha heating [Gorelenkov, 2005]. The computed linear TAE stability versus toroidal mode number n with and without NNBI ions is shown. The results indicate that NNBI pressure can cause plasmas that are stable to alpha pressure become unstable.

An example of a use of modeling for the design of diagnostics is shown in Fig.III.9.8. This indicates how relativistic corrections to reflectometry scattering at high electron temperatures complicate the design of the reflectometry diagnostic [Kramer, 2006].

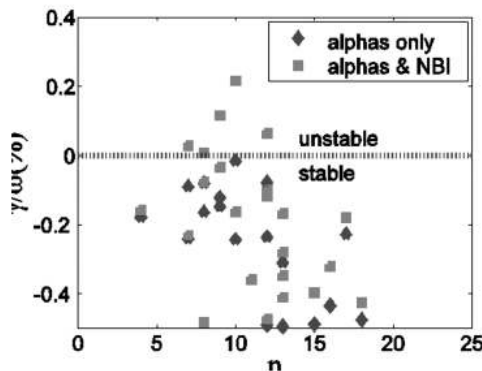


Fig.III.9.7 - computed linear TAE stability versus toroidal mode number n with and without NNBI

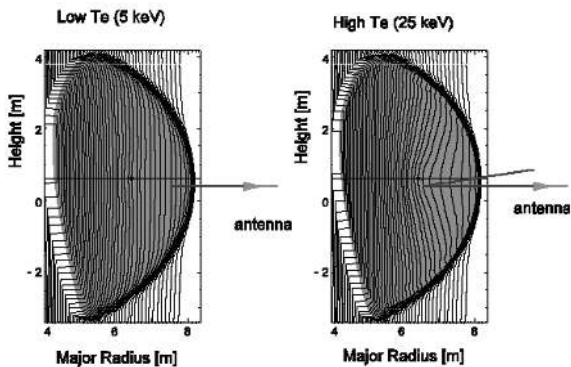


Fig.III.9.8 Relativistic corrections to reflectometry scattering at high electron temperatures complicate the design of the reflectometry diagnostic

Improvements of pTRANSP Development is continuing on the pTRANSP with the goal of improving the reliability of simulations. Near-term work (i.e., within a year) includes development of:

- 1) robust solvers for stiff predictive models such as GLF23;
- 2) a robust fixed / free boundary equilibrium solver of the Grad-Shafranov equation;
- 3) an NTM model [Halpern, 2006];
- 4) a pedestal model;
- 5) improved sawtooth triggering model; and
- 6) verification and validation checks.

Longer-term improvements include:

- 1) electron density profile prediction;
- 2) Scrape-off Layer model;
- 3) parallelization of the Monte Carlo fast ion package;
- 4) Monte Carlo model for ICRH.

Deficiencies

Obviously there remain many uncertainties in the modeling that limit our confidence in the reliability of predictions of ITER plasmas. Examples are:

- 1) validity and reliability of the transport models assumed;
- 2) torques and angular momentum transport;
- 3) poloidal rotation and the radial electric field;
- 4) effects of density profiles, and to what extent can they be controlled;
- 5) recycling and pumping of impurities;
- 6) wave-particle interactions

Collaboration possibilities

Collaborations to develop and use pTRANSP are welcome. The NTCC modules library² is a very fruitful method for sharing many of the modules used in pTRANSP. Submissions to the library are tested, documented, and peer reviewed. Use and submission is encouraged. A mode of closer collaboration would be to use pTRANSP via the FusionGrid. Presently the TRANSP code is being used at South West Institute of Physics via the FusionGrid³. This could be extended to include pTRANSP.

Acknowledgments:

This work is supported in part by the US DoE Contract No. DE-AC02-76CH03073

¹<http://tokamak-profiledb.ukaea.org.uk/>

²<http://w3.pppl.gov/ntcc/>

³<http://www.fusiongrid.org/>

References

[Batchelor, 1980] D. Batchelor, R. Goldfinger. 1980, Nucl. Fus., 20: 403
 [Bateman, 1998] G. Bateman, A.H. Kritz, A. J. Redd, et al. 1998, Plasma of Physics, 5: 1798
 [Brambilla, 1999] M. Brambilla. 1999, Plasma Phys. Cont. Fusion, 41:1
 [Budny, 1995] R. V. Budny, M. G. Bell, H. Biglari, et al.

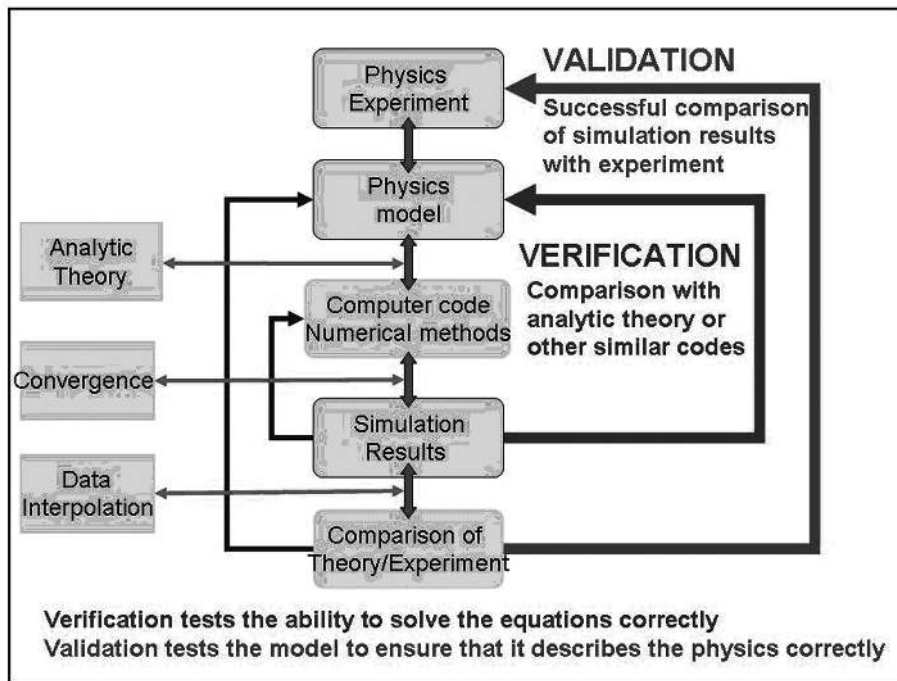
1995, Nuclear Fusion, 35: 1497
 [Budny, 2002] R. V. Budny. 2002, Nuclear Fusion, 42: 1383
 [Evrard 1995] M. Evrard, J. Ongena, D. van Eester. "Improved Dielectric Tensor in the ICRH module of TRANSP", 11th topical conference, Palm Springs, CA (USA), May 17-19, 1995. AIP Conference Proceedings 335, 397.
 [Fu 1993] G. Y. Fu, C. Z. Chang, K. L. Wong. 1993, Phys. of Fluids B, 5: 4040
 [Campbell, 2001] D. J. Campbell. 2001, Phys of Plasmas, 8: 204
 [Gao, 2000] Q. D. Gao, R. V. Budny, Jinhua Zhang, et al. 2000, Nucl. Fusion, 40: 1897
 [Gao, 2003] Q. D. Gao, R. V. Budny, F. Li, et al. 2003, Nucl. Fusion, 43: 982
 [Goldston, 1981] R. J. Goldston, D. C. McCune, H. H. Towner, et al. 1981, J. Comput. Phys., 43: 61
 [Gorelenkov, 1998] N. Gorelenkov, C. Z. Chang, W. M. Tang. 1998, Phys. of Plasmas, 5: 3389
 [Gorelenkov 2005] N. Gorelenkov, H. Berk, et al. 2005, Nucl. Fusion, 45: 226
 [Halpern, 2006] Federico D. Halpern, Glenn Bateman, et al. 2006, Phys. Plasmas, 13: 062510
 [Houlberg 1997] W. Houlberg, K. Shaing, S. Hirshman, et al. 1997, Phys. Plasmas, 4: 3230
 [Ignat, 1994] D. W. Ignat, E. J. Valeo, S. C. Jardin. 1994, Nuclear Fusion, 34: 837 ~ 852
 [Jardin, 1986] S.C. Jardin, N. Pomphrey, J. Delucia. 1986, J. Comput. Phys., 46: 481
 [Kessel, 2006] C. E. Kessel, R. V. Budny, K. Indireskumar.

21st IEEE/NPSS SOFE Conference Knoxville, TN (2006)
 [Kramer, 2006] G. J. Kramer, R. Nazikian, E. J. Valeo, et al. 2006, Nuclear Fusion, 46: S846 ~ S852
 [Mazzucato, 1998] E. Mazzucato. 1998, Rev. of Sci. Instruments, 69: 2201
 [Pankin, 2004] A. Pankin, D. McCune, R. Andre, et al. 2004, Computer Physics Communications, 159(3): 157 ~ 184
 [Strand 1998] P. Strand, H. Nordman, J. Weiland, J. P. Christiansen. 1998, Nucl. Fusion, 38: 545
 [Waltz 1997] R. E. Waltz, G. M. Staebler, W. Dorland, et al. 1997, Phys. Plasmas, 4: 2482

III.10 Verification and validation (J. Manickam)

The challenge of developing a reliable predictive code with complex scientific models, includes a process of verification and validation. The process of simulating a physics phenomenon generally includes:

1. Identifying the key features of the underlying physics
2. Determining a suitable model set of equations
3. Writing a computer code, which can solve the set of equations, and
4. Running the code and comparing the results with experimental data.



At each of these stages, choices are made, which impact the final conclusion. In order to achieve predictive capability, verification and validation, V&V, should be a critical component of the process, and applies at each of the four stages in different ways.

Formulating the physics/mathematical model for a simulation, rarely start from rigorous first principles, they are more likely to be based on reduced models, which are guided by analytic intuition. In this process, some physics features or terms in the equation

are determined to be non-essential, to the particular physics problem, and are either dropped or approximated. Once the equations are defined, the next step is to solve them, either analytically or numerically. The numerical method usually has inherent errors due to the choice of representation, grid size, time step etc. This can be overcome through convergence studies. Verification is the process for determining that the numerical solution correctly represents the model equations. The verification process is complete when the converged simulation results compare favorably with analytical theory estimates or other codes using the same physics model.

Verification is followed by validation, the process by which the physics/mathematical model is determined to correctly model the physics phenomenon of interest. This can be significantly more difficult than verification, since it may require substantial modification of the basic physics model, which would then trigger a new cycle of verification. Furthermore, difficulties can easily arise from the lack of experimental data, or from poor resolution. In fact, it might be necessary to design special experiments, specifically for code comparison. Too often, benchmarking is confused with validation. Benchmarking refers to comparing the output from two different codes, the results might agree, but there is no guarantee that they are correctly reproducing the physics, hence the importance of comparison with experiment. An equally important point for consideration is that even with proper validation, a code is generally applicable in a limited regime of parameter space. Extensions in parameter space, should trigger a whole new cycle of model building, verification and validation. This has important consequences for the challenge of developing reliable predictive codes, which should not be ignored.

The process of validation may be conducted at several levels. At the crudest level easily measured global parameters may provide validation. Where this breaks down, detailed profile information may be required. Finally to validate the first-principles model, we might require local 2D or 3D information. This is illustrated in the evolution of our understanding of beta limits, due to MHD. Introduction of the Troyon-Gruber empirical scaling law, provide a trivially computed estimate of the achievable beta, based on the toroidal field strength, plasma current and minor radius. This proved a valuable guideline until it became clear that many discharges did not reach the Troyon limit, and in some exceptional cases, they exceeded this limit. Closer analysis revealed the role of the safety-factor profile and the pressure gradients. The understanding gained in this analysis, in turn led to optimized shear regimes, commonly referred to as advanced tokamak regimes. The drive to obtain and sustain these regimes, in turn led to wall stabilization and the discovery of resistive wall modes. Feedback studies of these modes, requires detailed information on the perturbed fields, in the plasma and at the wall. From this example it is evident that validation is not just a numerical exercise

but a systematic refinement of the physics model, and crucial for the progress, we seek.

As the complexity of the physics models increases, it will be possible to simulate experimental diagnostics. This is a powerful technique for leveraging the simulation models to gain insight into the underlying physics. The value of such ‘synthetic diagnostics’ can be demonstrated by the following example. It is possible to estimate global transport coefficients and as the diagnostics improve, it will be possible to measure local fluctuations within a limited range of k-space. If a simulation is able to match this observation with a synthetic diagnostic, the underlying physics can be explored using the simulation code at other wavelengths with more confidence, and the role of the different instabilities in the nonlinear regime can be investigated, even though that space may not be accessible to the prevailing instruments. This argues for the systematic development of synthetic diagnostics for all major codes.

IV Major initiatives on fusion simulation

IV.1 U. S. scientific discovery through advanced computing (SciDAC) program & fusion energy science (W. M. Tang)

IV.1.1 Introduction

The development of a secure and reliable energy system that is environmentally and economically sustainable is a truly formidable scientific and technological challenge facing the world in the twenty-first century. This demands basic scientific understanding that can enable the innovations to make fusion energy practical. The “computational grand challenge” nature of fusion energy science is a consequence of the fact that in addition to dealing with vast ranges in space and time scales which can span over ten decades, the fusion-relevant problem involves extreme anisotropy, the interaction between large-scale fluid-like (macroscopic) physics and fine-scale kinetic (microscopic) physics, and the need to account for geometric detail. Moreover, the requirement of causality (inability to parallelize over time) makes this problem among the most challenging in computational physics. Nevertheless, there has been excellent progress during the past decade in fundamental understanding of key individual phenomena in high temperature plasmas [Tang05, Tang02]. Modern magnetic fusion experiments are typically not quiescent, but exhibit macroscopic motions that can affect their performance, and in some cases can lead to catastrophic termination of the discharge. Major advances have been achieved in the modeling of such dynamics, which require an integration of fluid and kinetic physics in complex magnetic geometry. Significant progress has also been made in addressing the dynamics governing

the interactions between plasmas and electromagnetic waves, especially in the radio-frequency (RF) range) of interest for plasma heating. Another key topic, where there have been exciting advances in understanding, is the degradation of confinement of energy and particles in fusion plasmas caused by turbulence associated with small spatial-scale plasma instabilities driven by gradients in the plasma pressure. While progress has been impressive, the detailed physics of the growth and saturation of these instabilities, their impact on plasma confinement, and the knowledge of how such turbulence might be controlled remain major scientific challenges [Tang05, Tang02, Idomura06].

Accelerated development of computational tools and techniques are needed to produce predictive models which can prove superior to empirical scaling. This will have a major impact on the fusion community's ability to effectively harvest the key physics from the proposed International Thermonuclear Reactor Experiment (ITER) - currently the top priority in the DoE Office of Science. The probability that ITER will achieve its goals can be significantly enhanced by development of the capability to numerically simulate the associated plasma behavior under realistic conditions. Unraveling the complex behavior of strongly nonlinear plasma systems is clearly a key component of the next frontier of computational fusion research and will advance the understanding of magnetically-confined plasmas to an exciting new level. Accelerated progress in the development of the needed codes with higher physics fidelity will be greatly aided by the interdisciplinary (computer science, applied mathematics, and specific applications) alliances championed by the US Scientific Discovery through Advanced Computing (SciDAC) Program [DOE 01] together with necessary access to the tremendous increase in compute cycles enabled by the impressive advances in supercomputer technology.

The scientific issues of magnetic fusion encompass a wide range of phenomena including those just mentioned, as well as others. However the dynamics of high temperature plasma does not respect these categorizations, and the understanding of overall plasma performance requires integrating all of these issues in a comprehensive simulation that includes interactions between phenomena which were previously studied as essentially separate problems. To achieve the ultimate goal of such integration, it becomes necessary to follow the evolution of the global profiles of plasma temperature, density, current and magnetic field on the energy-confinement time scale with the inclusion of relevant physics on all important time scales. While this is a formidable long term goal, the program now stands ready to begin such cross-disciplinary studies to develop more efficient models via improved algorithms and also to enhance the physics content of existing integrated codes. Pilot Fusion Energy Science SciDAC integration efforts have now begun development of frameworks for bringing together the disparate physics models, combined with the algorithms and computational infras-

tructure that enables the models to work together.

Supercomputing resources can clearly accelerate scientific research critical to progress in plasma science in general and to fusion research in particular. Such capabilities are needed to enable scientific understanding and to cost-effectively augment experimentation by allowing efficient design and interpretation of ambitious new experimental devices in the multi-billion dollar range such as ITER. In entering the exciting new physics parameter regimes required to study burning fusion plasmas, the associated challenges include higher spatial resolution, dimensionless parameters characteristic of higher temperature plasmas, longer simulation times, and higher model dimensionality. It will also be necessary to begin integrating these models together to treat non-linear interactions of different phenomena. Various estimates indicate that factors of 10^3 to 10^5 increases in combined computational power are needed. Associated challenges include advancing computer technology, algorithmic development, and improved theoretical formulation, all contributing to the improvement of overall "time-to solution" capabilities. As such, the Fusion Energy Science area is looking forward to being even more actively involved in the SciDAC Program as it moves forward to the next 5-year phase of "SciDAC II." In the following, a vision for SciDAC II is provided from the FES application area. It is motivated in large measure by the strong interest in future burning plasma projects such as ITER and some of the associated integrated modeling challenges. The perspectives here draw heavily from the summaries provided by the Principal Investigators of the well-established FES SciDAC portfolio - the Centers for: (i) Extended Magnetohydrodynamic Modeling (CEMM); (ii) Gyrokinetic Particle Simulation of Turbulent Transport (CGPS); (iii) Simulation of Wave-Plasma Interactions (CWPI); and (iv) the National Fusion Collaboratory (NFC) Project.

IV.1.2 Key science problems in fusion energy science

The key scientific categories and associated challenges identified in the assessment of the Fusion Energy Science (FES) Program by the US National Academy of Sciences [Kennel01] include: (i) macroscopic stability, which determines what limits pressure in plasmas and the means to control the associated mechanisms; (ii) wave-particle interactions, which determine how hot particles and plasma waves interact in non-linear regimes and how to use such knowledge for key tasks such as heating the plasma; (iii) microturbulence and transport, which determine what causes enhanced plasma transport and the means to minimize the associated negative impact on efficient plasma confinement; and (iv) plasma-material interactions, which determines how high-temperature plasmas and material surfaces can co-exist and the possible means to create optimal ways to do so. In addition, the integrated modeling of the physical processes from all of these areas

is needed to effectively harvest the physics knowledge from existing experiments and to aid the improved design of future devices. These important topics, which are critically relevant to the FES mission, are addressed in the existing and possible future extensions of the SciDAC FES Centers together with the new integrated modeling activities initiated in the Center for Edge Simulation of Plasmas, the Center for Simulation of Wave Interactions with MHD, and the most recently launched project, Center for Framework Application for Core-Edge Transport Simulations.

IV.1.3 Needed advances and innovations in computer science and applied math

FES is effectively utilizing the exciting advances in information technology and scientific computing, and tangible progress is being made toward more reliable predictions of the complex properties of high temperature plasmas. In particular, the FES SciDAC projects have brought together physicists, applied mathematicians, and computer scientists in close and productive working relationships, which provide a model for future research. Productive current alliances exist with SciDAC Integrated Software Infrastructure Centers (ISIC's) and Scientific Application Programs (SAP's), but outstanding challenges remain. To illustrate these points, some highlights in each area include:

CEMM: In partnership with the SciDAC ISIC for Terascale Optimal PDE Solvers (TOPS), this MHD project's two flagship codes, M3D and NIMROD have achieved significant performance improvement. For example, TOPS collaborations led to: (i) the implementation of the SuperLU solver library which produced a factor of 5 in computational time for nonlinear applications in NIMROD; and (ii) symmetrization of sparse matrices to enable use of the PETSc ICCG solver which produced a factor of 2 reduction in computational requirements. Also, collaborations with the Applied Partial Differential Equations Center (APDEC) led to an adaptive mesh refinement (AMR) MHD code which has proven particularly useful in modeling pellet fueling of tokamaks.

Needed advances/innovations under SciDAC II: These will include: (i) hardware with greater data access capability relative to peak CPU speed to help address large communication burden in NIMROD/M3D imposed by the stiffness of the mathematical problems; (ii) possible integration of the AMR capability into the two major codes, NIMROD/M3D; (iii) successful development and implementation of more efficient implicit schemes to enable effective utilization by the CEMM of up to 1000 processors or more on leadership-class computing platforms.

Estimate "Scale" (terascale, petascale ...) of associated computations expected to be performed under SciDAC II: Good use can be made of terascale computer capabilities if provided in a balanced way where increased processor speeds are matched with faster caches

and memory access times and improved inter-processor communication latency and bandwidth. Realistic MHD simulations of ITER-scale burning plasma experiments will demand such improvements.

CGPS: There have been extensive interactions between this microturbulence simulation project with the SciDAC ISICs including: (i) TOPS on optimizing the interface between the GTC code and PETSc; and (ii) SDM (scientific data management) on managing the terabytes data sets from GTC. Visualization capabilities for this center have been significantly enhanced with SAP collaborations with visualization experts at UC-Davis and at PPPL. Terascale computing is being aggressively used, and GTC, the Fusion Energy Science representative in the NERSC benchmark suite for testing most advanced computing platforms, provides an impressive example of "leadership class" computing. This well parallelized code has recently achieved 7.2 teraflops sustained performance with 4096 processors using over ten billion particles and with 20 to 25% single-processor efficiency on the Earth Simulator Supercomputer in Japan. Needed advances/innovations under SciDAC II: More realistic future simulations requires introducing additional physics into GTC which in turn entails enhanced support from ISICs and SAP alliances to address greater demands on code parallelization and optimization, solver efficiency, and data management and feature tracking. A PIC code such as GTC calculates the interaction of dynamical objects (particle points) with static objects (field grids), gathers the field information for the particles, and scatters the particle charge and current onto neighboring grids. The gather-scatter operations, which involve non-sequential memory access of field data, are the main computational bottleneck, due to the memory latency on all cache-based machines. Since particles sample the distribution function of the system, a very large number may be needed to capture all the non-linear physics, while reducing the statistical noise to a minimum. This puts a significant strain on the memory. Inter-processor communication in a PIC code can be minimized using domain-decomposition. The biggest general problem here is one of data locality due to the particle-grid interaction. The random positions of the particles inside each domain result in continuous non-sequential writes to memory during the charge deposition on the grid, which constitutes the most time-consuming step of PIC codes. A large number of operations, integer and floating point, are required to get the final grid array indexes where the charge is deposited. Low cache reuse results from these numerous random writes. Sorting the particles could improve this, as long as the time spent in the new routine (i.e., sorting plus charge depositing) is less than that of the original algorithm.

Estimate "Scale" (terascale, petascale ...) of associated computations expected to be performed under SciDAC II: With access to terascale and eventual petascale computational resources under SciDAC II, nearer-term CGPS computations will provide valuable new insights

in a timely way into: (i) noise-related phase-space density resolution issues impacting the ability to realistically simulate the long-time evolution of plasma microturbulence; and (ii) how nonlinear velocity space dynamics act to drive plasma transport to much more rapidly reach saturation. By using up to 100 times more particles than for the normal runs, these studies will achieve the very high phase space resolution to enable systematic studies of these important scientific questions. The ability of GTC to successfully carry out such investigations on advanced “leadership class” computational platforms such as the ESC, the CRAY X1E and XT3, the IBM Power line, and the IBM Blue-Genie L is well documented. Longer term, the CGPS plans to address integrated fusion simulations of ITER-scale plasmas and also the code integration of core and edge turbulence physics in collaboration with the new SciDAC ProtoFSP CESP. These are terascale/petascale problems which will likely require the multi-scale mathematical development and integration into GTC of new algorithms capable of addressing low-frequency, long-wavelength MHD modes as well as high-frequency, short-wavelength ion-cyclotron waves.

CWPI: This wave-plasma interactions simulation project’s utilization of terascale computing and associated productive interactions with SAP have focused on the dense-matrix solution of the complex linear wave equation. It has benefited from such alliances to accelerate progress on: (i) parallelization of the AORSA and TORIC codes which enabled 2D multi-scale field solutions; (ii) algorithmic improvements in handling non-Maxwellian dielectric operator to enable coupling of AORSA to CQL3D for self-consistent field solutions; and (iii) recasting of field algorithms in terms of real-space representation to enable 3D solutions for radio-frequency (RF) fields in general geometry.

Needed advances/innovations under SciDAC II: For future integrated simulations that combine RF with longer time-scale phenomena such as MHD and transport, it is particularly important to develop and implement more sophisticated wave solvers using a multi-scale adaptive spectral representation of the fields. Much more work of this kind is needed to drastically reduce CPU storage and run-time requirement, and enhanced collaborations with the SAP and the SciDAC ISICs as well as with the new SciDAC ProtoFSP “SWIM” Project will be required.

Estimate “Scale” (terascale, petascale ...) of associated computations expected to be performed under SciDAC II: With access to terascale computational resources, the CWPI intends to target: (i) a fully-integrated self-consistent field and particle distribution function solution for modeling RF heating; (ii) incorporation of PIC codes to explore nonlinear RF-edge interactions; and (iii) integrated solutions for the wave fields in the plasma core and edge regions to provide information on the amount of power that can be coupled into the plasma from a given launcher.

NFC: Although not a formal part of the FES

SciDAC Program, the National Fusion Collaboratory (NFC) has proven to be remarkably successful in providing vital infrastructure for national and international collaboration in experimental operation, data analysis, and simulation. FusionGrid services have enabled fusion scientists to use codes with less effort and better support, and the transport analysis code TRANSP, available as a FusionGrid service, has performed over 5800 simulations for ten different fusion devices throughout the world. It is also being used for machine and experimental designs for ITER. Shared display walls in tokamak control rooms and significantly enhanced remote collaboration via access grid nodes are having a large impact on productivity. The NFC is enabling greater utilization of the existing US experiments by more scientists via facilitation of real-time off-site interactions with the experiments. In addition, a unified FusionGrid security infrastructure has enabled more effective sharing of data and codes. For the future, the NFC can play a major leadership role in building collaborative infrastructure for the needed remote operation of experiments such as ITER and in fostering collaborative development and use of simulation codes as well as data analysis codes. With future support from either the SciDAC II Program and/or the Fusion Energy Science base program, this kind of effort can provide a valuable leadership role in establishing common data structures and protocols and a collaborative culture for integrating SciDAC FES project results into the broader fusion community, including the large experimental communities.

IV.1.4 Integration across FES SciDAC projects, SciDAC ISICs and SAP, and computing facilities

In many respects, the physics fidelity of the most advanced high performance computational codes, when properly benchmarked against theory, experimental results, and complementary codes, represent the state of understanding in any research discipline. The integrated modeling challenge in fusion energy science is to effectively harvest the knowledge gained from the associated simulations to provide the underpinning for predicting the behavior of fusion systems. Developing a comprehensive simulation capability for carrying out “virtual experiments” of such systems will be essential for the design and optimization of a portfolio of future facilities, including burning plasma experiments, technology testing facilities and demonstration power plants, necessary for the realization of commercially available fusion energy. A near-term application is to optimize the design of experimental burning plasma devices such as ITER, which will pave the way to both greater scientific understanding and speeding up the development of the first fusion power plant. A realistic integrated simulation capability would dramatically enhance the utilization of such a facility, and its application to concept innovation can be expected to lead to

further optimization of toroidal fusion plasma systems in general. The targeted goal is to deliver the ability to effectively simulate the entire plasma device with a validated predictive capability that reproduces trends from existing experimental regimes and can be applied with a reasonable level of confidence when extrapolated to new physics regimes.

A successful approach toward the timely achievement of the integrated modeling goal in FES will need to demonstrate significant advances at three levels. At the most fundamental level, improvements in physics understanding and theoretical descriptions for all physical processes in key areas that govern the performance of fusion systems will be needed. This should translate into a capability to perform realistic numerical simulations of individual components of a fusion device, utilizing available high performance computers to help quantitatively validate against accurate experimental measurements. Such an initial step has been successfully launched under the existing FES SciDAC Program. A second level is the optimization of physics code packages and demonstration of coupled simulations of several different physics processes. Under SciDAC-II, this element will require significantly greater collaborations with the mathematics and computer science community (via ISIC's and SAP's) for improvement of algorithm accuracy and efficiency along with the preparation of physics packages for compatibility with the next generation of high performance computer architectures. The associated advanced simulation capability should have extensive ability to better diagnose and interpret experiments. The third and final level is to integrate all physical processes needed in a seamless framework for the comprehensive computational simulation of fusion energy science experimental devices. Achieving such an integrated simulation capability, guided by the three-level phased approach just noted will require the availability of terascale (and eventually petascale) 'capability' or 'leadership class' computing facilities as well as significantly enhanced capacity computing resources, which can be made available through dedicated topical computing centers.

References

- [Tang 05] Tang W. M., Chan V. S. 2005, Plasma physics and controlled fusion, 47(2): R1-34
- [Tang 02] Tang W M. 2002, Physics of plasma, 9 (5): 1856-1872 Part 2
- [Idomura 06] Idomura Y, Watanabe T, Sugama, H. 2006, C. R. Physique, 7: 650-669
- [DOE 01] Department of Energy Office of Science's "Scientific Discovery through Advanced Computing (SciDAC) Program," (Department of Energy, Washington, DC, 2001)
- [Kennel 01] C. F. Kennel, et al. National Research Council, Final Report (National Academy Press, Washington, DC, 2001)

IV.2 EU integrated tokamak modelling (ITM) task force (A. Becoulet, F. Zonca)

At the end of 2003, the European Fusion Development Agreement (EFDA) structure set-up a long-term European task force (TF) in charge of "co-ordinating the development of a coherent set of validated simulation tools for the purpose of benchmarking on existing tokamak experiments, with the ultimate aim of providing a comprehensive simulation package for ITER plasmas" [<http://www.efda-taskforce-itm.org/>]. The resources are found within the European Associations, and so far mobilized through voluntary participation.

Integrated tokamak modelling is an extremely complex issue which poses at least three challenges in terms of integration. First, of course, the physics integration challenge: after several decades spent to develop the various physics ingredients at play in a tokamak plasma, there is an actual need to foster interactions between the different physics areas such as MHD, heat & particle transport, exhaust, energetic particle physics, etc. Significant new physics is expected, for instance when coupling edge to core physics (L-H transition, ELM etc), fast particle content to non linear MHD and/or to turbulent transport, etc. Most of them are expected to be dominant in ITER. The second challenge is the code integration. Developing a 'tokamak simulator' requires a significant effort from the community in terms of creating full sets of validated and benchmarked codes, and of setting-up standardised inputs/outputs to allow modules from different codes and providers to be linked to each others and to multiple databases. This also requires agreement on a common framework for code development and operation. The complexity, the international context, and the very long term aspects of the problem further require standardised and user-friendly frameworks. The third challenge to face is the discipline integration. The success of the ITM relies on close cross-discipline interactions, with input from theoreticians to build/improve the appropriate mathematical models, modellers to construct efficient, accurate codes from the models and experimentalists to provide data to validate models. The involvement of each community is crucial for success. The obvious questions of the relevant computer resources and numerical support are also to be addressed at the proper level.

The year 2004 was dedicated in Europe to structure the task force and plan the mid- and long-term activities necessary to such an endeavour. The work broadly aimed at reviewing the current status of modelling and at developing the longer term strategy of the TF, towards an integrated suite of codes, in order to optimize the European exploitation of the ITER project. The long term objectives aimed at structuring the EU modelling effort towards ITER and the existing fusion devices, strengthening the collaborative efforts between EU and the other ITER partners, and implementing more systematic verification and experimental valida-

tion procedures as well as documentation. The objectives also include the development of a code platform structure, easily enabling the coupling between codes and models, providing access to any device geometries and databases, and easing the more systematic code comparisons and confrontations between data and simulations.

After endorsement of the 2005-2006 work programme by EFDA, the actual work of the task force began in early 2005, through a first set of seven projects, divided into:

- five Integrated Modelling Projects (IMPs), addressing the modelling issues of fusion plasma physics which require a sufficiently high degree of integration:

- a. IMP1 in charge of equilibrium reconstruction and linear MHD stability analysis

- b. IMP2 addressing non linear MHD issues

- c. IMP3 in charge of providing the computational basis for a modular transport code, taking account of the core, the pedestal and the scrape-off layer. Ultimately, IMP3 will address the simulation of complete tokamak scenarios, e.g. for ITER.

- d. IMP4 in charge of developing a suite of unified, validated codes to provide quantitative predictions for the linear properties of a range of instabilities, including: ion-temperature-gradient (ITG) modes, trapped electron modes (TEM), trapped ion modes (TIM), electron-temperature-gradient (ETG) modes, micro-tearing modes, etc.

- e. IMP5 developing the computational basis for a modular package of codes simulating heating, current drive and fast particle effects

- a Code Platform Project (CPP), responsible for developing, maintaining and operating the code platform structure. Support to IMPs is included.

- a Data Coordination Project (DCP), supporting IMPs and CPP for Verification and Validation aspects and standardisation of data interfaces and access.

The European tokamak modelling community is thus structured and the seven projects are at work, with a careful time sequencing of a large number of cross-coupled tasks. As a first major milestone, to be reached in 2006, it was decided that IMP1 was in charge of providing an integrated suite of self-consistent codes (modules) for equilibrium reconstruction and linear MHD stability analysis, i) making full use of the prototype data structure and data access be put in place by DCP and ii) porting the modules on the prototype platform developed by CPP. This implies the complete disconnection of the equilibrium and linear MHD codes from the device geometry and diagnostic data, and a universal read/write access to data.

The first results already available are extremely encouraging. The TF is now in a position to propose a high performance object oriented database structure. This structure represents the full description of a tokamak experiment: physics quantities, subsystems characteristics and diagnostics measurements. It presents a high degree of organisation, being structured in vari-

ous “trees” and “sub-trees”, each of them corresponding to “Consistent Physical Objects”. This avoids “flat structures” with never-ending lists of parameter names. The “Consistent Physical Objects” are either subsystems (e.g. a heating system, or a diagnostic) and contain structured information on the hardware setup and the measured data by or related to this object, or code results (e.g. a given plasma equilibrium, or the various source terms and fast particle distribution function from an RF code) and contain structured information on the code parameters and the physics results. The database structure is based on XML schemas [<http://crppwww.epfl.ch/lister/euitmschemas>], allowing an actual programming language flexibility. The XML schemas are used to define the data structure (arborescence, type of the objects, ...). User-friendly tools (XML editors) allow a fast and easy design of the data structure. Small scripts (“parsers”) translate the schemas in many other languages (HTML, Fortran, C, ...), allowing an automated interfacing of the structure to any programming language used in the community. The data storage problem is also addressed, both in terms of data access and in terms of hardware. A short term storage system solution (1Tb) has been put in place by the TF through an MDS+ server hosted by ENEA [<http://fusfis.frascati.ena.it/FusionCell>]. The IMPs storage needs are estimated around 4Tb at the end of 2006, and more than 15 Tb on a longer term basis (see below). The access layer is presently based on MDS+, which is the most widely used data access system in the fusion community at moment, and is interfaced already with many languages. MDS+ is convenient for storing multi-dimensional arrays, and has no problem with large data size, but it is not really object oriented (arrays of objects are not possible), and is rather slow for large numbers of data calls. The idea of a universal access layer is thus under consideration within DCP. The access to data would become device independent, extensible through plug-in technology (MDS+, HDF5, ...), providing a single read/write interface to any data manipulation.

In parallel, a code platform structure is under development by CPP. The idea is to provide modellers with a user-friendly environment, on which they would ultimately have access to (any) device geometry description, to the various systems and physics data bases, and to the codes, modules and models they need to solve the problem they address. The platform would then allow them, by automatically coupling these various elements, to build-up the desired computer application (i.e. the ‘simulator’) and then get access to the necessary hardware resource (computer and storage). The terms of reference of the platform also specify that the modellers would find access to all the existing information about the verification and validation information relevant to the elements they use, as well as to all the existing documentation, pre- and post-processing tools. A complete specification document has been edited by DCP and is presently used to evalu-

ate several frameworks, existing among the OpenSource community. The TF is now entering into a prototyping phase, making use of one or two selected frameworks in a test version in charge of demonstrating the feasibility of such a concept. The prototype platform will encapsulate the embryo of device geometry descriptions, the existing versions of the data structure and data access layer (MDS+), and the suite of self-consistent codes (modules) for equilibrium reconstruction and linear MHD stability analysis provided by IMP1. It will also give access to a number of data servers and computers, large enough to demonstrate the flexibility. IMP1, DCP and CPP expect by the end of 2006 to be in a position to demonstrate a first complete chain of manipulation tools and standards, around a set of fully modularized equilibrium reconstruction and linear MHD stability codes for tokamaks.

The other four IMPs are progressing on a slightly longer term basis, keeping the full compatibility with DCP and CPP as a constraint of course. Concerning IMP2, initial work on resistive wall modes (RWMs), sawteeth and edge localised modes (ELMs) has started. One expects on one side state-of-the-art models for such non linear MHD instabilities, to be validated and then delivered under self-standing documented modules and on the other side a dedicated development programme at the first principle resolution level. IMP3 is in charge of integrating the various codes and modules developed in the other projects into the discharge evolution codes and also to address the major integrated transport issues. At this level, an ambitious edge code benchmarking activity is underway (in connection with ITPA) involving SOLPS, EDGE2D/NIMBUS and UEDGE codes as well as JET, DIII-D and AUG data, and MDS+ is used to couple SOLPS with the ASCOT Monte Carlo code. IMP4 has structured a very ambitious turbulence and micro-stability first principles code verification and code-code benchmarking exercise, both for core (based on the Cyclone case) and edge physics. Finally, IMP5 has also structured its activity and resources around ion, electron and fast particle physics, in order to develop the computational basis for a modular package of codes simulating heating, current drive and fast particle effects. This covers ECRH, ICRH, NBI, LH, alpha particle and fast particle interaction with instabilities. With the long-term goal of reaching self-consistent calculations validated against experiments, the priority is given to realistic modelling applicable to ITER standard and advanced scenarios.

On the hardware level, Europe is also pro-active and several initiatives are being worked out at moment. Let us quote, just focusing on plasma fusion activity, the joint effort between Europe and Japan (aka the 'broader approach') which contains a fusion super computer centre to be located in Japan, and the idea to support the ITM-TF activity within Europe with specific European resources such as a dedicated super computer for fusion and/or a more systematic use of GRID technology for fusion. The ITM-TF is also supporting the creation of

a tokamak simulation 'gateway' concept, where modellers, by connecting, would have access to all the tools discussed before in this section, including data storage, computers and support.

Obviously this significant European modelling effort is to be conducted in close connection with other ITER partners, with ITER international team and ITPA. The TF has already initiated bi-lateral contacts with US and Japan, and discussions with ITER and ITPA in order to promote a common attitude towards full compatibility between the various developments and tools. A quality process must be progressively put in place in the tokamak modelling activity. This is certainly vital for ITER and the future.

IV.3 Fusion simulation activities in Japan

(A. Fukuyama, N. Nakajima, Y. Kishimoto, T. Ozeki, M. Yagi)

IV.3.1 Introduction

Computer simulation has been playing a key role in plasma physics and nuclear fusion research in Japan. Various complicated phenomena have been clarified by proof-of-principle simulations and large-scale nonlinear phenomena are being studied by first-principle simulations, especially in nonlinear MHD dynamics and turbulent transport. Though the time and spatial scales of the phenomena in magnetic fusion plasmas spread over very wide ranges, the range of observable scales in a simulation was limited by shortage of available computer resources. Recent advances in understanding nonlinear plasma physics and computer technology, however, are changing the situation. Multi-scale simulations consistently describe the interaction between the phenomena with different time and/or spatial scales, which have been separately simulated in the past, e.g., microscopic turbulence and macroscopic MHD instabilities. On the other hand, disparate separation of scales requires another approach to describe whole plasma over a whole discharge. Integrated modeling composed of various modules governing phenomena within a limited scale and interacting with each other on longer time and/or spatial scales.

In this subsection, recent fusion simulation activities in Japan are briefly reviewed. Multi-scale simulations in NIFS and JAEA are described in subsections 2 and 3, respectively. Integrated modeling initiative, BPSI, is introduced in subsection 4. A modeling code system, TASK, and integrated modeling activities in JAEA are described in subsection 5 and 6. The plan of ITER-BA computer simulation center is mentioned in the final section.

IV.3.2 Multi-scale simulations in NIFS

Theoretical studies and computer simulation researches of the magnetic confinement fusion have been

promoted at the National Institute for Fusion Science (NIFS), for the purposes of comprehending and systematizing physics of plasma confinement. Two approaches extending over general toroidal magnetic configurations such as the Large Helical Device (LHD) and ITER are pursued in domestic and international collaborations with a large variety of researchers in universities or institutes as well as in the LHD experimental group. One is an integrated model-based approach, where a so-called integrated simulation code applicable to the LHD will be developed through comparisons of the simulation results with the LHD experimental data. The other is a hierarchy model-based approach, where simulation models in each space-time hierarchy are intensively developed; then, the simulation models will be extended so as to include various physics and/or effects in adjacent hierarchies. Hereafter, the present status of such activities will be reported.

Time evolution of the rotational transform and the radial electric field due to transport are re-formulated and are incorporated into an integrated simulation code for three-dimensional magnetic configurations. Temporal changes of the rotational transform in the NBI-heated LHD experiment are investigated [Nakamura 2006]. The transport code, TASK [Fukuyama 2004] combined with the newly developed model will be extended to TASK/H.

Simulation codes in various space-time hierarchies are intensively developed in two directions; one direction from macro- to micro- scales, and the other direction from micro- to macro-scales. As a macro-scale simulation model, an MHD simulation code MINOS has been developed in order to study low- n MHD activities in LHD experiments [Miura 2006]. MINOS employs the MHD equilibrium obtained by HINT [Harafuji 1989], where existence of nested flux surfaces is not assumed. In order to extend the MHD model into two-fluid ones, properties of the two-fluid equilibrium are rigorously examined by taking account of various fluid closure models. Simultaneously, a simulation code based on a reduced set of two-fluid equations has been developed in order to clarify multi-scale-interactions among micro-instabilities, macro-scale-MHD instabilities and zonal flows [Ishizawa 2006].

Interactions between MHD modes and energetic particles in tokamak and helical plasmas, for example TAE, EPM etc, have been investigated with a hybrid simulation code for MHD and energetic particles, MEGA [Todo 2005a, Todo 2005b], which is now extended for applications to two-fluid background plasmas [Todo 2006]. The intermittent beam ion loss in a TFTR experiment was reproduced with a reduced simulation model [Todo 2003]. In order to treat multi-phases of matters, such as gaseous, liquid, and solid phases, the CAP code is now under development, which will be used to analyze the pellet ablation process in LHD [Ishizaki 2006].

As an approach from micro to meso scales, a gyrokinetic-Vlasov code GKV has been developed with the aim of understanding the anomalous transport

mechanism in general toroidal fusion plasmas [Watanabe 2002, Sugama 2003, Watanabe 2004, Watanabe 2005]. The ion temperature gradient turbulence and the zonal flow damping with the geodesic acoustic mode oscillations are successfully simulated by the GKV code which precisely captures phase-space structures of the distribution function [Sugama 2005, Sugama 2006, Watanabe 2006].

The theory and computer simulation research activities at NIFS organized as the multi-scale simulation project are intensively pursued in collaboration with universities and institutes toward the prediction of the behavior of LHD and ITER plasmas.

IV.3.3 NEXT: numerical experiment of tokamaks

The NEXT (Numerical EXperiment of Tokamak) project is aimed at understanding the complex properties of fusion plasmas and predicting the physical processes in the next generation of tokamaks, such as ITER, using recently advanced computer resources. The main objectives of the NEXT project are

- (1) to understand complex physical processes in present-day and next-generation tokamak plasmas
- (2) to predict and evaluate the plasma performance of tokamak reactors, such as ITER, and
- (3) to contribute to the progress in plasma physics and related research areas through large scale computer simulation

To achieve the goals of the programme, we are developing numerical simulation codes which are applicable to the prediction of the properties of the core plasma and the divertor plasma on an equal footing. For core plasmas, the main interest is in the analysis of complex transport and MHD phenomena. The simulation codes that have been developed are based on plural models; electrostatic toroidal delta- f particle codes based on the gyro-kinetic model [Idomura 2000, 2002, 2003,], electrostatic and electromagnetic toroidal codes based on the gyro-Landau-fluid model [Miyato 2004, Li 2004, 2005], an electromagnetic slab particle code based on the gyro-kinetic model [Matsumoto 2003, 2005], reduced MHD model [Ishii 2002, 2003], and compressible MHD model [Kagei 2003].

Special attention has been paid to developing high resolution global turbulent transport codes which can cover a wide wave number and frequency region for example including the meso-scale ion temperature gradient mode and the micro-scale electron temperature gradient mode, and in addition secondary excited large scale structures such as zonal flows, GAM, streamers, and low frequency long wavelength modes [Idomura 2003, Miyato 2005]. Simulation codes for dense and cold divertor plasmas are being developed with particle including the collisional/relaxation process [Takizuka 2001], and fluid models combined with Monte Carlo techniques for neutrals and impurities [Shimizu 2003].

Such codes are being executed on massively parallel

computers. The NEXT programme incorporates with other fields of research where complex plasma behavior plays a crucial role, such as in astrophysics, accelerator plasmas, and laser plasmas. The NEXT project involves research in parallel computing technology and in the architecture of massively parallel computers

IV.3.4 BPSI: burning plasma simulation initiative

The purpose of burning plasma simulations is to predict the behavior of burning plasmas and to develop reliable and efficient schemes to control them. It should describe whole plasma (core, edge, divertor and wall-plasma interaction) over a whole discharge (startup, sustainment, transient events and termination) with a reasonable accuracy validated by experimental observations and within available computer resources. Accomplishment of such simulations requires well-organized development of a simulation system according to the gradual increase of our understanding and model accuracy.

The Burning Plasma Simulation Initiative (BPSI) in Japan is a research collaboration among universities, NIFS and JAEA since 2002. The targets of BPSI are (1) to develop a framework for collaboration of various plasma simulation codes, (2) to promote physics integration of phenomena with different time and space scales, and (3) to encourage introducing advanced technique of computer science. In order to develop the framework, we are working on a common interface for data transfer and execution control and a standard data set for data transfer and data storage. We are implementing them in a reference simulation core code TASK. The standard dataset is going to be extended to describe three-dimensional helical configurations. Examples of physics integration include transport during and after a transient MHD events, transport in the presence of magnetic islands, and core-SOL plasma interface. We have been evaluating parallel computing on PC clusters and scalar-parallel machines and grid computing using Globus and ITBL.

The activity of BPSI covers domestic workshops supported by the Research Institute for Applied Mathematics (RIAM, Kyushu Univ), NIFS and JAEA and US-Japan JIFT workshops with participants from EU and Korea. Development of integrated modeling codes based on BPSI is described in the following two subsections. As a basis for physics integration, multi-scale simulations for multiple-scale turbulence [Smolyakov 2002, Yagi 2002], MHD and turbulence coupling [Yagi 2005], and turbulence and transport coupling [Yagi 2006] have been also carried out.

IV.3.5 TASK: integrated simulation code system

The integrated code TASK (Transport Analysing System for tokamak) [Fukuyama 2004] is a core code of the integrated modeling of tokamak plasmas in BPSI.

It has a highly modular structure and includes the reference implementation of a standard dataset and program interface for data exchange and module execution. Since most of the necessary libraries as well as its own open-sourced graphic libraries are included, the portability of the code is high. The code has been developed by the use of CVS (Concurrent Version System) and a Fortran77 version of the code is now available from the web site as an open source, although the next version will be based on Fortran95.

At present, the modules of TASK are composed of

EQ: 2D equilibrium module (fixed or free boundary condition, toroidal rotation)

TR: 1D diffusive transport module (radial transport, various transport models)

WR: 3D geometrical optics module (ray or beam tracing, EC, LH)

WM: 3D full wave module (antenna excitation, eigenmode analysis, IC, AW)

FP: 3D Fokker-Planck module (relativistic, bounce-averaged, radial transport)

DP: Wave dispersion module (local dielectric tensor, arbitrary $f(v)$)

PL: Data interface module (data exchange, data conversion, profile database)

LIB: Common libraries

More modules, TX (dynamical transport module), WA (linear stability module) and WI (integro-differential full wave analysis), are under development.

The status of the plasma is always kept in the PL modules. At the beginning of a calculation in each module, necessary data, such as device data, equilibrium data, fluid plasma profile, kinetic plasma distribution, electromagnetic field data, are imported from PL. The results of calculation are also exported to PL. Experimental profile data stored in the ITPA profile database are also available through the PL module.

The TASK code has been applied to the analyses of ICRF heating [Fukuyama 2000], electron cyclotron current drive [Fukuyama 2001], Alfvén eigenmode excited by energetic ions [Fukuyama 2002], and comparison of turbulent transport models [Honda, 2006]. Results of predictive simulation of various operation scenarios of ITER have been reported in the ITPA topical meetings. Benchmark tests of the transport module TASK/TR and the transport code TOPICS developed in JAEA has been also carried out.

Improvement of the modules (refinement of modular structure, conversion to Fortran95), improvement of the models (edge plasma model, sawtooth model and so on), systematic comparison with experimental data, and integrated simulation with other code for stability analysis and peripheral plasma transport are under way.

IV.3.6 Integrated modeling activities in JAEA

Integrated modeling for burning plasmas is programmed in the Japan Atomic Energy Agency. In order

to simulate the burning plasma which has a complex character with wide time and spatial scales, a simulation code cluster based on the transport code TOPICS is being developed by the integration of heating and current drive, the impurity transport, edge pedestal model, divertor model, MHD and high energy behavior model [Ozeki 2006]. Developed integration models are validated by fundamental researches of JT-60U experiments and the simulation based on first principles in our strategy.

An integrated model of MHD stability and the transport is being developed for three different time scale phenomena of NTMs ($\sim \tau_{\text{NTM}}$), beta limits ($\sim \tau_{\text{Alfven}}$) and ELMs (intermittent of τ_E and τ_{Alfven}) [Hayashi 2005]. The integrated calculation is realized by coupling the modified Rutherford equation with the transport code of TOPICS including the ECCD code, the MHD stability calculation of MARG2D/ERATO using the down stream data from the TOPICS code, and the alternative calculations of the MARG2D and TOPICS codes. The degradation of the pedestal due to the medium-n mode and the recovery of the pedestal structure are obtained.

An integrated SOL/divertor model is being developed for interpretation and prediction studies of the behavior of plasmas, neutrals and impurities in the SOL/divertor regions [Kawashima 2006]. The code system consists of the 2-D fluid code for plasma (SOLDOR), the neutral Monte Carlo code (NEUT2D), the impurity Monte-Carlo code (IMPMC) and the particle simulation code (PARASOL). Physical processes for neutrals and impurities are studied with the Monte Carlo (MC) method to accomplish highly accurate simulations. The features of the so-called SOLDOR/NEUT2D code, are as follows; 1) a high-resolution oscillation-free scheme for solving fluid equations, 2) neutral transport calculation under the fine meshes, 3) success in reduction of MC noise, 4) optimization on the massive parallel computer. As a result, our code can get a steady state solution within 3 ~ 4 hours and enables effective parameter survey. The detached plasma simulation on JT-60U reproduces the X-point MARFE, explaining the radiation peaking (3~4 MW/m³) from the chemically sputtered carbon.

IV.3.7 ITER-BA computer simulation center

As a part of the Broader Approach Activities in support of the ITER project (ITER-BA) which is under negotiation between Japan and EURATOM, a computer simulation center (CSC) is planned to be established at Rokkasho in Japan. It will be one of the three activities in the International Fusion Energy Research Center (IFERC). The working group on CSC reported that the mission of CSC is to establish a Centre of Excellence (COE) for the simulation and modeling of ITER, JT-60SA and other fusion experiments, and for the design of future fusion power plants, in particular DEMO. A high-performance super computer is expected to be

made available in 2012. The agreement on ITER-BA will be established soon.

References

- [Fukuyama 2000] A. Fukuyama, E. Yokota, T. Akutsu. 2000, Proc. of 18th IAEA Fusion Energy Conf., IAEA-CN-77/TH/P2-26, Sorrento, Italy
- [Fukuyama 2001] A. Fukuyama. 2001, Fusion Eng. Des., 53(1): 71 ~ 76
- [Fukuyama 2002] A. Fukuyama, T. Akutsu. 2002, Proc. of 19th IAEA Fusion Energy Conf., IAEA-CN-94/TH/P3-14, Lyon, France
- [Fukuyama 2004] A. Fukuyama, S. Murakami, M. Honda, et al. 2004, Proc. of 20th IAEA Fusion Energy Conf., IAEA-CSP-25/CD/TH/P2-3, Villamoura, Portugal
- [Harafuji 1989] K. Harafuji, T. Hayashi, T. Sato. 1989, J. Comput. Phys., 81: 169
- [Hayashi 2005] N. Hayashi, T. Takizuka, T. Ozeki. 2005, Nucl. Fusion, 45: 933 ~ 941
- [Honda 2006] M. Honda, A. Fukuyama. 2006, Nucl. Fusion, 46(5): 580-593
- [Idomura 2000] Y. Idomura, M. Wakatani, S. Tokuda. 2000, Phys. Plasmas, 7: 3551
- [Idomura 2002] Y. Idomura, S. Tokuda, Y. Kishimoto. 2002, New J. Phys., 4: 101.1 ~ 101.13
- [Idomura 2003] Y. Idomura, S. Tokuda, Y. Kishimoto. 2003, Nucl. Fusion, 43: 234 ~ 243
- [Ishii 2002] Y. Ishii, M. Azumi, Y. Kishimoto. 2002, Phys. Rev. Lett., 89: 205002
- [Ishi 2003] Y. Ishii, M. Azumi, Y. Kishimoto, et al. 2003, Nucl. Fusion, 43: 539 ~ 546
- [Ishizaki 2006] R. Ishizaki, N. Nakajima, M. Okamoto, to be reported in 21st IAEA Fusion Energy Conf. (Chengdu, China, 2006)
- [Ishizawa 2006] A. Ishizawa, N. Nakajima, M. Okamoto, et al. to be reported in 21st IAEA Fusion Energy Conf. (Chengdu, China, 2006)
- [Kagei 2003] Y. Kagei, M. Nagata, Y. Suzuki, et al. 2003, Plasma Phys. Control. Fusion, 45: L17 ~ L22
- [Kawashima 2006] H. Kawashima, K. Shimizu, T. Takizuka, et al. 2006, Plasma Fusion Res., 1: 031
- [Li 2004] J. Q. Li, Y. Kishimoto. 2004, Physics of Plasmas, 11(4): 1493 ~ 1510
- [Li 2005] J. Q. Li, Y. Kishimoto, N. Miyato, et al. 2005, Nucl. Fusion, 45(11): 1293 ~ 1301
- [Mataumoto 2003] T. Matsumoto, S. Tokuda, Y. Kishimoto et al. 2003, Phys. Plasmas, 10 (1): 195 ~ 203
- [Matsumoto 2005] T. Matsumoto, H. Naitou, S. Tokuda et al. 2005, Phys. Plasmas, 12: 092505
- [Miura 2006] H. Miura, N. Nakajima, T. Hayashi et al. to be published in Fusion Sci. and Tech. Phys. July 2006 (in press)
- [Miyato 2004] N. Miyato, Y. Kishimoto, J. Q. Li. 2004, Phys. Plasmas, 11: 5557 ~ 5564
- [Miyato 2005] N. Miyato, J. Q. Li, Y. Kishimoto. 2005, Nucl. Fusion, 45 (6): 425 ~ 430

[Nakamura 2006] Y. Nakamura, et al. 2006, to be reported in 21st IAEA Fusion Energy Conf., Chengdu, China

[Ozeki 2006] T. Ozeki, N. Aiba, N. Hayashiet al. 2006, Fusion Sci. and Tech. Phys., 50, 68 ~ 76

[Shimizu 2003] K. Shimizu, T. Takizuka, et al. 2003, J. Nucl. Mater., 313-316: 1277

[Smolyakov 2002] Smolyakov, A. I., M. Yagi, Y. Kishimoto, et al. 2002, Physical Review Letter 89 (12): 125005-1 4

[Sugama 2003] H. Sugama, T.-H. Watanabe, W. Horton. 2003, Phys. Plasmas, 10(3): 726 ~ 736

[Sugama 2005] H. Sugama, T.-H. Watanabe. 2005, Phys. Rev. Lett., 94: 115001

[Sugama 2006] H. Sugama, T.-H. Watanabe. 2006, Phys. Plasmas, 13: 012501

[Takizuka 2001] T. Takizuka, M. Hosokawa, K. Shimizu. 2001, Trans. Fusion Tech., 39: 111

[Todo 2003] Y. Todo, H. L. Berk, B. N. Breizman. 2003, Phys. Plasmas, 10, 2888

[Todo 2005a] Y. Todo, K. Shinohara, M. Takechi, et al. 2005, Phys. Plasmas, 12, 012503

[Todo 2005b] Y. Todo, N. Nakajima, K. Shinohara, et al. in Fusion Energy, 2004 (Proc. 20th Int. Conf. Vilamoura, 1-6 November 2004), IAEA, Vienna, TH/3-1Ra

[Todo 2006] Y. Todo, to appear in Proc. 19th Int. Conf. Numer. Simul. Plasmas, (Nara, 12-15 July 2005), a special issue of J. Plasma Phys. (2006)

[Watanabe 2002] T. H. Watanabe, H. Sugama. 2002, Phys. Plasmas, 9 (9): 3659 ~ 3662

[Watanabe 2004] T.-H. Watanabe, H. Sugama. 2004, Phys. Plasmas, 11(4): 1476 ~ 1483

[Watanabe 2005] T.-H. Watanabe, H. Sugama. 2005, Transp. Theo. Stat. Phys., 34: 287 ~ 309

[Watanabe 2006] T. H. Watanabe, H. Sugama. 2006, Nucl. Fusion, 46: 24

[Yagi 2002] M. Yagi, S.-I. Itoh, M. Kawasaki, et al. 19th IAEA Fusion Energy Conference, IAEA-CN-94/TH/1-4 (Lyon, France, 14-19 October 2002)

[Yagi 2005] M. Yagi, S. Yoshida, S.-I. Itoh, et al. 2005, Nuclear Fusion, 45(7): 900 ~ 906

[Yagi 2006] M. Yagi, T. Ueda, S.-I. Itoh, et al. 2006, Plasma Phys., Control. Fusion, 48: A409 ~ A418

V Cross-disciplinary research in fusion simulation

V.1 Applied mathematics: models, discretizations, and solvers (D. E. Keyes)

Computational plasma physicists inherit decades of developments in mathematical models, numerical algorithms, computer architecture, and software engineering, whose recent coming together marks the beginning of a new era of large-scale simulation.

As expectations for computational plasma physics progress from simple "insight" into actual numbers to guide engineering design and investment, there is an

increase in the complexity of virtually all aspects of the modeling process. There are several areas of applied mathematics for which research and development is needed to accompany the rapidly increasing expectations for simulation. They fall into the following three categories:

- **Managing model complexity** Physicists want to use increasing computing capability to improve the fidelity of their models. For many problems, this means introducing models with more physical effects, more equations, and more unknowns. In multiphysics modeling, the goal is to develop a combination of analytical and numerical techniques to better represent problems with multiple physical processes. These techniques may range from analytical methods to determine how to break a problem up into weakly interacting components, to new numerical methods for exploiting such a decomposition of the problem to obtain efficient and accurate discretizations in time. A similar set of issues arises from the fact that many systems of interest have processes that operate on length and time scales that vary over many orders of magnitude. Multiscale modeling addresses the representation and interaction of behaviors on multiple scales so that results of interest are recovered without the (unaffordable) expense of representing all behaviors at uniformly fine scales. Approaches include the development of adaptive methods, i.e., discretization methods that can represent directly many orders of magnitude in length scales that might appear in a single mathematical model, and hybrid methods for coupling radically different models (continuum vs. discrete, or stochastic vs. deterministic), each of which represents the behavior on a different scale. Uncertainty quantification addresses issues connected with mathematical models that involve fits to experimental data, or that are derived from heuristics that may not be directly connected to physical principles. Uncertainty quantification uses techniques from fields such as statistics and optimization to determine the sensitivity of models to inputs with errors and to design models to minimize the effect of those errors.

- **Discretizations of spatial models** Simulations of plasmas and the interaction of a burning plasma with materials have, as core components of their mathematical models, the equations of magnetohydrodynamics or radiation transport, or both. Computational magnetohydrodynamics and transport and kinetic methods have as their goal the development of the next generation of spatial discretization methods for these problems. Issues include the development of discretization methods that are well suited for use in multiphysics applications without loss of accuracy or robustness. Historically, the use of low order discretizations of partial differential equations predominates. Such discretizations lead to very large and sparse systems of algebraic equations, which overwhelm the storage and bandwidth capabilities of likely future computational platforms, relative to floating point processing. High-order discretizations and alternative formulations such as integral equations

should be considered to address trends in computer architecture. Meshing methods specifically address the process of discretization of the computational domain, itself, into a union of simple elements. This process is usually a prerequisite for discretizing the equations defined over the domain. This area of work includes the management of complex geometrical objects arising in technologically realistic devices.

• **Managing computational complexity** Once the mathematical model has been converted into a system of equations for a finite collection of unknowns, it is necessary to solve the equations. The goal of efforts in solvers and “fast” algorithms is to develop algorithms for solving these systems of equations that balance computational efficiency on hierarchical multiprocessor systems, scalability (the ability to use effectively additional computational resources to solve increasingly larger problems), and robustness (insensitivity of the computational cost to details of the inputs). An algorithm is said to be “fast” if its cost grows, roughly, only proportionally to the size of the problem. This is an ideal algorithmic property that is being obtained for more and more types of equations, through multilevel methods for partial differential equations and multipole methods for interacting particles. Discrete mathematics and algorithms make up a complementary set of tools for managing the computational complexity of the interactions of discrete objects. Such issues arise, for example, in traversing data structures for calculations on unstructured grids, in optimizing resource allocation on multiprocessor architectures, or in scientific problems that are posed directly as combinatorial problems.

In this section, we concentrate our discussion on solvers, since the limitations of solvers effectively limit many other generalizations desired above, such as coupling together multiple types of physics, refining resolution or increasing discretization order, and performing sensitivity analyses. The software issues for solvers are much the same for other mathematical issues. Scalable software tools for discretizing and solving PDEs on highly resolved meshes enable physicists to function at the frontier of algorithmic technology while concentrating primarily on their application - that is, refining models and understanding and employing their results - rather than, for instance, debugging split-phase communication transactions deep within a parallel solver. Modern scientific software engineering is characterized by: abstract interface definition, object orientation (including encapsulation and polymorphism), componentization, self-description, self-error-checking, self-performance-monitoring, and design for performance, portability, reusability and extensibility. As an exemplar of scientific software engineering, we mention PETSc, the Portable, Extensible Toolkit for Scientific Computing [Balay 2005], first released in May 1992, and employed in a variety of community and commercial CFD codes and some MHD codes, among many other applications.

Layered Structure of Modern Mathematical Software

At the top level of a modern software library for discretization or solution is an abstract interface that features the language and objects (parameters, fields, etc.) of the application domain (mathematics, physics, etc.) and hides implementation details and call options with conservative parameter defaults. An example of this within the realm of linear solvers is MATLAB's $x = \bar{A}/b$, which requires the user to know nothing about how the matrix \bar{A} is represented or indeed about any of its solution-salient properties (such as symmetry, definiteness, sparsity, etc.) or how the mathematical objects, vectors and matrices, are distributed across storage. The top level description is intended to offer ease of use, correctness, and robustness. However, it might not be particularly efficient to solve problems through the top-layer interface, and the user does not at this level exploit significant knowledge about the system being solved.

The middle level is intended to be accessed by experienced users. Through it is offered a rich collection of state-of-the-art methods and specialized data structures beyond the default(s). The parameters of these methods are exposed upon demand and the methods are typically highly configurable. Accessing the software at this level gives the user control of algorithmic efficiency (complexity), and enables the user to extend the software by registering new methods and data structures that interoperate with those provided. At this level, the user may also expose built-in performance and resource monitors, in the pursuit of comprehending performance. For example, in the realm of linear solvers, a user might elect a domain-decomposed multigrid-preconditioned Krylov iterative method. All associated parameters would have robust defaults, but he could specify the type of Krylov accelerator, its termination criteria, and whether any useful by-products, such as spectral estimates of the preconditioned operator are desired. For the multigrid preconditioner, typical user-controllable parameters include the number of successively coarsened grids, the type of smoother to be used at each level and the number of smoothing sweeps, the prolongation and restriction operators, and the means of forming coarsened operators from their predecessors. For the (domain-decomposed) smoothers, one may have many further parameters. Flexible composability is possible; e.g., the smoother could be another Krylov method. Extensibility is possible, e.g., the coarsening method may be something supplied by the user, or something that comes from an externally linked third-party package.

The bottom level is for implementers. It provides support for a variety of execution environments. It is accessed for portability and implementation efficiency. For instance, different blocking parameters may be appropriate for machines with different cache structures. Different subdomain partitions and message granularities may be appropriate to exploit locally shared mem-

ories, if present.

Demand for scalable solvers

The principal demand for scalable solvers arises from multiscale applications. Here we give operational definitions of “multiscale” in space and time and see why scalable solvers are needed.

Multiple spatial scales exist when there are hard-to-resolve features, such as interfaces, fronts, and layers, typically thin and clustered around a surface of codimension one relative to the computational domain, whose width is small relative to the length of the domain. An example would be a thin sheet embedded in three-dimensional space, though features of greater codimension may also exist, e.g., a thin tube or a small “point” source. The computational domain is usually taken as small as possible subject to the constraint that one must be able to specify boundary conditions that do not interfere with the phenomena of interest. Boundary layers, combustion fronts, hydrodynamic shocks, current sheets, cracks, and material discontinuities are typical multiscale phenomena in this sense. Multiple spatial scales are also present in isotropic phenomena, such as homogeneous turbulence or scattering, when the wavelength is small relative to the target. Multiple spatial scales demand fine mesh spacing relative to the domain length, either adaptively or uniformly.

Multiple temporal scales exist when there are fast waves in a system in which only slower phenomena, such as material convection, diffusion, or other waves, are of interest. The physicist must isolate the dynamics of interest from the multitude of dynamics present in the system, and model the rest of the system in a way that permits discretization over a computably modest range of scales. He may rely on physical assumptions or mathematical closures. Often, assumptions of quasi-equilibrium or filtration of (presumed energetically unimportant) fast modes are invoked since it is not feasible for an explicit integrator to resolve the fastest transients while respecting Courant-like stability limits. For example, fast reactions may be assumed to be in instantaneous equilibrium relative to slow. Fast waves (e.g., acoustic waves in aerodynamics, surface gravity waves in physical oceanography, and magnetosonic waves in plasma dynamics) may be projected out. The dynamics is, in practice, often reduced to a computable manifold by enforcing algebraic or elliptic constraints. The discrete algebraic systems that must be solved to enforce these constraints at every iteration to keep the solution on the manifold are typically ill-conditioned (due to the spatial multiscale nature of the problem) and of extremely high algebraic dimension (millions or billions of degrees of freedom on terascale hardware).

To enforce the constraints, scalable implicit solvers must be called at every step. In this context, “scalable” refers both to complexity of operations and storage, and to parallel implementation on many processors. Classical implicit solvers, such as Gaussian elimination and Krylov iteration [Greenbaum 1997] are not generally, in

and of themselves, sufficient for this task. Both have operation count complexities that grow superlinearly in the discrete dimension of the problem. Depending upon the problem and the particular method, both may have storage complexity that grows superlinearly as well. This implies that even if one adds processors in linear proportion to the discrete problem size (in so-called “weak” or “memory constrained scaling”), the execution time grows without bound. Only hierarchical algorithms, such as multigrid, multipole, and FFT, are algorithmically scalable in this context - their operation counts and storage typically grow only as fast as $O(N \log N)$. FFTs are widely exploited in Poisson projections for structured problems. However, they are being replaced by multigrid [Briggs 2000], which is less fragile, in many contexts. In particular, algebraic multigrid methods extend $O(N \log N)$ optimal complexity to many unstructured problems. Fortunately, multigrid methods often have enough parameters to be tuned to be nearly scalable in a parallel sense as well. Since multigrid methods typically use other direct and iterative linear methods as components, a well-stocked scalable solver toolkit has a wide range of composable solvers available.

A linear solver has been long-regarded as a simple blackbox presenting a relatively straightforward interface. Nevertheless, this unpretentious module is asymptotically the bottleneck to massively parallel scaling in any implicit or semi-implicit MHD code, and in many others. To see why this is the case, consider that most physics applications discretized on a mesh of N degrees of freedom require $O(N)$ work for a basic work step, e.g., evaluating the residual of the conservation laws over the mesh for an implicit problem, or evaluating the right-hand side of a transient problem for the instantaneous rate of change of the state variables. The constant of the $O(N)$ may be large, to accommodate a variety of physical models and constitutive laws, but weak memory-constrained scaling of the problem to large sizes is routine. If carried out by domain decomposition, and if the operator is local, excellent communication-to-computation ratios follow the surface-to-volume scaling of the subdomains [Keyes 1997]. On the other hand, conventional solvers suffer from an $O(N^p)$ scaling for some $p > 1$. Suppose $p = 1.5$, which would be typical of diagonally preconditioned conjugate gradients for a 2D problem. If the computation is well balanced on 64 processors, with the physics phase and the solver phase each costing 50% of the execution time, and if the problem is weakly scaled up to 64K processors, preserving all constants and exponents (Fig. V.1.1), the solver will cost 97% of the execution time! We note that many contemporary users will be scaling in the coming decade from 64 nodes in a departmental cluster to 64K nodes, which are available already on the IBM BG/L machine. We also note that many contemporary implicit and semi-implicit large-scale simulations have reached the point in which 90% of the execution time is spent in $Ax=b$ on problem sizes

that require a number of processors far less than 64 K. These applications require an optimal $O(N \log N)$ scalable solver now.

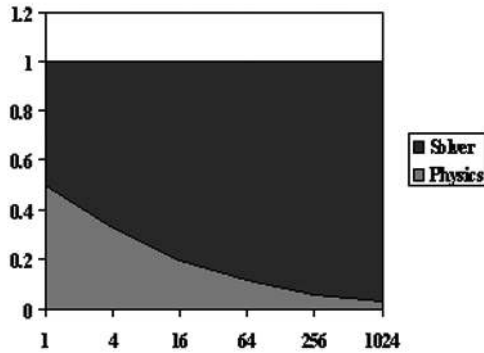


Fig.V.1.1: Fraction of time spent in the solver and in the physics phases of a typical PDE simulation as the problem is scaled by a factor of one thousand, assuming that the computation is originally well balanced on one processor and that the complexity of the solver phase grows like the 3/2ths power of the discretization size, whereas the physics phase grows linearly

Solving the PDE is just one forward map (from inputs to outputs) in this process. Together with analysis, sensitivities and stability are often desired. Solver toolkits for PDEs should support these follow-on desires, which are just other instances of solvers. For instance, stability may be a matter of doing an Eigen analysis of a linear perturbation to the base nonlinear solution. Sensitivity may be a matter of solving an augmented set of equations for the principal unknowns and their partial derivatives with respect to uncertain parameters. No general purpose PDE solver can anticipate all needs. Extensibility is important. A solver software library improves with user feedback and user contributions.

The solver toolchain

The toolchain has become a central concept in solver software design. This is a group of inter-related tools presenting functional abstractions and leveraging common distributed data structure implementations, which ultimately inherit the structure of the mesh on which they are based. The solver tool chain is part of a longer toolchain that reaches upwards through discretization to the application and downwards through performance tools to the hardware.

Within the solver part of the toolchain, the solution of square nonsingular linear systems is the base. Literally dozens of methods - most of them iterative - through combinatorial composition of accelerators and preconditioners, are provided to fulfill this function. Linear solvers are, in turn, called by eigensolvers, mainly during the shift-and-invert phase of recovering eigencomponents other than that of the maximum eigenvalue.

Similarly, linear solvers are called by nonlinear solvers, during each iteration of Newton-like methods. Nonlinear solvers, in turn, are called by stiff implicit

integrators on each time step. Stiff integrators are also called by optimizers to solve inverse problems or compute sensitivities. A solver toolchain is depicted in Fig. V.1.2. It does not include every type of solver that physicists may want; for instance, least-squares methods are not shown here. This constellation of software was assembled to respond to particular needs of users with large-scale mesh-based finite-discretization PDE simulations.

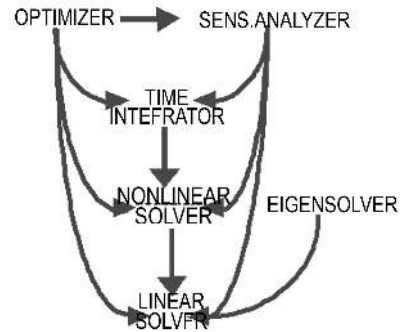


Fig.V.1.2: Solver toolchain

Illustrations from the TOPS solver project

To illustrate this chapter, we consider three different collaborations through which TOPS [Keyes 2001] has engaged magnetohydrodynamicists modeling magnetically confined fusion plasmas.

Nimrod [Sovinec 2004] is a toroidal geometry MHD code discretized via Fourier expansion in the periodic toroidal direction and high-order finite elements in each identically meshed poloidal crossplane. At each time step, several complex nonsymmetric linear systems must be solved in each crossplane, with, for typical contemporary resolutions, 10 K to 100 K unknowns. These sparse linear systems were solved with diagonally preconditioned Krylov iteration, consuming approximately 90% of the execution time. High-order discretizations lead to linear systems that typically lack diagonally dominance and convergence was slow and not very robust. Nimrod presented straightforward symptoms and a straightforward $Ax=b$ interface. A natural trial was to replace the Krylov solver with a parallel direct solver, SuperLU_DIST [Li 2003], a supernodal Gaussian elimination code supported by the TOPS project. The concurrency available in SuperLU is ultimately limited, as it is in any direct solver, by sparsity, and parallel orchestration is disturbed by the dynamic pivoting required in Gaussian elimination on nonsymmetric systems, which gives rise to sophisticated heuristics for pre-factorization scaling and ordering, as well as iterative refinement. Despite the challenges of parallel direct factorization and backsolving, SuperLU has achieved parallel speedups in the hundreds for finite element-type problems with algebraic dimension in the millions, with hundreds of millions of nonzeros in the system matrix. Incorporated into Nimrod to replace the iterative linear solver with no other reformulation, SuperLU achieved solver time improvements of up to two

orders of magnitude in the individual crossplane problems, leading to reduced overall running times of up to a factor of 5 relative to the slowly converging Krylov iteration [Sovinec 2005]. This is in line with expectations from Amdahl's Law for improving the solver execution and shifting the bottleneck to the remaining nonsolver portions of the code. It is well-known that direct methods are competitive with iterative methods on sparse, two-dimensional problems; therefore simulation codes with heavy requirements for such kernels should offer run-time swappable linear solvers including members of both categories.

M3D [Breslau 2002, Park 1999] is an MHD code with greater geometrical generality than Nimrod in that toroidal symmetry is not presumed in the domain or in the poloidal crossplane discretization. As a result, M3D can model configurations such as the experimental stellarator geometry sometimes employed to control the stability of fusion plasmas. Fourier decomposition does not generally apply in the toroidal direction, so M3D employs finite differences in this direction, and finite elements on the triangulated poloidal crossplane meshes, either low-order C0 elements in the standard release or higher-order C1 elements. To achieve parallelism, M3D employs domain decomposition in both toroidal and poloidal directions. The velocity and magnetic fields in M3D are expressed via a Hodge decomposition, through scalar potentials and streamfunctions. As in Nimrod, there are many linear solves per crossplane per timestep, in which Laplacian-like or Helmholtz-like operators are inverted to advance the potentials and streamfunctions. M3D employs PETSc [Balay 2005] for these linear solves, and at the outset of the TOPS project, it relied on one-level additive Schwarz preconditioned GMRES iteration for each such system, with incomplete factorization being employed within each subdomain of each crossplane. One-level additive Schwarz is capable of achieving optimal conditioning for diagonally dominant Helmholtz problems, but is known to degrade in condition number and therefore number of iterations to convergence for pure Laplace problems. Moreover, some of the Poisson problems in each M3D crossplane at each timestep are of Neumann type, so there is a nontrivial nullspace. Presented with the symptom of nonscalable linear solves, requiring 70-90% of the execution time, depending upon the type of problem being run, TOPS collaborators assisted in several improvements. First, they noted that the only asymmetry in the system matrices came from the implementation of boundary conditions, which were modified to achieve symmetry. Second, they implemented a nullspace projection method for the Neumann Poisson problems. Third, they hooked a variety of algebraic multigrid solvers from Hypre [Falgout 2002] into PETSc, to provide dynamic selection of linear solvers. Fourth, they selected three different iterative linear solver combinations, one for each of three different classes of Poisson problems that produced the lowest running times on problem-architecture combina-

tions typical of current M3D operations. The result of this collaboration, most of which was accomplished underneath the PETSc interface, is an M3D that runs 4-5 times faster relative to a pre-collaboration baseline on a typical production problem. Greater savings ratios are expected as problems scale to the sizes required for first-principles simulations of the International Thermonuclear Experimental Reactor (ITER).

The preceding two illustrations of scalable solver enhancements to fluids codes, and collaborations in other science and engineering domains in the TOPS project, are at the $Ax=b$ level. Potentially, there is much to be gained by a tighter coupling of solver research and CFD application development, as illustrated by a collaboration on a standard test case in MHD modeling known as the GEM challenge magnetic reconnection problem [Birn 2001]. Magnetic reconnection refers to the breaking and reconnecting of oppositely directed magnetic field lines in a plasma, or a fluid of charged particles. In this process, the energy stored in the magnetic field is released into kinetic and thermal energy. The GEM problem is designed to bring out the requirement for adaptive meshing in the limit, but it can be run on a fixed mesh and provides a stiff nonlinear system of boundary value problems for the fluid momenta and the magnetic field. A standard case is two-dimensional with periodic boundary conditions - a bona fide idealized temporal multiscale problem. TOPS collaborators worked with a plasma physicist [Reynolds 2006] to compare a nonlinearly implicit method with an explicit method on a fixed-mesh problem. The explicit code respected a CFL stability limit, and therefore ran at a fine timestep. The nonlinearly implicit code ran at a timestep up to two orders of magnitude higher than the CFL limit and showed no loss of accuracy relative to the explicit code. Even after surrendering more than an order of magnitude of this timestep size advantage due to the necessity of solving nonlinear systems on every timestep, the implicit method was approximately a factor of five faster per unit physical time simulated, "out of the box." Prospects exist for preconditionings that could substantially boost the implicit advantage. Similar opportunities for scalable implicit solvers exist throughout computational physics, from magnetohydrodynamics to aerodynamics, from geophysics to combustion.

Future of solver software

Applied computational scientists and engineers should always be "on the lookout" for new and better solution algorithms. A lesson of 60 years of history of floating point algorithms is to be humble about present capabilities. Alongside the punctuated discovery of new solution algorithms, however, are other more predictable research thrusts. We mention five such thrusts, each of which complements in an important way the discovery of new solution algorithms: interface standardization, solver interoperability, and vertical integration with other enabling technologies, automated architecture-adaptive performance optimiza-

tion, and automated problem-adaptive performance optimization.

Interface Standardization. In the recent past, there have been several attempts to establish standards for invoking linear solvers. Examples include the Finite Element Interface, the Equation Solver Interface, Hypre's "conceptual interfaces," and PETSc's linear solver interface, which has become the de facto TOPS interface through the process of absorbing valuable features from all of the others. Fortunately, it is possible to support many independent interfaces over the same core algorithmic functionality, just as it is possible to provide many independent solver libraries beneath a common interface. For $Ax=b$, the TOPS Solver Component (TSC) [Smith 2005] interface has the following object model: A solver applies the inverse action of an operator (typically representing the discretization of a differential operator) to a vector (typically representing field data) to produce another vector. The layout of the data that make up the operator and the vectors in memory and across processors need not be specified. However, since some users require it, TOPS has viewers that provide access to the layout and to the actual data. Available views include the classic linear algebra view (indices into R^n or C^n), as well as several that preserve aspects of the spatial origin of vectors as fields: a structured grid view on "boxes" of data in a Cartesian index space, an unassembled finite element view, a hierarchically structured grid view, etc. The TSC is compatible with the Common Component Architecture (CCA) definition for scientific code interfaces.

Solver interoperability. Because there is no solver that is universally best for all problems or all hardware configurations, users and developers like to mix and match solver components. TOPS has made it possible for many popular solvers to be called interoperably - in place of or as parts of each other. However, only a finite number of well published solver components can ever be included in this manner. TOPS also allows users to "register" custom solver components that support a minimal object model for callback. This feature is especially useful in allowing legacy code to become a component of a TOPS preconditioner.

Vertical integration. The data structures required by solvers are often complex and memory intensive, and the information they contain (for instance, the number of distinct physical fields in a single mesh cell, or the neighbor list for an unstructured grid entity) is potentially valuable in other computational phases, such as mesh refinement, discretization adaptivity, solution error estimation, and visualization, where it might otherwise have to be recomputed. For example, the coarsening procedure in a multilevel solution algorithm may be directly useful in systematically downgrading detail in a discrete field for graphical display. TOPS intends to work with the providers of other components, such as meshers and visualizers, to amortize such work and reduce the total number of copies of what is essentially the same metadata.

Architecture-adaptive performance optimization. It is well known as a result of the ATLAS project [Whalley 2001] that arithmetically neutral data layout issues (blocking and ordering) can have an enormous impact in performance in dense linear algebra. The performance of sparse linear algebra subroutines is, if anything, even more sensitive to such issues, and an additional issue of padding by explicitly stored zeros to obtain greater uniformity of addressing is added to the mix. TOPS is working directly with the developers of OSKI [Vuduc 2005] to obtain the benefit of data layout optimizations demonstrated in that project, which for some sparse linear algebra kernels can approach an order of magnitude.

Application-adaptive performance optimization. Because optimal iterative methods tend to have many (literally up to dozens) of parameters that can be tuned to a specific application, and even to a specific application-architecture combination, users are frequently overwhelmed by parameter choices and run with safe but inefficient defaults. Examples of such tuning parameters include the number of levels in a multigrid method, the number of vectors in a subspace in a Krylov method, the level of fill in an incomplete factorization, and the degree of overlap in a domain decomposition method. Machine learning can be employed to assist users in the choice of these methods, on the basis of previous runs of similar problems, whose features (such as a measure of symmetry or diagonal dominance or number of nonzeros per row) are stored together with performance outcomes. Some preliminary examples of such adaptive optimization of a solver over a pool of matrices arising from unstructured finite element grids in poloidal crossplanes generated during execution of the resistive MHD code M3D are given in [Bhowmick 2006].

References

- [Balay 2005]S. Balay, K. Buschelman, V. Eijkhout, et al. 2005, PETSc Users Manual, ANL 95/11 Revision 2.3.0.
- [Birn 2001]J. Birn, J. F. Drake, M. A. Shay, et al. 2001, Geospace Environmental Modeling (GEM) Magnetic Reconnection Problem, *J. Geophys. Res.* 106(A3): 3715-3719
- [Breslau 2002]J. Breslau, M3DP Users Guide, w3.pppl.gov/jchen/doc/jbreslau.pdf, 2002
- [Briggs 2000]W. L. Briggs, V. E. Henson, S. F. McCormick. 2000, *A Multigrid Tutorial*, 2nd edition, SIAM, Philadelphia
- [Bhowmick 2006]S. Bhowmick, V. Eijkhout, Y. Freund, et al. 2006, Application of Machine Learning in Selecting Sparse Linear Solvers, *Int. J. High Performance Computing Applications* (submitted)
- [Falgout 2002]R.D. Falgout, U. M. Yang. 2002, Hypre, A Library of High-performance Preconditioners, in "Computational Science - ICCS 2002 Part III", P.M.A. Sloot, et al., eds., *Lecture Notes in Computer Science*, 2331: 632-641, Springer

[Greenbaum 1997]A. Greenbaum. 1997, Iterative Methods for Solving Linear Systems, SIAM, Philadelphia.

[Keyes 1997]D. E. Keyes. 1997, How Scalable is Domain Decomposition in Practice?, Proceedings of the 11th International Conference on Domain Decomposition Methods, C. H. Lai, et al. (eds.), pp. 282-293, ddm.org.

[Keyes 2001]D. E. Keyes, et al. 2001, TOPS Home Page, www-unix.mcs.anl.gov/scidac-tops.org

[Li 2003]X.S. Li, James W. Demmel. 2003, ACM Trans. Math. Soft., 29(2): 110-140

[Park 1999]W. Park, E. V. Belova, G. Y. Fu, X. Z. Tang. 1999, Phys. Plasmas, 6: 1796-1803

[Reynolds 2006]D. R. Reynolds, R. Samtaney, C. S. Woodward. 2006, J. Comp. Phys. (to appear)

[Smith 2005]B. F. Smith et al. TOPS Solver Component, <http://www-unix.mcs.anl.gov/scidac-tops/solver-components/tops.html>, 2005

[Sovinec 2004]C. R. Sovinec, A. H. Glasser, T. A. Gianakon, et al. 2004, J. Comp. Phys., 195: 355-386

[Sovinec 2005]C. R. Sovinec, C. C. Kim, D. D. Schnack, et al, and the NIMROD Team. 2005, J. Physics, 16: 25-34

[Vuduc2005]R. Vuduc, J. W. Demmel, K. A. Yelick. 2005, J. Physics, 16: 521-530

[Whaley 2001]R. Clint Whaley, Antoine Petitot, J. J. Dongarra. 2001, Automated Empirical Optimization of Software and the ATLAS Project, Parallel Comput., 27(1-2): 3-35

V.2 Computer science (K. Li)

Computer science is the discipline that anchors the computer industry which has been improving processor performance, communication bandwidth and storage capacity on the so called “Moore’s law” curve or at the rate of doubling every 18 to 24 months during the past decades. The exponential improvements not only have revolutionized how we live, but also have changed how we conduct research. During the past few years, science disciplines including Fusion have shifted to data-driven e-science that unifies theory, simulations, and experiments by exploration of large datasets [GS04]. The roles of computer science have evolved to include not only next-generation supercomputer architecture, compilers, runtime systems, but also methods, software tools, and infrastructure for data exploration to accelerate science discoveries. This section outlines some trends and challenges in computer architecture, software systems, and data exploration that are relevant to science disciplines and fusion research.

Trends in CPU architecture

The most relevant issues to Fusion research in computer architecture are parallel architectures and their implications to programming. Since the architecture of supercomputers is closely related to CPU architecture, we will first look at the main trend in CPU architecture and then the trends in parallel architectures.

A main trend in CPU architecture is a multi-core CPU design where a number of relatively simple, low-

power CPU cores are placed on the same chip to deliver high aggregate computing performance. The main reason for this trend is that the superscalar CPU architecture that we have enjoyed during the past two decades depends heavily on aggressive instruction-level parallelism (ILP) and high-frequency clocks and has now hits the wall of power consumption, due to the increasing difficulties in moving processor fabrications to new-generation technologies. The multi-core CPU architecture, on the other hand, uses many simple CPU cores, each consuming much less power. Together, they exploit process-level parallelism (PLP) or thread-level parallelism (TLP) to achieve high aggregate performance with the available transistors on a chip and with a constrained power budget.

The computer industry started making multi-core processors during the past several years. While AMD, IBM and Intel are shipping dual-core processor chips, SUN Microsystems has recently shipped 8-core processors where each core can execute 4 simultaneous threads sharing the same set of function units, allowing 32 threads to execute in parallel and access shared memory via a large coherent second-level cache [KAO05]. CISCO has 188 32-bit special-purpose CPU cores on a single chip without coherent shared caches [EAT05]. The computer industry views this architecture as the main way to continue the processor performance improvement on the Moore’s law curve in the next decades.

We expect the multi-core processors to develop in two phases. During the first phase, we anticipate a dramatic increase in the number of cores on a single chip. This is because by using simple CPU cores, one can increase the substantial number of cores with the same fabrication technology, as a simple CPU core typically requires an order of magnitude fewer transistors than a complex core. Since the industry needs some time to revert their course from designing complex CPU cores to simple ones, we expect this phase to take two to three years. At the end of the first phase, we should expect the number of cores to reach the range of 16 to 64 for general-purpose processor chips since the processor industry will be using the next-generation fabrication technology.

After the first phase (or during the second phase), we expect that the number of cores for a general-purpose processor chip to slow down its increasing rate to the chip density improvement rate. If the chip density improves 4 to 6 times during the next five years, the number of cores on a general-purpose CPU chip should reach or exceed 128 by that time.

This trend raises several challenging issues in architecture, software systems, and parallel programming for future parallel computers.

Trends in parallel architecture

There are two trends in parallel architecture. The first is the continuing trend in using a cluster of commodity PC nodes as parallel machine. The main rationale of this approach is that it is relatively inexpensive

because of the sheer PC volume in the market place. PC cluster can deliver impressive performance because PCs track technology well.

PC cluster has evolved to become a mature approach to constructing fairly large-scale parallel computers due to the development of commodity systems network interconnect. About twenty years ago, Intel's iPSC/2 supercomputer used a hypercube of Ethernet links to connect 386-based PCs running a small OS kernel with special message-passing software to support MPI-like message-passing programming model [ARL88]. In the 90s, research projects [VCGS92, BLAD94] worked on protected user-level communication to substantially reduce the end-to-end communication latency. These efforts laid the foundation of building low-latency, high-bandwidth networks [DRMC*98, RCGH02] for larger-scale clusters.

The main advantage of this approach is that each node can be relatively "fat" with a large amount of memory and disk storage. The disadvantage of this approach is that a parallel machine of this kind typically consumes a large amount of space and power and its scale is typically limited to fewer than 10,000 processors.

We believe that this trend will continue because systems networks have now become commodity [BCFK*95, ITA00] and it is easy for a science team to construct its own cluster for small or medium-scale simulations and data explorations. By doing so, the scientists can perform their software development and small runs without remotely using large-scale supercomputers which are often high-cost and inconvenient.

The second trend is to use a high-density approach to build very high-end supercomputers. An example of this approach is the IBM Bluegene/L machine [AAAA*02]. The system is built out of a large number of low-power nodes, which utilizes IBM PowerPC embedded CMOS processors, embedded DRAM, and system-on-a-chip techniques that allow for integration of all system functions including compute processor, communications processor, 3 cache levels, and multiple high speed interconnection networks with sophisticated routing onto a single ASIC. Each node has a relatively modest clock rate but an excellent "performance to power" ratio. The entire machine is built with a high-density packaging method that packs 1,024 nodes or 2,048 processors into a single rack.

The main advantage of this approach is that it can push the scale of a supercomputer to use over 100,000 processors by consuming about a similar amount of power that a cluster approach does with an order of magnitude fewer processors. As a result, the Bluegene/L currently dominates the top spots in the top500 list. The main disadvantage of this approach is that its node is relative "thin" with relatively small amount of memory and disk space. As a result, programmers need to pay special attentions to decompose their data structures to fit in to the limited memory space on the thin nodes. Applications whose data structures cannot be

decomposed to fit into the thin nodes will not be able to use such supercomputers.

We expect a supercomputer using the high-density approach to reach 10 million CPU cores in the next few years, as the number of cores per chip will increase by two orders of magnitude during this time period.

Trends in programming future parallel computers

The dramatic increase of CPU cores in future supercomputer raises several challenges in computer science that require significant research. However, we anticipate several near-term trends in programming future parallel computers.

We expect to see a shift in programming model and methodologies for the next-generation parallel machines. We believe that applications using high-end supercomputers will have to do more than using only the message-passing model. The main difficulty with the message-passing programming model alone is that the future supercomputers are expected to require applications to decompose their data structures into two orders-of-magnitude finer pieces than the current applications for Bluegene/L, which are already quite difficult. This is because the average memory per CPU core is expected to be two orders of magnitude smaller than that on Bluegene/L.

One approach is to consider a hybrid programming model between shared memory and message passing. As the future multi-core processor chips are likely to support coherent shared memory and parallel computers are likely to support only message-passing among nodes, we may need to consider algorithms and programming techniques to construct parallel programs where the code that runs on an individual CPU chip uses the multi-threaded, shared-memory programming model and using the message-passing programming model (such as MPI) to communicate among the CPU chips in a parallel computer.

Another approach is to consider a combination of coherent and non-coherent memory programming model for shared address space parallel machines. Some parallel machines such as Cray T3D, T3E, or XT3 have supported a non-coherent shared memory address space. Languages such as Split-C or UPC try to exploit the non-coherent shared address space by using explicit get and put primitives. Currently, these languages do not consider a large number of CPU cores on each node, but they can be extended to have an abstraction for many CPU cores, leading to a combination of shared memory and non-coherent shared address space programming models.

In addition, we expect programmers to pay substantial attention to deal with the increasingly unbalanced memory performance in future supercomputers. Although the multi-core processor trend indicates that the number of CPU cores will increase by two orders of magnitude in the next five years, the memory bandwidth is not expected to increase by more than an order of magnitude due to pin limitations. This implies that

multi-core architecture accelerates hitting the memory wall [WM95]. In order to exploit the potential performance of multiple CPU cores, we will need to consider algorithms and programming techniques to further improve the temporal and spatial localities of programs to tolerate the dramatic increasing performance gaps between processor and memory, and between processor and disk storage subsystems.

Data exploration

Science disciplines including Fusion are experiencing a data avalanche. This is largely due to the exponential improvement of instruments, compute infrastructure, and storage technologies during the past decades. The most exciting aspect of the explosive data growth is to bring an equivalent explosion of knowledge from the data explosion. We are changing from theoretical research to data intensive research. The new trend is to collect or generate massive amounts of data, analyse them to discover new knowledge, achieve scientific discoveries with digital information, and publish knowledge digitally. New ways to explore massive amount of data may lead to new knowledge or new discoveries. Since new instruments have extraordinary precision, the data quality is rapidly improving. Analysing the data to find the subtle effects missed by previous studies requires algorithms that can simultaneously deal with huge datasets and that can find very subtle effects.

An important direction for data exploration is feature tracking and searching in large datasets. Since ITER equipment and large-scale simulation generate immense amount of high-dimensional data, it is difficult to track evolving desired features and it is difficult to search for observe patterns and visually follow regions of interest. Early computer science research on extracting and tracking voxel regions of 3D regular and curvilinear computational fluid dynamics datasets shows that it is possible to help scientists explore tracked features via visualization [SW97]. However, previous work dealt with relatively small datasets. The challenging research issue for computer science is to develop desired feature tracking and searching algorithms for very large, high-dimensional datasets.

A recent trend in data exploration of large, high-dimensional datasets is to develop dimension reduction and indexing techniques by using approximations. By using approximation algorithms, it is often possible to reduce the computation complexity dramatically. For example, it has been shown that one can construct sketches from high-dimensional feature vectors and use Hamming distance to approximate L_1 or L_2 distance effectively [LCL04, LJWC*06]. Locality-Sensitive Hashing [IM98, Cha02] can be used to approximately index similar data objects in high-dimensional space using a fixed number of hashing tables. We expect to see more such approximation methods for data explorations of very large datasets in the near future.

In order to effectively explore very large datasets, scientists need to visualize features on large-display systems. Recent research in computer science shows that

it is possible to build scalable, wall-size, seamless displays from an array of display devices such as projectors [WABC*05]. Scalable display walls have now become mature technologies and they have been used in many national labs as the main infrastructure to visualize large datasets for science discoveries.

Data exploration for large datasets is still a developing area of research in computer science. Scientists including Fusion scientists must continue working with computer science researchers to attack the challenge to accelerate science discoveries by building tools and developing techniques on data management, data analysis and learning, and data visualization for large datasets in a distributed environment.

References

- [AAAA*2002] N R Adiga, et al. 2002, An Overview of the BlueGene/L Supercomputer, IEEE/ACM Proceedings of Supercomputing 2002, Baltimore, Maryland
- [ARL1988] Ramune Arlauskas. 1988, iPSC/2 System: A Second Generation Hypercube. Proceedings of the 3rd Conference on Hypercube Concurrent Computers and Applications: Architecture, Software, Computer systems, and General issues - 1: 38-42, Pasadena, California
- [BLAD*1994] Matt Blumrich, Kai Li, Richard Alpert, et al. 1994, Virtual Memory Mapped Network Interface for the Shrimp Multicomputer. ACM/IEEE Proceedings of the 21st Annual International Symposium on Computer Architecture. Pages 142-153. Chicago, Illinois
- [BCFK*1995] N. Bode, D. Cohen, R. Felderman, et al. 1995, IEEE Micro, 15(1): 29-36
- [CHA2002] M. Charikar. 2002, Similarity Estimation Techniques from Rounding Algorithms. Proceedings of the 34th Annual ACM Symposium on Theory of Computing, pages 380-388. Montreal, Quebec, Canada
- [DRMC*1998] Dave Dunning, Greg Regnier, Gary McAlpine, et al. 1998, The Virtual Interface Architecture. IEEE Micro, 18(2): 66-76
- [EAT2005] Will Eatherton. 2005, The Push of Network Processing to the Top of the Pyramid. Keynote Address, ACM Symposium of Architectures for Networking and Communication Systems. Princeton, New Jersey
- [GS2004] Jim Gray, Alexander S. Szalay. 2004, IEEE Data Engineering Bulletin, 27(4): 3-11
- [IM1998] P. Indyk, R. Motwani. 1998, Approximate nearest neighbors: Towards removing the curse of dimensionality. In Proceedings of the 30th Annual ACM Symposium on Theory of Computing, 604-613, Dallas, Texas
- [ITA2000] InfiniBand Trade Association. InfiniBand Specification, Release 1.0, October 2000. (<http://www.infinibandta.org/home>)
- [KAO2005] Poonacha Kongetira, Kathirgamar Aingaran, Kunle Olukotun. 2005, IEEE MICRO, 25(2): 21-29
- [LCL2004] Qin Lv, Moses Charikar, Kai Li. 2004, Image Similarity Search with Compact Data Structures. Proceedings of the 13th ACM Conference on Information and

Knowledge Management (CIKM), pages 208-217, Washington, DC, 2004

[LJWC*2006] Qin Lv, William Josephson, Zhe Wang, Moses Charikar, Kai Li. 2006, Ferret: A Toolkit for Content-Based Similarity Search of Feature-Rich Data. Proceedings of ACM SIGOPS EuroSys 2006, Leuven, Belgium

[RCGH2002] R. Recio, P. Culley, D. Garcia, et al. 2002, An RDMA Protocol Specification (version 1.0) Technical Report, RDMA Consortium (<http://tools.ietf.org/html/draft-ietf-rddp-rdmap-00>)

[SW1997] Debra Silver, Xin Wang. 1997, IEEE Transactions on Visualization and Computer Graphics, 3(2): 129-141

[VCGS1992] Thorsten von Eicken, David E. Culler, Seth Copen Goldstein, et al. 1992, Active Messages: a Mechanism for Integrated Communication and Computation. ACM/IEEE 19th International Symposium on Computer Architecture. 256-266. Gold Coast, Australia

[WABC*2005] Grant Wallace, Otto J. Anshus, Peng Bi, et al. 2005, IEEE Computer Graphics and Applications, 25(4): 24-33

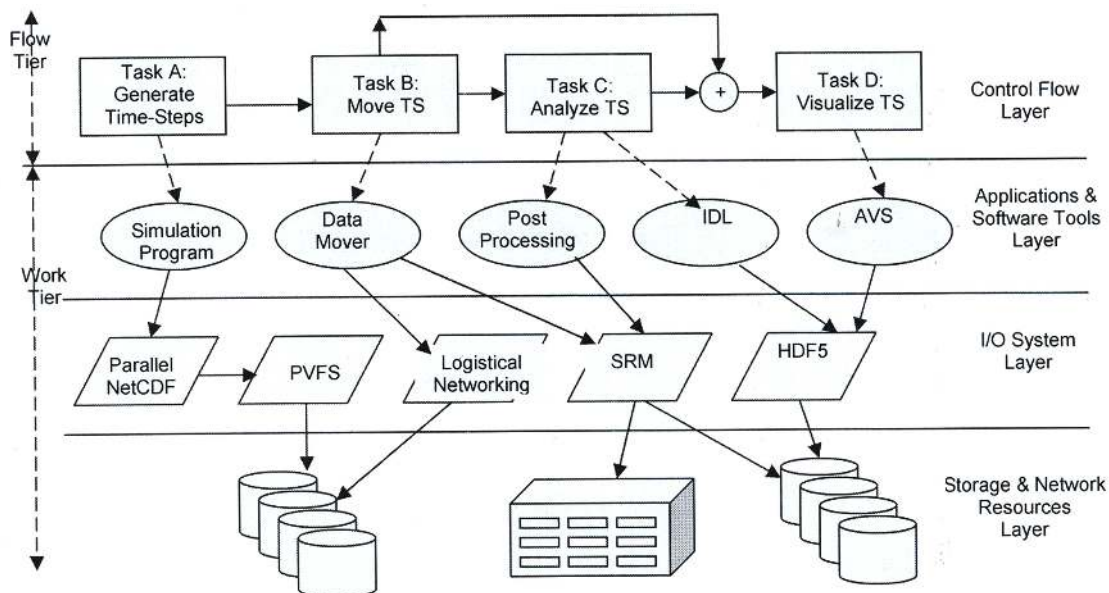
[WM1995] W. Wulf, S. McKee. 1995, ACM SIGArch Computer Architecture News, 23(1): 20

V.3 Scientific data and workflow management (S. Klasky, M. Beck, B. Ludaescher, N. Podhorszki, and M. A. Vouk)

With the increasing volume and complexity of data produced by leadership class simulations and high-throughput experiments, understanding the science is largely hampered by the lack of comprehensive, end-to-end data and workflow management solutions ranging from initial data acquisition to final analysis and visualization. In the following section we highlight some of the challenges and ongoing work towards meeting these challenges.

Motivating Case. Consider a fusion simulation where a group of scientists need to run a simulation on a parallel machine, storing the output data effectively on a parallel file system, archiving the intermediate checkpoint and analysis data, concurrently running an analysis of one or more steps dynamically, then examining the results either statistically or with a visualization tool. [Klasky 2006] Clearly, there are significant data and workflow management challenges, but also opportunities present in such a scenario.

Oversimplifying, we can consider the following Scientific Data Management (SDM) architecture for addressing these challenges to consist of the following layers as shown below



- The bottom layer consists of computational resources and basic services (high-end computers, storage devices, OS).

- The first software layer provides local and distributed storage and efficient data access capabilities and other general “middleware” capabilities.

- The next layer includes specialized software components, e.g., for data mining, analytics (e.g. PCA), and visualization. These components can be considered services (or actors) by the top layer.

- The top (application) layer deals with workflow automation and integrates underlying components into an end-to-end solution for the end-user scientist.

The following challenges and requirements often arise, especially when large data volumes are involved:

Code Monitoring and Adaptation. An important part of any long-running simulation is monitoring of its progress and outputs. This real-time feedback enables scientists to decide whether (a) to stop a simulation, (b) change a set of parameters (e.g. the number


of paths in the Monte Carlo routine for higher accuracy), (c) adjust the simulation code (e.g. invoke an analysis routine), (d) utilize different system resources (e.g. duplicate to increase throughput and guarantee termination within the expected timeframe), or (e) continue. These adjustments can potentially lead to better science and avoid unnecessary use of computational cycles, data storage to file systems, and data transfers to archives. As easy as it sounds, manually orchestrating this complex scientific workflow is a daunting task, so automation is necessary.

Workflow automation tools, while still maturing, already play an important role in effective and efficient analysis of the monitored data. However, the demands on the workflow automation system and the analysis tools used for monitoring increase as science grows more sophisticated (e.g. across multiple spatial and temporal scales with hundreds of variables and thousands of dimensions). First, proper interpretation of this high-dimensional data requires more than a simple monitoring of a few variables but a search for a subset of data of interest and even advanced multivariate features extraction and tracking. Second, scientists want to be able to plug-in into a workflow system an analysis routine written in their language of preference (Matlab, IDL, R) and to run it efficiently. Third, as more simulation data gets monitored, efficient storage of this data, utilization of storage resources for “mainstream” data analysis and sharing the results of this analysis across distributed sites become more demanding. Finally, a workflow engine that invokes the appropriate analysis components automatically should be dynamically and easily updatable to allow explicit modification of the data analysis pipeline in both loosely and tightly coupled manner with modifications applied as new data enters the pipeline. It should support the efficient termination of a specific execution request, halting all related pre- and post-processing activities when the simulation is explicitly stopped or any intermediate component fails. It should also allow us to capture dynamic workflow evolution by recording metadata about the runs and analyses steps that were performed (i.e. data and workflow provenance).

Interactive Debugging of HPC-codes. A task that is quickly becoming overwhelming is the debugging of complex simulations. While parallel debugging tools exist, they are not commonly used because of their complexity and cost. Instead, scientists tend to insert print statements into their code to output information as they try to understand a certain runtime phenomenon. This information routinely needs to be processed further to gain insight. Unfortunately, it is extremely rare that a single debug run generates sufficient insight to solve the problem. Instead, multiple runs, with slightly different parameter settings and slightly different output statements, are usually needed for debugging. Again, workflow automation tools can significantly help in this process. A workflow could be set up that executes the simulation and performs the re-

quired data analysis repeatedly with a variety of input parameters. An adaptive workflow system would easily support modification based on the available variables. Data and workflow provenance tracking can provide a mechanism for recording the runs and their results.

Other Special Requirements. As workflows are increasingly used in production environments, it becomes increasingly important that they are able to effectively manage large data sets and perform long-distance data transfers efficiently. This requires a multi-pronged approach including handling of streaming data between machines different from the machine executing the workflow engine, persistent archiving of data and handling of MxN data transfers (dynamically restructuring the data coming from a cluster with M processors to a cluster with N processors) between simulations and the associated data post-processing steps.

The advent of high-performance computing engines and networks is bringing new opportunities but also challenges for data-intensive and compute-intensive IT solutions for scientific discovery. e.g., numerical and scientific problem-solving environments (PSEs), closer to a broad base of users with widely differing needs and experiences. Use of a PSE is typically associated with a number of additional activities such as collection of data, submission of data and programs to a computational system, execution of simulation and computational codes, movement of data from one platform to another, storage of data, analytics (including visual analytics) of the results, and so on. From the perspective of the users, the key issues are functionality, usability, and quality of service of such systems. A practical bottleneck for more effective use of available computational and data resources is often in the IT knowledge of the end-user, in the area of design of resource access and use of processes, and the corresponding execution environments, i.e., in the scientific workflow environment of end user scientists. The scientific community now expects on-demand access to services which are not bound to a fixed location (e.g., as a specific lab) and fixed resources (e.g., particular operating system), but which can be used over (mobile) personal access device of a scientist (e.g., laptop or a PDA or a cell phone) [Atkins 2003, MOUNT 2004]. The need is for environments where application workflows are dramatically easier to develop and use (from art to commodity), thus expanding the feasible scope of applications possible within budget and organizational constraints, and shifting the scientist’s effort away from data management and application development to concentrating it on scientific research and discovery (Fig. 13 ?).

An integrated view of these activities is provided by the notion of Scientific Workflows. Scientific workflows mean a series of structured activities and computations that arise in scientific problem-solving. Workflows have been drawing enormous attention in the database and information systems research and development communities (e.g., [GEORGAKOPOULOS 1995]). Similarly, the scientific community has developed a num-

ber of problem-solving environments, most of them as integrated solutions [HOUSTIS 2000], and finally, component-based solution support systems are also proliferating [CRNKOVIC 2002, CCA06]. Scientific workflows merge advances in all these areas to automate support for sophisticated scientific problem-solving [LUDASCHER 2006, LUDAESCHER 2005, MOUNT 2004, VALAY 2000, VOUK 1997, SINGH 1996]. Some of the heaviest users of computing are in the sciences. It is no longer possible for scientists to carry out their day-to-day activities without heavy use of computing. This holds in fields and problem areas as diverse as computational medicine, biology, chemistry, genetics, environment, fusion and combustion. Indeed, scientific workflows, as we understand them, are crucial to the success of major initiatives in high-performance computing (HPC).

As parallel computing expands, their standards encourage scientists to construct complex distributed solutions that span the networks, and through web-based interfaces invite incorporation into still more complex systems that may include interactions with economic and business flows. Workflows represent the logical culmination of this trend. They provide the necessary abstractions that enable effective usage of computational resources, and development of robust problem-solving environments that marshal high-performance computing resources. Scientific workflows are expected to co-exist and cooperate with other user workflows (e.g., institutional business workflows, educational workflows, legislative workflows, etc.). As such they must support compatible interfaces and quality of service in the broader sense (which includes reliability, fault-tolerance, security, privacy, data provenance, auditability, etc.).

Characteristics

In many science and engineering areas, the use of computation is not only heavy, but also complex and structured with intricate dependencies. Graph-based notations, e.g., generalized activity networks (GAN), are a natural way of representing numerical and human processing. These structured activities are often termed studies or experiments. They have some common features:

1. Scientific problem-solving usually involves the use of a number and variety of analysis tools, typically invoked in a routine manner. For example, the computations involve much detail (e.g., sequences of format translations that ensure that the tools can process each other's outputs), and often-routine verification and validation of the data and the outputs. There may be also a lot of changes in the workflow as scientists explore new options. As scientific data sets are consumed and generated by the pre- and post-processors and simulation programs, the intermediate results are checked for consistency, and validated to ensure that the computation as a whole remains on track. Process is tracked and provenance information is generated,

2. Semantic mismatches among the tools and data

must be handled. Some of the tools are designed for performing simulations under different circumstances or assumptions, which must be accommodated to prevent spurious results. Heterogeneous databases are extensively accessed; they also provide repositories for intermediate results. When the computation runs into trouble, semantic roll-forward (fault-tolerance, fail-over) must be attempted; just as for business workflows, roll-back is often not an option.

3. Many large-scale scientific computations of interest are long-term, easily lasting weeks if not months. They can also involve much human intervention. This is especially so during the early stages of process (workflow) design. However, as they are debugged, the exceptions that arise need to be handled automatically. Thus, in the end, the production runs should require no more than semiskilled human support. The roles of the participating humans involved must be explicitly represented to enable effective intervention by the right person.

4. The computing environments are heterogeneous. They include supercomputers as well as networks of workstations and supercomputers. This puts additional stress on the run-time support and management. Also, users typically want some kind of a predictability of the time it would take for a given computation to complete, and some run-time status and tracking, and provenance information collections. Making estimates of this kind is extremely complex and requires performance modeling of both computational units and interconnecting networks.

Framework

The key to the solution is an integrated framework that is dependable; supports networked or distributed workflows, a range of couplings among its building blocks, a fault-tolerant data- and process-aware service-based delivery, and ability to audit processes, data and results. Key characteristic of such a framework and its elements are [CRNKOVIC 2002, LUDASCHER 2006]: Reusability (elements can be re-used in other workflows), substitutability (alternative implementations are easy to insert, very precisely specified interfaces are available, run-time component replacement mechanisms exist, there is ability to verify and validate substitutions, etc), extensibility (ability to readily extend system component pool, increase capabilities of individual components, have an extensible architecture that can automatically discover new functionalities and resources, etc), customizability (ability to customize generic features to the needs of a particular scientific domain and problem), and composability (easy construction of more complex functional solutions using basic components, reasoning about such compositions, etc.).

In order to automate scientific problem solving processes, one has to understand limitations of the existing, manual, approaches. Some of the limitations stem from the way we construct our software, some from the way we orchestrate our processes and analyse the results,

and are inherent in the information technology we use.

Storage management

Logistical Networking is the foundation of storage management in distributed research communities for many Fusion Simulation Projects. The general approach taken in Logistical Networking is the creation of a highly generic abstraction of storage that can model a great variety of disk-like storage resources, and which can also be used to model the movement of data between storage resources in networks ranging from Local Area Networks to the global Internet.

Having defined and experimented with Logistical Networking, the focus of recent work has been the creation of libraries implementing standard storage API such as stdio, netCDF, HDF5 which write directly to Logistical Networking storage resources rather than to a local file system. This provides a means to inject the data generated by simulations directly into global workflows, without the need for an additional step transferring data from local to wide area storage systems. Conversely, these libraries allow data to be inspected and read by programs directly from repositories that are distributed in the wide area. This is of particular importance when only a small part of a massive dataset is to be read, and so localizing the entire dataset before reading is terribly wasteful. In the extreme, when only descriptive metadata is read, the cost of data localization may be so much greater than the cost of reading that it becomes prohibitive.

A key part of the Logistical Networking work currently being performed for the Fusion community is the creation of directories to keep track of distributed, replicated data and to provide common namespaces and points of synchronization. Such directories are being customized to the needs of Fusion researchers, which are possible because they are implemented at the user application level, as opposed to being embedded components of a traditional file or database system.

The major point of differentiation for the Fusion Simulation community in building on Logistical Networking is the ability to replicate files freely among a collection of storage resources located at collaborating sites, and to then access the data in a manner that makes data location transparent. This means that increased replication has the effect of increasing data access performance through greater proximity between the application and the storage resource, as well as greater fault tolerance and general system stability through transparent "fail-over" from more local to more distant data copies.

Another factor is the ability to customize the organization of data in structures that mimic database systems without the need to incorporate full-fledged database systems into the scientific software stack. Logistical networking provides a degree of control over low-level storage structures and algorithms that is not generally available except through direct access to disk storage at a very low level. As the scale of data intensive computation continues to increase, file systems derived from conventional Unix/Linux mechanisms strug-

gle to support modes of use that were never anticipated in those original designs. Scientific communities often have design requirements that are more demanding than normal file system access while at the same time being restricted in important ways. For instance many communities can use a write-once discipline for their largest and most widely distributed data, but not for smaller files used for configuration and for the storing the results of data analysis. Logistical Networking allows the available restrictions to be used to ease the problems of massive data scale and geographical distribution.

References

- [Klasky 2006] Scott A. Klasky, Bertram Ludaescher, Manish Parashar, 2006, The Center For Plasma Edge Simulation Workflow Requirements. 22nd International Conference on Data Engineering Workshop, Atlanta GA
- [Atkins 2003] D. Atkins et al, 2003, "Report of the National Science Foundation Blue-Ribbon Advisory Panel on Cyber-infrastructure," NSF-CISE051203, <http://www.nsf.gov/od/oci/reports/atkins.pdf>.
- [MOUNT 2004] R. Mount et al., 2004, Department of Energy, Office of Science report, "Data Management Challenge". <http://www.er.doe.gov/ascr/Final-report-v26.pdf>.
- [GEORGAKOPOULOS 1995] D. Georgakopoulos, M. Hornick, and A. Sheth, 1995, "An Overview of Workflow Management: From Process Modeling to Workflow Automation Infrastructure," *Distributed and Parallel Databases*, 3(2): 119-153
- [HOUSTIS 2000] Elias N. Houston, John R. Rice, Efstratios Gallopoulos, Randall Bramley (editors), 2000, *Enabling Technologies for Computational Science Frameworks, Middleware and Environments*, Kluwer-Academic Publishers, Hardbound, ISBN 0-7923-7809.
- [CRNKOVIC 2002] I. Crnkovic, M. Larsson (editors), 2002, *Building Reliable Component-Based Software Systems*, Artech House Publishers, ISBN 1-58053-327-2
- [CCA06] <http://www.cca-forum.org/>, accessed February 2006.
- [LUDASCHER 2006] B. Ludäscher, et al. 2006, *Scientific Workflow Management and the Kepler System, Concurrency and Computation: Practice & Experience*, Special Issue on Scientific Workflows. 18: 1039-1065.
- [LUDAESCHER 2005] B. Ludaescher, C. A. Goble, editors. *ACM SIGMOD Record, Special Section on Scientific Workflows*, volume 34(3), September 2005, pp 3-4
- [VALAY 2000] Balay R. I, Vouk M. A, Perros H. "Performance of Network-Based Problem-Solving Environments," 2000, Chapter 18, in *Enabling Technologies for Computational Science Frameworks, Middleware and Environments*, editors Elias N. Houston, John R. Rice, Efstratios Gallopoulos, Randall Bramley, Hardbound, Kluwer Academic Publishers, Norwell, MA, ISBN 0-7923-7809-1
- [VOUK 1997] Vouk M. A, M. P. Singh. "Quality of Service and Scientific Workflows," 1997, in *The Quality of Numer-*

ical Software: Assessment and Enhancements, editor: R. Boisvert, Chapman & Hall, Oxford, United Kingdom pp.77-89.

[SINGH 1996] Singh M. P, Vouk M. A. 1996, "Scientific workflows: scientific computing meets transactional workflows," Proceedings of the NSF Workshop on Workflow and Process Automation in Information Systems: State-of-the-Art and Future Directions, Univ. Georgia, Athens, GA, USA., pp.SUPL28-34

V.4 Collaborative tools (J. Manickam)

A successful next generation fusion experiment, such as the International Thermonuclear Experimental Reactor (ITER) project, will need experimentalists, theorists, and computational scientists to collaborate efficiently, to understand the overwhelming amount of information from experiments, codes, and theory. The task is large and, at this stage, imperfectly defined. There is a need for an integrated framework for collaborative services, which will address these issues on several fronts. The main elements of such a framework are a physical, and computational infrastructure, and a well-defined suite of fusion analysis codes that are made accessible to the fusion community for general use.

Prior projects in the US for collaborative research have been mostly oriented towards addressing the needs of the experimental community, to the exclusion of large first-principles simulation codes. An early project focused on file systems, audio/video communications, and web-based tools to demonstrate remote, interactive operations on a large US facility, the DIII-D tokamak at General Atomics [1]. The most recent effort under the first Scientific Discovery through Advanced Computing program (SciDAC), the National Fusion Collaboratory[2], specialized in grid computing using the Access Grid [3], it is a collection of projectors, cameras, and microphones, linked by networked computers to enable audiovisual collaboration between remote participants: videoconferencing. The Access Grid also provides interfaces to enable collaborative visualization, data-sharing, and remote control of instruments. The grid offers a hierarchy of services, ranging from the desktop computer to large TV monitor based interactive communication to room-size tiled display walls. In the US fusion community, there are nodes at MIT, General Atomics, PPPL, and ORNL. The full list of AG nodes worldwide is available at Ref. [3]. The grid had significant success with one particular transport sim-

ulation code, TRANSP [4], including the use of web-monitoring tools.

The ITER experiment will be characterized by its international scope, with widely separated groups of researchers who need to collaborate, to propose and participate in each experiment campaign, to analyse or do simulations, and discuss and understand the results. Another key difference from present experiments is that a single experimental shot on ITER may last for thousands of seconds, in contrast to present high-power machines like JET, which operate for tens of seconds. Significantly more data is generated in the longer discharge, but more critically, it must be analysed in near real time, to assess and predict the plasma evolution and guide it successfully. Thus three new factors must be addressed: data access on a significantly larger scale, a much larger group of researchers needing to extract data at the same time, and the ability to analyse the data in near real time. In order to obtain the best return from the investment and to advance the physics understanding, there is also a need to concurrently run theory-based simulation codes for comparison with experiment. This requires seamless, rapid, and collaborative high-level data analysis and simulation capabilities for both between-shot and longer time-scale analysis. There is presently no widely adopted or viable framework to support such extensive collaborative research. However, existing fusion experiments together with new ones planned to begin operation in the near future, such as EAST in China and KSTAR in South Korea would benefit from the availability of a collaborative framework.

In order to start the discussion of collaborative analysis of a tokamak experiment, we begin with a minimal code-suite, see Fig.V.4.1. This consists of an ideal MHD equilibrium code to fit the experiment; a transport code to analyse the time evolution on the slow, transport time scale, and MHD stability codes. Many examples and extensions of this set exist. Experiments already interpret many of their measurements by running an ideal MHD equilibrium code, EFIT[5], to obtain a constrained fit to the equilibrium at chosen time points. A transport code can then be run to evolve the plasma equilibrium on the slower transport time scales, where the plasma pressure (density, electron and ion temperatures) and magnetic fields are assumed to change by diffusive processes (thermal and particle transport and resistivity, whose diffusion coefficients are specified as functions of space or plasma variables).

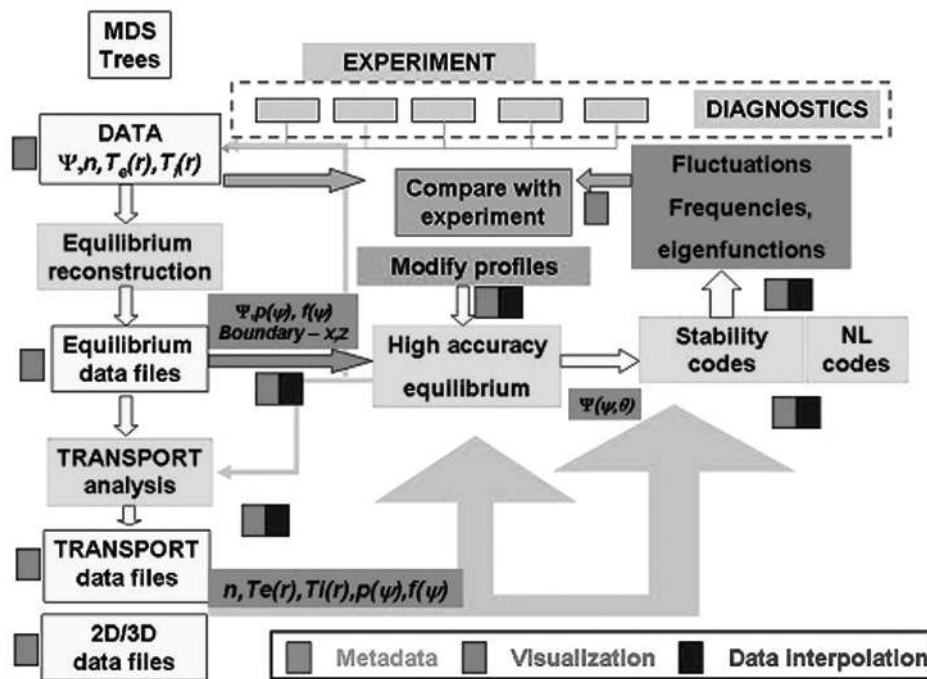


Fig.V.4.1 A schematic diagram of the flow of data from experiment and diagnostics to primary and secondary analysis codes. It shows opportunities to identify data and metadata sets, apply data interpolation and visualization

The transport code calculates a new ideal MHD equilibrium every few time steps, using its own solver, self-consistently with the transported profiles. The new equilibria can also be tested regularly for stability. The resulting equilibrium is often not suitable for direct input to further simulations, which require higher accuracy. Thus, a second equilibrium calculation, with the same or a different code, is often used to refine the equilibrium. An ideal MHD stability code is then used to determine the stability properties, particularly to low- n modes, where n refers to the toroidal mode number. If necessary, the equilibrium can be further analysed, or a nonlinear simulation code used to study its evolution. Stability to slower growing instabilities can be checked by applying a resistive MHD stability code. At each stage, the result can be visualized and compared to experimental measurements or used to predict the plasma behavior.

A number of the basic codes are readily available. They use a number of input/output data formats, but most stability codes read a number of different equilibrium code outputs. Some standard equilibrium formats and translation packages exist, such as XPLASMA and I2MEX in the National Transport Code Collaboratory [6].

A representative list of fusion simulation codes used in the US is shown in Table V.4.1. This is not a comprehensive list; there are many other worthy codes in use in the US fusion community. In addition, it should be noted that, many of these codes have international counterparts, which are also not indicated. In addition to modeling experimental data, another major area for collaboration is ‘first-principles’ based simulation, which can be extended in the future to include inte-

grated modeling. The ultimate goal is to have a predictive capability, based on first-principles’ physics including verification and validation, V&V, rather than the current practice of using empirical scaling.

Large scale simulations and integrated modeling of the plasma over a wide range of temporal and spatial scales are currently a major area of fusion science research and will become increasingly important in the future. In general, they involve much more complex code and data coupling issues. Some of the more important issues are: a) simulations typically generate many more variants of output data for a given study than an experiment; b) There is a need to address data from multiple simulations, arising from both numerical convergence and parameter scans; c) Results must be tracked through many layers of transformations from raw experimental data to interpreted, calibrated data to the results of the final simulation; Scientific approximations may be introduced at each step and must be recorded; and, d) Access permissions and authorizations must be respected.

Another major need is in the area of shared visualization, there is a need for a protocol and capability to connect and update multiple locally shared displays. The protocol will need to consider issues such as window movements and information overlapping in a multi-user environment.

Equally important is the need to develop collaboration mechanisms and policies appropriate for fusion scientists. Web-based monitoring of simulations spanning several hours or even days, assisted by visualization, will be crucial tools for advancing physics understanding.

Equilibrium	Free boundary	EFIT	Lang Lao – GA	
		ESC	Leonid Zakharov – PPPL	
		TSC	Stephen Jardin – PPPL	
	Fixed Boundary	JSOLVER	Charles Kessel – PPPL	
		VMEC	Steve Hirshman – ORNL	
MHD Stability	Linear Ideal	BALLOON	Morrell Chance – PPPL	
		DCON	Alan Glasser – LANL	
		ELITE	Philip Snyder – GA	
		GATO	Alan Turnbull – GA	
		PEST	Janardhan Manickam – PPPL	
	Nonlinear resistive	M3D	Guo-Yong Fu – PPPL	
		NIMROD	Carl Sovinec – U. of Wisconsin	
Micro-stability	Linear	FULL	Greg Rewoldt – PPPL	
		GS2	Bill Dorland – U. of Maryland	
		GTC-NEO	Weixing Wang – PPPL	
		GTC	Zhihong Lin – UC Irvine	
	Nonlinear	GEM	Scott Parker – U of Colorado	
		GYRO	Ron Waltz – GA	
	Wave-particles	Energetic particles and MHD	NOVA	Nikolai Gorelenkov – PPPL
			M3D-K	Guo-Yong Fu – PPPL
		RF waves	AORSA	Don Batchelor – ORNL
			TORIC	Paul Bonoli – MIT
Boundary Physics	Neutrals	DEGAS-2	Darren Stotler – PPPL	
	Edge-Core	XGC	Chaing-Sook Chang – NYU	
	Edge-core	BOUT	Xue Qiao Xu – LLNL	

The responsible person and their institution are shown on the right. Many of these codes have international as well as other US counterparts, which are not indicated here.

Validation and Verification (V&V) will be a major activity in experimental operations. This requires access to data from experiment and from analysis and simulation codes. The chaining of applications and the comparison of simulation results with experiment, which is likely to require chaining codes to put the two sets of data into the same variables, will encourage the use of standardized data formats or data interpolation schemes. The importance of the raw simulation results means that links to them should be included in the transformed data in the same way that the sources of the experimental data are tracked. In addition, V&V for numerical codes, the ability to store and visualize code output directly is crucial. Visualization methods should be capable of looking directly at the code variables on the code grid, for debugging and for ensuring numerical stability and convergence. Numerical problems frequently manifest as oscillations that develop very fine scale, grid-to-grid variation, easy to detect when viewed on the original grid, but not on an interpolated one.

An effective collaborative framework must also acknowledge the fact that human experts are, and will remain for the foreseeable future, indispensable to running sophisticated experiments and simulations. The

framework must also address means to streamline the process of identifying, contacting, and interacting with people.

References

- [1] T.A. Casper, et al. 1998, Computers in Physics, 12: 230
- [2] <http://www.fusiongrid.org>
- [3] <http://www.accessgrid.org/>
- [4] <http://w3.pppl.gov/transp>
- [5] <http://web.gat.com/efit>
- [6] <http://w3.pppl.gov/ntcc>

Acknowledgement

The authors thanks for following colleagues for useful discussions and for support of the Workshop on ITER Simulation: V. Chan, L. Chen, T.S. Fan, Z. Gao, B.L. Hu, X.W. Hu, Y.P. Huo, D. Li, J.G. Li, J.Q. Li, Y.X. Liu, J.R. Luo, Z.W. Ma, C.H. Pan, Y. Pan, Y.D. Pan, Z.Y. Pu, X.G. Wang, Y.L. Ye, H. Zhou, S.Z. Zhu.